EVALUATION OF HOURLY SOLAR RADIATION MODELS TO ESTIMATE RADIATION ON INCLINED SURFACES IN DRY ZONE OF SRI LANKA

Abeyrathna A.R.M.U.E.

128352L

Degree of Master of Engineering

Department of Mechanical Engineering

University of Moratuwa
Sri Lanka

December 2017

EVALUATION OF HOURLY SOLAR RADIATION MODELS TO ESTIMATE RADIATION ON INCLINED SURFACES IN DRY ZONE OF SRI LANKA

Abeyrathna A.R.M.U.E.

128352L

Thesis submitted in partial fulfillment of the requirements for the degree Master of Engineering

Department of Mechanical Engineering

University of Moratuwa

Sri Lanka

December 2017

DECLARATION

I declare that this is my own work and this thesis does not incorporate without acknowledgement any material previously submitted for a degree or diploma in any other University or institute of higher learning and to the best of my knowledge and belief it does not contain any material previously published or written by another person except where the acknowledgement is made in the text.

Also, I hereby grant to University of Moratuwa the non-exclusive right to reproduce and distribute my thesis, in whole or part in print, electronic or other medium. I retain the right to use this content in whole or part in future works (such as articles or books).

Signature: ..... Date: .....

Abeyrathna A.R.M.U.E.

The above candidate has carried out research for the Masters Thesis under my supervision

Signature: ..... Date: .....

Prof. R.A Attalage

ABSTRACT

An analysis of global, beam and diffuse solar radiation on horizontal and 7° tilt about east west axis and facing due south orientation at Hambanthota was carried out to assess the solar resource potential in dry zone of Sri Lanka. The calculated monthly averaged daily insolation for dry zone was found to be varying between 16.30 MJ/m^2/day to 22.75 MJ/m^2/day with the annually averaged daily insolation of 20.07 MJ/m^2/day. Calculated annually averaged beam horizontal radiation was 10.87 MJ/m^2/day and diffuse horizontal radiation was found to be 9.19 MJ/m^2/day while 0.56 was the annual average clearness index indicating that partly cloudy sky throughout the year. Horizon brightness coefficients of Perez et al (1990) was modified using diffuse radiation data of Hambanthota. Modified model was used for the estimation of titled radiation on due south faced surfaces. Diffuse tilted daily insolation and global tilted insolation for -45° to +45° inclined surfaces with 1° increments was estimated and monthly and annual optimum tilt angles were derived. The calculated monthly optimum tilt angle varied between -26° to +27° while having annual optimum tilt angle of -2°. Hence, tilting towards due south by same angle as latitude is not the recommended optimum tilt for fixed axis systems. Optimum tilt angle for beam radiation was derived and it was found that annual optimum tilt angle for beam radiation is 6° facing towards the due south. The derived maximum solar resource potential was 2068 kWh/m^2 per annum for fixed system at -2° tilt angle and 2169 kWh/m^2 per annum for monthly tracking system which is 5% higher than the horizontal potential. It is proposed to assess the solar resource potential for tilted surfaces with different surface azimuth angles by using modified Perez et al (1990) model in future. It is also possible to modify the coefficients of circumsolar brightness components of Perez et al (1990) model for better results.

Key Words: Diffuse Solar Radiation, Isotropic Models, Anisotropic Models, Optimum Tilt angle, Hambanthota.

ACKNOWLEDGEMENT

I am very much grateful to Prof. R.A Attalage, Deputy Vice Chancellor of the University of Moratuwa for giving me his utmost support and guidance for this research. I am very much grateful to the course coordinator of M.Eng/PG Diploma on Energy Technology Dr. Himan Punchihewa, Senior lecturer, Department of Mechanical Engineering, University of Moratuwa, for giving his fullest support in every stage of this research. This research was carried out under the supervision of Prof. R.A Attalage, senior professor, Department of Mechanical Engineering, University of Moratuwa. I am indebted to him for the valuable guidance, and kind hearted co-operation and encouragement extended throughout the research. I would like to extend my sincere thanks to Mr. M.M.R. Pathmasiri, Director General (SEA), Mr. H.A. Vimal Nadeera, Deputy Director General - Operatins (SEA), who gave their co-operation and utmost support by giving access to radiation data of Hambanthota Solar Park. It is a great pleasure to remember the kind co-operation extended by the colleagues in the post graduate programme who helped me to continue the studies from start to end. Finally, I appreciate everybody, who helped me in numerous ways at different stages of the study, which was of utmost importance in bringing out this effort a success.

TABLE OF CONTENTS

LIST OF FIGURES

Page

LIST OF TABLES

Page

LIST OF APPENDICESS

LIST OF NOMENCLATURE

Roman Letters

A	=	Apparent solar irradiation at zero air mass, Anisotropy index, Altitude of the location in kilometres, Apparent solar irradiation at zero air mass
B	=	Atmospheric extinction coefficient
C	=	Diffuse radiation factor
c_ω	=	Cloud cover index
$\overline{c_\omega}$	=	Monthly averaged daily cloud cover index
F_1	=	circumsolar brightness factor
F_2	=	horizon brightness factor
F'	=	Klucher's modified clearness index
G	=	Total scattered intensity, Total horizontal radiation
G_0	=	Incident intensity
G_b	=	Beam radiation on horizontal surface
G_{bn}	=	Beam normal radiation
G_{bt}	=	Beam radiation on tilted surface
G_d	=	Diffuse radiation on horizontal surface
G_{dt}	=	Diffuse radiation on tilted surface
G_g	=	Ground reflected radiation on horizontal surface
G_{gt}	=	Ground reflected radiation on tilted surface
G_o	=	Extra-terrestrial radiation on horizontal surface
G_{on}	=	Extra-terrestrial normal radiation
G_{sc}	=	Solar Constant
G_t	=	Total radiation on tilted surface
$G_{\lambda,0}$	=	Monochromatic intensity at x=0
H	=	Daily total horizontal radiation
H_b	=	Daily beam radiation on horizontal surface
H_{bn}	=	Daily beam normal radiation
H_{bt}	=	Daily Beam radiation on tilted surface
H_d	=	Daily diffuse radiation on horizontal surface
H_{dt}	=	Daily diffuse radiation on tilted surface

H_g = Daily ground reflected radiation on horizontal surface

H_{gt} = Daily ground reflected radiation on tilted surface

H_o = Daily extra-terrestrial radiation on horizontal surface

H_{on} = Daily Extra-terrestrial normal radiation

H_t = Daily Total radiation on tilted surface

$\bar{H}$ = Monthly averaged daily total horizontal radiation

$\overline{H_b}$ = Monthly averaged daily beam radiation on horizontal surface

$\overline{H_c}$ = Monthly averaged clear day radiation on horizontal surface

$\overline{H_{bn}}$ = Monthly averaged daily beam normal radiation

$\overline{H_{bt}}$ = Monthly averaged daily Beam radiation on tilted surface

$\overline{H_d}$ = Monthly averaged daily diffuse radiation on horizontal surface

$\overline{H_{dt}}$ = Monthly averaged daily diffuse radiation on tilted surface

$\overline{H_g}$ = Monthly averaged daily ground reflected radiation on horizontal surface

$\overline{H_{gt}}$ = Monthly averaged daily ground reflected radiation on tilted surface

$\overline{H_o}$ = Monthly averaged daily extra-terrestrial radiation on horizontal surface

$\overline{H_{on}}$ = Monthly averaged daily Extra-terrestrial normal radiation

$\overline{H_t}$ = Monthly averaged daily Total radiation on tilted surface

I = Hourly total horizontal radiation

I_b = Hourly beam radiation on horizontal surface

I_{bn} = Hourly beam normal radiation

I_{bt} = Hourly Beam radiation on tilted surface

I_d = Hourly diffuse radiation on horizontal surface

I_{dt} = Hourly diffuse radiation on tilted surface

I_g = Hourly ground reflected radiation on horizontal surface

I_{gt} = Hourly ground reflected radiation on tilted surface

I_o = Hourly extra-terrestrial radiation on horizontal surface

I_{on} = Hourly Extra-terrestrial normal radiation

I_t = Hourly Total radiation on tilted surface

k_T = Hourly clearness index

K_T = Daily clearness index

$\overline{K_T}$ = Monthly average daily cleanness index

K_λ = Monochromatic extinction co-efficient

L = Latitude angle

m_h = Air mass

n = Julian day of the year

r = Radius of the particle

r_b = Hourly beam radiation tilt factor

r_d = Diffuse radiation tilt factor

r_t = Daily global irradiance to hourly global irradiance conversion ratio

R = Distance between the molecule and the point of observation

R_b = Daily beam radiation tilt factor

R_h = Relative humidity

$\overline{R_b}$ = Monthly averaged daily beam radiation tilt factor

$\overline{R_h}$ = Monthly averaged daily relative humidity

S = Averaged hours of sunshine

S_0 = Averaged maximum possible hours of sunshine

$\overline{S}$ = Monthly averaged daily hours of sunshine

$\overline{S_0}$ = Monthly averaged daily maximum possible hours of sunshine

t = Midpoint of the hour

T = Temperature

T_{max} = Daily maximum temperature

T_{min} = Daily maximum temperature

$\overline{T}$ = Monthly averaged daily temperature

$\overline{T_{max}}$ = Monthly averaged daily maximum temperature

$\overline{T_{mın}}$ = Monthly averaged daily maximum temperature

x = Size of the scattering particle

Greek Letters

α = Altitude angle, Polarisability of the particle

β = Tilt angle

γ = Solar azimuth angle

γ_p = Surface azimuth angle

Γ	=	Day angle
δ	=	Declination angle
Δ	=	Brightness
ε	=	Sky clearness
θ	=	Incident angle
θ_z	=	Zenith angle
λ	=	Wave length
ρ_g	=	Ground albedo
τ_λ	=	Monochromatic transmittance
ω	=	Hour angle
ω_s	=	Sunshine/sunset angle
ω_{sr}	=	Sunrise angle on tilted surface
ω_{ss}	=	Sunset angle on tilted surface

LIST OF ABBREVIATIONS

Abbreviation	Description
ASHRAE	American Society of Heating, Refrigerating and Air-Conditioning Engineers
AST	Apparent Solar Time
LST	Local Solar Time
PV	Photovoltaic
SLSEA	Sri Lanka Sustainable Energy Authority
WMO	World Metrological Organization

1 INTRODUCTION

1.1 Background

Out of all renewable energy sources, solar energy is one of the most feasible sources of sustainable energy. Solar energy is environment and nature friendly and does not contribute in damaging the ecological system. Small scale solar systems are practicable at remote areas where grid systems are not available and large scale thermal systems are more beneficial with current energy and environment crisis. But major design drawback is the unpredictable nature of solar irradiance. Existing Solar radiation data are the best source of information for estimating the average incident radiation required for the planning and evaluation of suitable solar energy systems. Prediction of the availability of solar radiation is difficult, since its availability is dependent on weather and climate conditions. The availability of complete data of solar radiation is invaluable for planning and evaluation of conversion systems based on solar energy.

There are different forms of data on solar radiation, which are suitable to be used for variety of purposes in the design and development of solar energy systems. Often solar radiation data are available as hourly, daily and monthly averaged daily data. Most of the solar radiation models found in the literature for the estimation of radiation is mainly based on the data collected at weather stations in the United States, Canada, Australia and the countries of the northern Europe.

In Sri Lanka, the solar radiation databases for areas of interest are not readily available. Sri Lanka Metrological Department recodes sunshine hours at few weather stations and total radiation in Colombo station. Sri Lanka Sustainable Energy Authority (SLSEA) recodes solar radiation data in Hambanthota solar park and Kilinochchi since 2011. These data can be used for deriving relevant solar radiation models to predict the hourly, daily and averaged solar radiation availability of the dry zone in Sri Lanka.

1.2 Present status of solar energy applications in Sri Lanka

SLSEA has been commissioned and operates Sri Lanka's first solar power plant at Hambanthota with the capacities of 500 kW and 737 kW since 2010 as pilot project and these two plants has operated with annual plat factors of 17.69 and 17.91 respectively (Sri Lanka Energy Balence 2015, 2017). 10 MW solar plant at Welikanda with single axis hourly tracking system (about north south axis) was commissioned in December, 2016. A total of 39,312 solar photovoltaic modules has been installed in a land extend of 19.95Ha in Welikanda having generation capacity of 23 GWH per annum. (windforce, 2017). Another 10 MW solar plant at Hambanthota was commissioned in December, 2016 without tracking system. A total of 48,000 polycrystalline solar panels with construction costs of 2.5 billion rupees has been installed (Sri Lanka commissions 10MW solar power plant, 2017). Ceylon electricity board has commissioned 60 kW hybrid power plat with solar, wind and diesel in Eluwathivu island. With all these new addition Sri Lanka has total of 21.36 MW grid connected solar system apart from net metering systems. Another solar photovoltaic (PV) plants with total capacities of 50 MW is also under consideration.

Net metering in Sri Lanka which was introduced in 2010 has reached 30 MW with 4200 roof top installations providing approximately 38.8 GWh per annum to the national grid by the end of 2015 (Sri Lanka Energy Balence 2015, 2017).

Since, the solar energy is mostly used in non-commercial forms, the total usage of energy is not yet quantified properly. However, solar energy is the most frequently used in day to day life and drying, heating and electricity production are the most common uses of solar energy in the country. Solar energy utilization in Sri Lanka by end of year 2015 is given in Table 1.1

Table 1.1 - Solar energy utilization in Sri Lanka

Typical User Groups	Typical Applications	Scale of use by end 2012
Solar photovoltaic	Net-metering	4,200 installation
	Household lighting	About 120,000 units
Grid connected PV	For sale to utility	4 power plants
Solar Thermal	Hot water systems (Commercial and domestic scale)	widespread
Informal use	Household and agricultural use	widespread

Source: (Sri Lanka Energy Balence 2015, 2017)

By the end of year 2015, it is generated 1.9 GWh of energy had been generated by 1.4 MW of installed capacity at three solar power plants. It is about 0.1% of the total non-conventional renewable energy generation of year 2015 (Sri Lanka Energy Balence 2015, 2017).

1.3 Problem statement

Although the earth's extra-terrestrial radiation is held at a constant about 1367 W/m^2, the amount of energy available in the terrestrial region is highly varied due to several factors. The porous atmosphere around the earth is consists of various gases such as CO_2, CO, O_3, N_2, O_2, atmospheric water vapour and dust. Due to the presence of these components in the atmosphere, the amount of solar energy received by the earth surface is reduced and due to the variation of these components from location to location, the net amount of solar energy availability at the ground level is also varied accordingly. There are two distinct models developed to assess the horizontal radiation on the given surface called parametric models and decomposition models. Parametric models asses the global horizontal radiation and decomposition models quantify the amount of diffuse radiation on horizontal surface. But there are some site specific parameters incorporated into those models which are needed to be derived by performance measurements in the site in which the solar radiation is to be assessed.

However, in solar energy applications it is essential to estimate the solar radiation on tilted surfaces to maximise the energy harnessing by using optimum tilt angels. However, estimating of the diffuse radiation components on the tilted plane is

complicated even though estimating of beam and ground components are straight forward. Amount of the diffuse radiation is defend on the sky clouds pattern and there are two distinct types of sky models available on literature called isotropic and anisotropic to estimate the diffuse radiation components on tilted planes depend on the nature of the sky. Isotropic models have been developed by assuming that intensity of the sky diffuse radiation is uniform over the entire sky dome and anisotropic models have been developed by dividing sky radiation component into three components as circumsolar, sky dome and horizon brightening components. However, most of these models are location based and has been developed by countries in temperate zone and none of these models have validated with measured Sri Lankan solar radiation data. Hence, solar resource availability estimations of Sri Lankan locations based these models may not present the actual solar radiation potential in Sri Lanka. Therefore, development of new model using measured data for Sri Lanka is important and such model can be used in future for estimation of solar resource availability new solar energy applications

1.4 Aim and objectives

The aim of this research is to identify best fit model/s to predict the availability of solar radiation availability in the dry zone of Sri Lanka. Therefore, the objectives set for this study are;

- Identify the different parameters affecting the Global Solar Radiation
- Identify the existing models to predict global solar radiation for different sky conditions
- Identify most appropriate model(s) to estimate the global radiation for dry zone
- Develop new model (modify an existing model) for dry zone
- Estimate monthly and annually averaged hourly and daily global, beam and diffuse horizontal solar resource potential in Dry zone of Sri Lanka
- Estimate monthly and annually averaged hourly and daily global, beam and diffuse solar resource potential on tilted surface in Dry zone of Sri Lanka
- Estimate of monthly and annual optimum tilt angle for dry zone of Sri Lanka

1.5 Outcomes

- Mathematical model to predict hourly diffuse radiation on tilted surface in dry zone of Sri Lanka
- Estimation of monthly and annually averaged hourly and daily global, beam and diffuse horizontal solar resource potential in Dry zone of Sri Lanka
- Estimation monthly and annually averaged hourly and daily global, beam and diffuse solar resource potential on tilted surface in Dry zone of Sri Lanka
- Estimation of monthly and annual optimum tilt angle for dry zone of Sri Lanka

1.6 Scope of the study

The scope of this study is limited to analyse hourly radiation data on horizontal and tilted surfaces in order to drive suitable diffuse radiation model for dry zone of Sri Lanka. In addition to that, estimation of monthly and annually averaged hourly and daily global, beam and diffuse radiation on both horizontal and tilted surfaces and driving the annual, monthly and daily optimum surface tilt angles for dry zone of Sri Lanka is presented as outcomes of this study.

1.7 Outline of the study

In the first chapter of this study, describes the solar energy utilization characteristics of Sri Lanka and the potential for solar energy harnessing, particularly in dry zone. The fundamentals of solar radiation are described in Chapter 2 which includes solar geometry such as solar angles and sun earth angles, extra-terrestrial radiation, terrestrial radiation and atmospheric attenuation. In addition to that basic formulas of solar radiation on horizontal and tilted surfaces, parametric solar radiation models, solar radiation decomposition models, solar insolation estimation methods on tilted surfaces are also discussed in Chapter 2. The research methodology is described in details in Chapter 3. The results of the study are discussed in Chapter 4 and finally Chapter 5 is dedicated to present the findings and conclusions of this study.

2 REVIEW OF THE LITRATURE

2.1 FUNDAMENTALS OF SOLAR RADIATION

2.1.1 The Sun and Earth

The sun is the star in our solar system. The sun is almost spherical with average diameter of 1.393×10^9 m (about 109 times with respect to Erath) and mass of 1.989×10^{30} kg (330,000 times the Earth). It is believed that Sun formed 4.6 billion years ago due to gravitational collapse of a molecular cloud. Sun is classified as G-type star (G2V) where G2 stands for surface temperature (5777 K) and V stands for energy is generated by nuclear fusion. Generated energy is transmitted to the earth by radiation.

The earth is an almost spherical planet with a diameter of 1.27×10^7 m. The average period of rotation of the earth about its axis is 24 hours and average period of revolution around the sun is 365.25 days. The mean distance between sun and earth is known as one astronomical unit and equals to 1.495×10^{11} m. However, Earth's orbit is not symmetrical and estimated to have ± 1.7 % annual variation. Minimum distance between sun and earth occurs at 21st of December and maximum distance occurs at 21st of June. Therefore, earth receives 7% more radiant energy in December than in June. However, the local climate of the earths is not only dependent on the mean distance but also on the angle of the incidence solar radiation at the particular location.

Sun subtends only 0° 32' angle at earth surface due to the large distance between sun and earth. Therefore, solar radiation at earth surface can be considered as parallel and with a travelling speed of 3.8×10^8 ms^{-1} in the vacuum it takes 8 min and 20 seconds to receive solar radiation by earth. Even though brightness of sun varies from its centre to outside it is assumed that brightness is uniform with an energy output of 63 MW/m^2 constituting a total energy output of 3.8×10^8 MW. The radiation outside the earth atmosphere is known as extra-terrestrial radiation and within the atmosphere is known as terrestrial radiation. The radiation received on the unit area of surface perpendicular to the direction of the propagation of sun at one astronomic unit distance outside the atmosphere is known as Solar Constant I_{SC} and has value of 1367 W/m^2. Figure 2.1 shows relationship of sun and earth schematically.

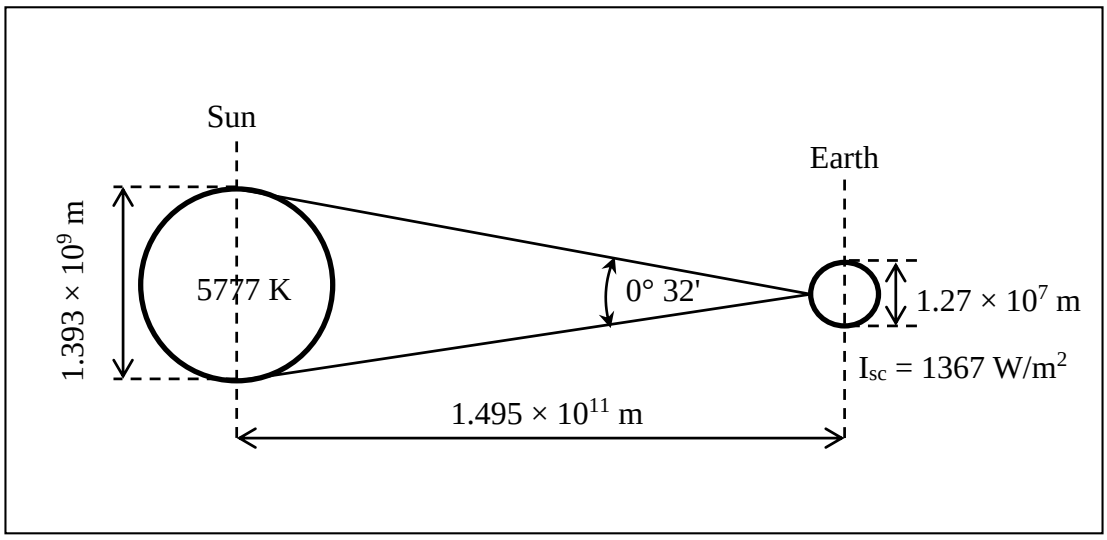

Figure 2.1 - The Sun-Earth relationship

(Source: Soteris, 2009)

2.2 Solar Geometry

Radiant energy received on earth surface from the sun varies with location, day of the year, time of the day and other metrological conditions. However extra-terrestrial radiation varies only with the location and time. Therefore, clear understanding on solar geometry is necessary in the estimation of solar energy. The earth's rotation axis is 23.45° inclined to the ecliptic axis which is normal to the ecliptic plane. Earth transits through the orbit keeping this inclined angle constant throughout the year. This result the changes in relative distance on a point on the earth's surface with respect to the sun. Figure 2.2 shows the relative position of the earth on 21st of June and 21st of December. Radiation incident angle on southern hemisphere in June and northern hemisphere in December is lower than to northern hemisphere in June and southern hemisphere in December. Further, Arctic circle in June and Antarctic circle in December receive 24 hours sun rays while Antarctic circle in June and Arctic circle in December doesn't receive at all. This variation of the solar incident angle on earth leads to make seasonal climatic variation on earth.

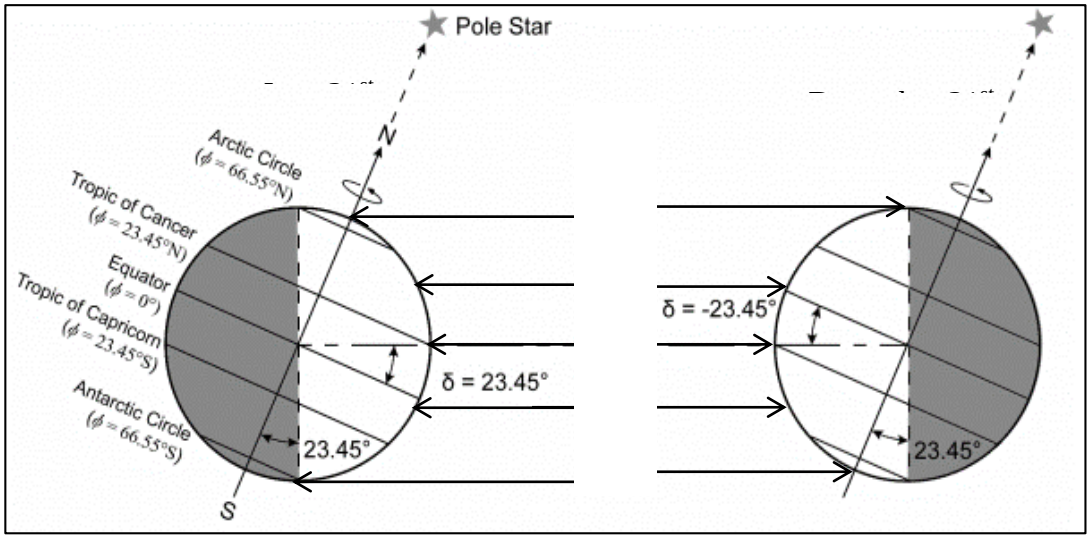

Figure 2.2 - Relative position of the earth on 21st of June and 21st of December

(Source: "The Sun as a Source of energy: Part 1: Solar Astronomy". n.d.)

The earth's surface has been divided in to five climatic zones due to climatic effects caused by its tilt angle. The zone between the latitudes of 23.45° either sides of equator is known as tropical zone where the sun is overhead at least once a year. The zones between latitudes of 23.45° to 66.55° (90°-23.45°) in both hemispheres are known as temperate zones where the sun appears above the horizon each day. The zones beyond the 66.55° in both hemispheres are known as frigid zones where the sun appears below/above at least one full day.

2.2.1 Sun-Earth angles

In order to identify the position of the point on earth's surface three basic sun earth angles have been defined as declination angle δ, Latitude angle L and hour angle ω. Angle between solar radiation and earth's rotational axis varies from -23.45° to +23.45° throughout the year and this angle is known as solar declination angle δ. The earth's axis is tilted towards (north pole towards the sun and south pole outwards the sun) the sun on the 21st of June making +23.45° declination angle and tilted away (north pole outwards the sun and south pole towards the sun) the sun on the 21st of December making -23.45° declination angle. Figure 2.3 shows schematic representation of earth's orbit and declination angles in equinoxes and solstices.

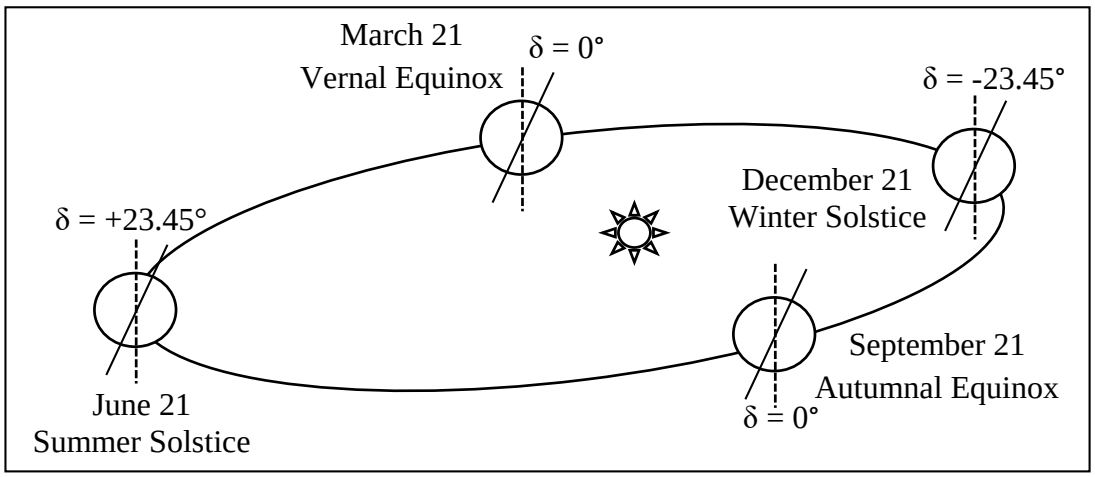

Figure 2.3 - Declination angles in equinoxes and solstices

This cyclic variation of solar declination causes seasonal weather changes in the earth. Even though solar declination angle varies all over the time it can be considered as constant during any given day for engineering calculations. Equation suggested by Cooper in 1969 for calculating declination angle is given in Equation 2.1.

$$\delta = 23.45 \sin\left[360 \times \left(\frac{284 + n}{365}\right)\right] \qquad 2.1$$

Where,

n : Julian day of year

Another equation called Spencer formula was introduced by Spencer in 1971 to calculate the declination angle which is given in Equation 2.2

$$\delta = \frac{180}{\pi}(0.006918 - 0.399912\cos\Gamma + 0.070257\sin\Gamma - 0.006758\cos 2\Gamma + 0.000907\sin 2\Gamma - 0.002697\cos 3\Gamma + 0.00148\sin 3\Gamma) \qquad 2.2$$

Where,

Γ : day angle given in Equation 2.3

$$\Gamma = \frac{360(n-1)}{365} \qquad 2.3$$

However, American Society of Heating, Refrigerating and Air-Conditioning Engineers ASHRAE in 2007 recommended Cooper (1969) equation to calculate Declination angle. Variation of the declination angle throughout the year is shown in Figure 2.4 which is calculated using cooper (1969) equation.

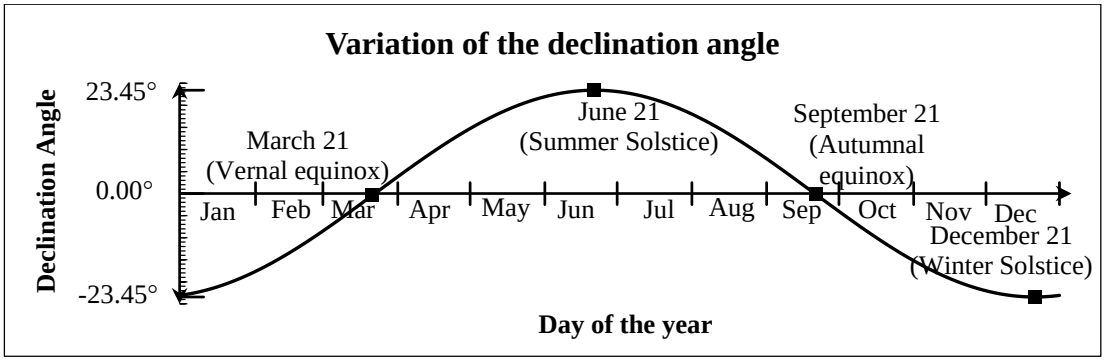

Figure 2.4 - Variation of the declination angle

Solar radiation receiving angle of the any point of the earth is varying on the position of the point in earth. Any point of the earth can be described using latitude L and longitude angle of the point. Latitude describes the angle between point on the earth's surface and the equatorial plane. Rotational speed of the earth is 15° per hour and hour angle ω defined as angle which earth has to rotate to bring meridian plane of any point to face the sun. Figure 2.5 describes the latitude angle L, hour angle ω and declination angle δ for a point P on the northern hemisphere.

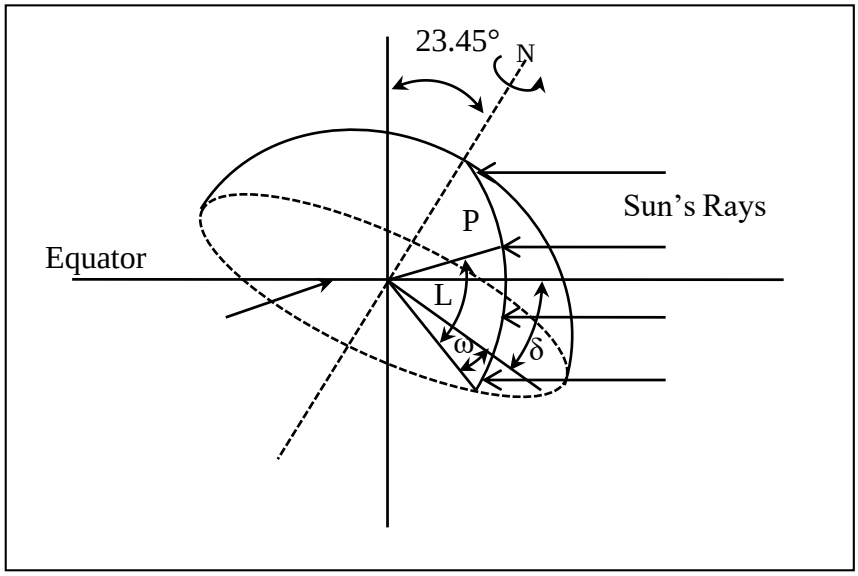

Figure 2.5 - Basic Sun-Earth angles

Value of the hour angle at solar noon is considered as zero. Therefore, value of the hour angle indicates the time of the day with respect to the solar noon. As convention morning hour angles are considered as negative and afternoon angles are considered as positive.

2.2.2 Solar angles

The solar angles are defined with respect to an observer on a tangential plane at a given point on the earth's surface. These solar angles are derived using basic sun earth angles. There are three basic solar angles called zenith angle θ_z, Altitude angle α and solar azimuth angle γ. In addition to those three, additional two angles have been introduced for a tilted surface as incident angle θ and surface azimuth angle γ_p.

The zenith angle θ_z is defined as angle of incident of solar radiation on the tangential plane at a point on the earth. Altitude angle α is the angle between the solar radiation incident and its projection on the earth. Altitude angle goes from 0° at sunrise through a maximum value at solar noon and again to 0° at sunset. Negative altitude angle indicates that sun is below the horizon. The negative altitude angles are used in defining on twilights which indicate the time period between complete darkness to sunrise in the morning and sunset to complete darkness in evening. Morning twilight is defined as the time period between altitude angle of -18° to 0° in morning and evening twilight is defined as altitude angle of 0° to -18° in evening. Twilights are again dived into tree periods as civil twilight (altitude angle -6° to 0°), nautical twilight (altitude angle -12° to -6°) and astronomical twilight (altitude angle -18° to -12°). The altitude angle and zenith angle are complementary by its definition. Therefore, altitude angle could be expressed as Equation 2.4,

$$\theta_z + \alpha = \frac{\pi}{2} \qquad 2.4$$

Solar azimuth angle γ is the angle on the tangential plane between the direction of due south and the projection of the solar rays on the plane. Eastwards values of azimuth are considered as negative as convention. Figure 2.6 shows the definition of zenith angle, altitude angle and solar azimuth angle with reference to the tangential plane.

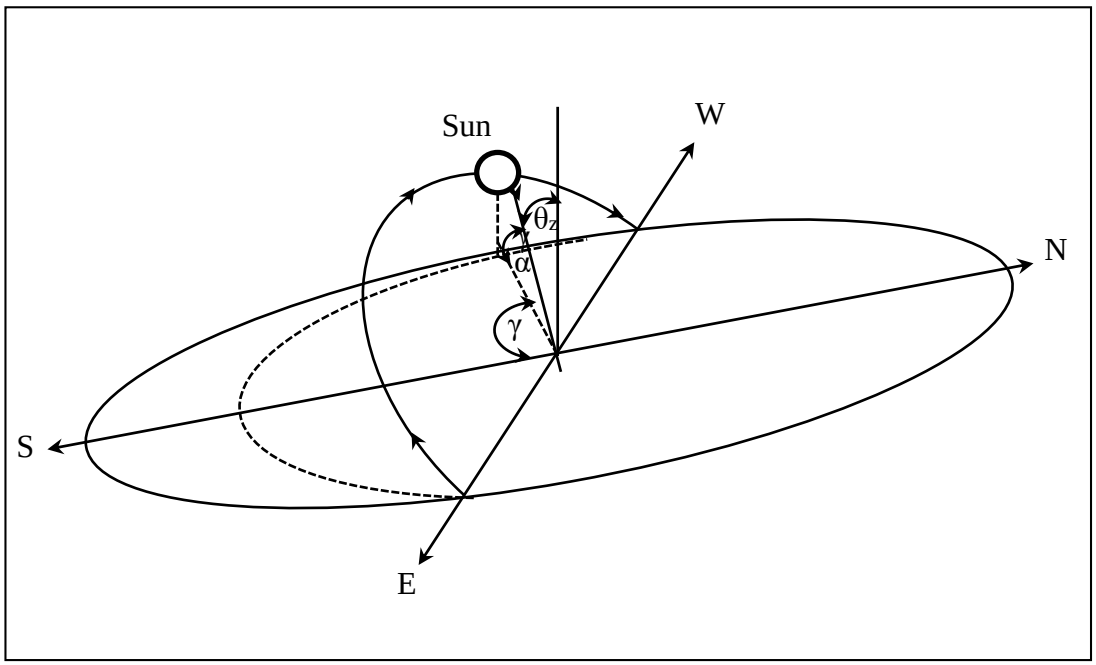

Figure 2.6 - Basic Solar angles on tangential plane

Zenith angle, altitude angle and solar azimuth angle are varies with the time and location of the earth surface. The zenith angle could be calculated using Equation 2.5 and altitude angle can be calculated using Equation 2.6 for a given solar time and location.

$$\cos\theta_z = \cos\delta\cos\omega\cos L + \sin\delta\sin L \qquad 2.5$$

$$\sin\alpha = \cos\delta\cos\omega\cos L + \sin\delta\sin L \qquad 2.6$$

Solar azimuth angle could be calculated using Equation 2.7 for a given solar time and location.

$$\sin\gamma = \frac{\cos\delta\sin\omega}{\cos\alpha} \qquad 2.7$$

for $\cos\omega > \frac{\tan\delta}{\tan L}$

If not, the sun is behind the east-west line and azimuth angle is $-\pi+|\gamma|$ for the morning hours and $\pi-\gamma$ for evening hours.

Value of the altitude angle is zero at the sunshine and sunset. Therefore, hour angle at sunshine and sunset known as sunshine/sunset angle ω_s could be calculated Equating altitude angle to zero of Equations 2.5 and 2.6.

$$\cos\omega_s = -\tan\delta\tan L \qquad 2.8$$

Day length is the duration from sunshine to sunset. So that day length could be expressed using Equation 2.9.

$$\text{Day length} = \frac{2}{15}\cos^{-1}(-\tan\delta\tan\mathrm{L}) \qquad 2.9$$

The incident angle θ is defined as the angle measured on the tilted surface between the solar rays and the normal to the tilted surface. For the tilted surfaces, tilt angle β is defined as angle of the surface to the tangential plane of location and surface azimuth angle γ_p is defined as angle measured on the tangential plane between the projection of normal to surface and due south. Figure 2.7 illustrates the incident angle, surface azimuth angle and tilt angle in the zenith system.

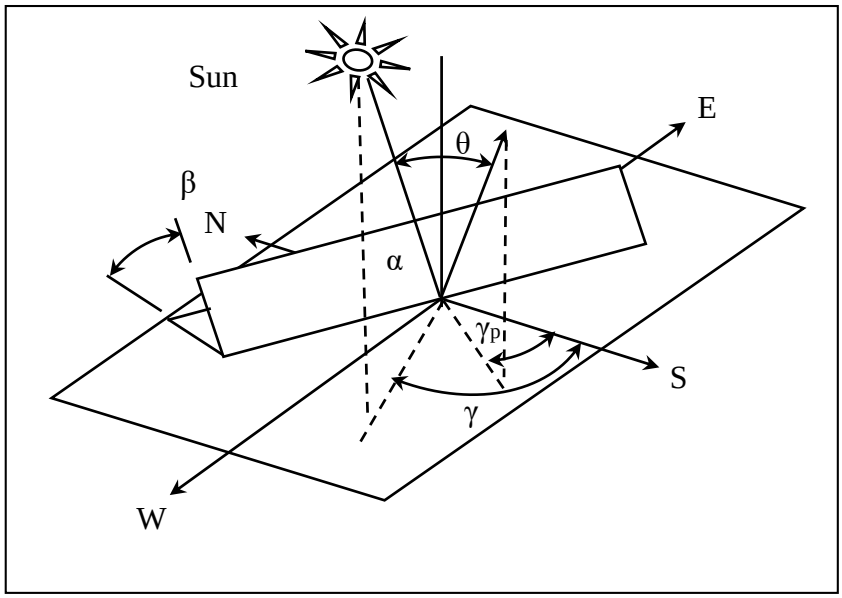

Figure 2.7 - Basic Solar angles on tilted plane

Incident angle could be calculated using Equation 2.10

$$\begin{aligned}\cos\theta = {} & \sin\mathrm{L}\sin\delta\cos\beta - \cos\mathrm{L}\sin\delta\sin\beta\cos\gamma_p \\ & + \cos\mathrm{L}\cos\delta\cos\omega\cos\beta + \sin\mathrm{L}\cos\delta\cos\omega\sin\beta\cos\gamma_p \\ & + \cos\delta\sin\omega\sin\beta\sin\gamma_p\end{aligned} \qquad 2.10$$

Similar to the sunrise/sunset angle on horizontal surface sunrise/sunset angle on tilted surface ω_{ss} could be expressed using Equation 2.11

$$\omega_{ss} = \min\{\omega_s, \cos^{-1}[-\tan(\mathrm{L}-\beta)\tan\delta]\} \qquad 2.11$$

2.2.3 Angles for tracking surfaces

Some solar collector systems track the sun by different ways to minimize the angle of incidence thus to maximise the energy intensity of the collector. The tracking systems are classified according their movement as single axis and two axes. Single axis tracking systems are classified as East-West axis tracking, North-South axis tracking or parallel to the earth's axis. Various types of tracking systems are shown in Figure 2.8.

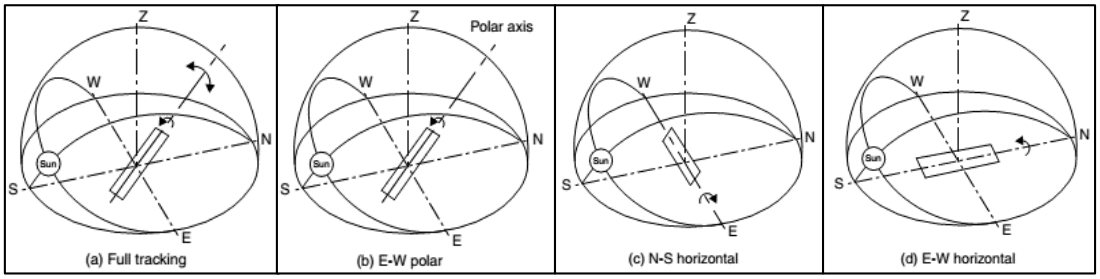

Figure 2.8 - Various tracking surfaces

(Source: Soteris, 2009)

Full tracking

In two axes tracking surface is kept to face the sun all time. Therefore, incident angle is always zero for the two axis tracking systems. Tilt angle is always equal to the solar zenith angle and surface azimuth angle is equal to the solar azimuth angle.

Therefore, Equations 2.12 to 2.14 are applicable to two axis tracking systems.

$$\cos\theta = 0 \qquad 2.12$$

$$\beta = \theta_z \qquad 2.13$$

$$\gamma = \gamma_p \qquad 2.14$$

Tilted North-South axis tracking with daily adjusted tilt angle

For a surface moved about north-south axis with a single daily adjusted tilt angle i.e. plane is normal to direction of propagation at solar noon, incident angle could be expressed using Meinel and Meinel (1976) relationship given in Equation 2.15

$$\cos\theta = \sin^2\delta + \cos^2\delta\cos\omega \qquad 2.15$$

Tilt angle of this type of surface is fixed for each day and could be calculated using Equation 2.16.

$$\beta = |L - \delta| \qquad 2.16$$

Surface azimuth angle of this type of tracking surface for day will be 0° or 180° as given in Equation 2.17.

$$\gamma_p = \begin{cases} 0° & \text{if } (L - \delta) > 0 \\ 180° & \text{otherwise} \end{cases} \quad 2.17$$

Polar north-south axis with east-west axis tracking

Incident angle for the surface that tracks the sun continuously about an axis parallel to the earth's axis of rotation (polar axis) is given in Equation 2.18

$$\cos\theta = \cos\delta \quad 2.18$$

Tilt angle of this surface varies continually and can be calculated using Equation 2.19 and surface azimuth angle can be calculated using Equation 2.20.

$$\tan\beta = \frac{\tan L}{\cos\gamma_p} \quad 2.19$$

$$\gamma_p = \tan^{-1}\left(\frac{\sin\theta_z \sin\gamma}{\cos\theta' \sin L}\right) + 180C_1C_2 \quad 2.20$$

Where,

$$\cos\theta' = \cos\theta_z \cos L + \sin\theta_z \sin L \cos\gamma \quad 2.21$$

$$C_1 = \begin{cases} 0 & \text{if } \left(\tan^{-1}\frac{\sin\theta_z \sin\gamma}{\cos\theta' \sin L}\right)\gamma \geq 0 \\ +1 & \text{otherwise} \end{cases} \quad 2.22$$

$$C_2 = \begin{cases} +1 & \text{if } \gamma \geq 0 \\ -1 & \text{otherwise} \end{cases} \quad 2.23$$

Horizontal east-west axis with north-south axis tracking

Incident angle for the surface that tracks the sun continuously about horizontal east-west axis can be calculated using Kreith and Kreider (1978) relationship given in Equation 2.24.

$$\cos\theta = (1 - \cos^2\delta\sin^2\omega)^{1/2} \quad 2.24$$

Tilt angle of this kind of tracking surface is given by Equation 2.25.

$$\tan\beta = \tan\theta_z |\cos\gamma| \quad 2.25$$

Surface azimuth angle of this type of tracking surface for day will be 0° or 180° as given in Equation 2.26.

$$\gamma_p = \begin{cases} 0° & \text{if } |\gamma| < 90 \\ 180° & \text{otherwise} \end{cases} \quad 2.26$$

Horizontal north-south axis with east-west axis tracking

Incident angle for the surface that tracks the sun continuously about horizontal north south axis could be calculated using Kreith and Kreider (1978) relationship as given in Equation 2.27.

$$\cos\theta = (\cos^2\theta_z + \cos^2\delta\sin^2\omega)^{1/2} \quad 2.27$$

Tilt angle of this kind of tracking surface is given by Equation 2.28.

$$\tan\beta = \tan\theta_z \left|\cos(\gamma_p - \gamma)\right| \quad 2.28$$

Surface azimuth angle of this type of tracking surface for day will be 90° or -90° as given in Equation 2.29.

$$\gamma_p = \begin{cases} 90° & \text{if } \gamma > 0 \\ -90° & \text{otherwise} \end{cases} \quad 2.29$$

2.3 Reckoning of time

In solar time, the time Sun crosses the meridian of the observer is considered as solar noon. Solar energy calculations are based on this solar time and normally it is known as Apparent Solar Time (AST). This AST usually does not match with the Local Standard Time (LST). The orbital velocity of the Erath's is varying around the year and does not uniform. Therefore, AST is slightly varying with compared to the uniformly running clock. This variation of the AST is known as Equation of Time (ET) and it is arising due to variation of the length of the day around the year against mean length of 24 hours. The ET in minute could be calculated using Equation 2.30.

$$ET = 9.87\sin(2B) - 7.53\cos(B) - 1.5\sin(B) \quad 2.30$$

Where,

$$B = (n - 81)\frac{360}{364} \quad 2.31$$

The LST of an Earth's point is based on the centre meridian of the observer's time zone. Therefore, difference between observer's actual longitude and meridian of the time zone should be considered when calculating the AST. The AST could be calculated using Equation 2.32 for a given location.

$$AST = LST + ET + 4(SL - LL) - DS \quad 2.32$$

Where,

SL : Standard Longitude

LL : Local Longitude

DS : Daylight Saving

2.4 Extra-terrestrial and Terrestrial Solar Radiation

2.4.1 Definitions

Beam (direct) Radiation

The solar radiation received to any point, without having been scattered or reflected by the atmosphere is known as beam radiation or direct radiation.

Diffuse (sky) radiation

The solar radiation received to any point, after scattered by the atmosphere is known as diffuse or sky radiation.

Ground Reflected radiation

The solar radiation received to any point, after reflection by the ground surface or nearby mountains, buildings etc. is known as ground reflected radiation.

Global (total) radiation

The sum of the beam, beam and ground reflected radiation is known as global or total radiation.

Irradiance

The rate of the radiant energy incident on a unit area of a surface is known as Irradiance. The symbol G is used for solar irradiance and measured by W/m^2.

Irradiation/Radiant Exposure

The amount of incident radiant energy per unit surface over the specified time period is known as Irradiance or radiant exposure.

Insolation

Usually solar irradiance is known as Insolation. The symbol I is used for an hour and H is used for a day. In addition to that symbol $\overline{H}$ is used for monthly averaged daily insolation values.

In conjunction with above symbols G, H,$\overline{H}$ and I subscripts o, b, d, g, n, t are used. Subscript o is used for the extra-terrestrial radiation. Subscripts b, d, g, are used for beam (direct), diffuse (sky) and ground reflected radiation respectively. Subscripts n

and t are used for radiation on plane normal to direction of propagation and radiation on tilted planes. If neither t nor n specified it implies that terms are for the horizontal surface.

2.4.2 Extra-terrestrial solar radiation

The solar radiation at the entrance to the earth's atmosphere, i.e. outside the earth atmosphere is known as extra-terrestrial solar radiation. The intensity of extra-terrestrial radiation is varying throughout the year due to variation of sun earth distance. The extra-terrestrial radiation at a plane normal to the solar rays at mean sun earth distance is known as Solar Constant G_{sc} and value is adapted to 1367 W/m^2. Spencer (1971) introduced mathematical equation to calculate Intensity of the extra-terrestrial radiation G_{on} on a plane normal to the soar rays on the nth day of the year using solar constant which is expressed in Equation is 2.33.

$$G_{on} = G_{sc}\left[1 + 0.033\cos\left(\frac{360n}{365}\right)\right] \quad 2.33$$

Extra-terrestrial radiation on given day could be calculated with reasonable accuracy using Equation 2.33. More accurate equation introduced by Iqbal (1983) is given by the Equation 2.34.

$$G_{on} = G_{sc}\,(1.000110 + 0.034221\cos\Gamma + 0.001280\sin\Gamma + 0.000719\cos 2\Gamma + 0.000077\sin 2\Gamma) \quad 2.34$$

Where,

Γ : day angle given by equation 2.3

However, in most engineering calculations Equation 2.33 is used to calculate the extra-terrestrial radiation in a given day.

The extra-terrestrial radiation on horizontal surface G_o (plane parallel to the earth surface) could be calculated using extra-terrestrial normal radiation G_{on} and zenith angle θ_z which is expressed in Equations 2.35.

$$G_o = G_{on}\cos\theta_z \quad 2.35$$

G_o could be expressed using equations 2.5, 2.33 and 2.35 as Equation 2.36.

$$G_o = G_{sc}\left[1 + 0.033\cos\left(\frac{360n}{365}\right)\right](\cos\delta\cos\omega\cos L + \sin\delta\sin L) \quad 2.36$$

Extra-terrestrial insolation values could be fined by integration equation 2.36 over the period of time which is expressed in equation 2.37.

$$\int_{\omega_1}^{\omega_2} G_o = \int_{\omega_1}^{\omega_2} G_{sc}\left[1 + 0.033\cos\left(\frac{360n}{365}\right)\right](\cos\delta\cos\omega\cos L + \sin\delta\sin L)\ d\omega \quad 2.37$$

Result is given in equation 2.35.

$$I_o = \frac{12 \times 3600 \times G_{sc}}{\pi}\left[1 + 0.033\cos\left(\frac{360n}{365}\right)\right] \times \left[\cos L\cos\delta\,(\sin\omega_2 - \sin\omega_1) + \frac{\pi(\omega_2 - \omega_1)}{180}\sin L\sin\delta\right] \quad 2.38$$

Daily extra-terrestrial insolation values could be obtained by substitution of sunshine angle and sunset angle to equation 2.38. Resulting equation is given in 2.39

$$H_o = \frac{24 \times 3600 \times G_{sc}}{\pi}\left[1 + 0.033\cos\left(\frac{360n}{365}\right)\right] \times \left[\cos L\cos\delta\sin\omega_s + \left(\frac{\pi\omega_s}{180}\right)\sin L\sin\delta\right] \quad 2.39$$

Monthly averaged daily extra-terrestrial values $\overline{H_o}$ could be calculated using mean day of each month. Recommended mean dates of each month which are given in Table 2.1.

Table 2.1 - Day number and recommended average day for each month

Month	Day number	Average day of the month		
		Date	Julian day of the year n	Declination angle δ (°)
January	i	17	17	-20.92
February	31 +i	16	47	-12.95
March	59 +i	16	75	-2.42
April	90 +i	15	105	9.41
May	120 +i	15	135	18.79
June	151 +i	11	162	23.09
July	181 +i	17	198	21.18
August	212 +i	16	228	13.45
September	243 +i	15	258	2.22
October	273 +i	15	288	-9.60
November	304 +i	14	318	-18.91
December	334 +i	10	344	-23.05

2.4.3 Earth's Atmosphere

The atmosphere of the Earth is an envelope of several air layers containing various gaseous, dust, liquid and solid particulate matter and clouds covering entire surface of earth. The earth's atmosphere extends about 9600 km from the earth surface and these gaseous layers are attracted to earth due to gravitational force of earth. The structure of atmosphere consists with five main layers and four transition layers in between. The density of the atmosphere rapidly decreases with altitude and temperature varies according to the layer. Figure 2.9 (a) describes the various layers of the earth's atmosphere and Figure 2.9 (b) shows the temperature profile of the atmosphere.

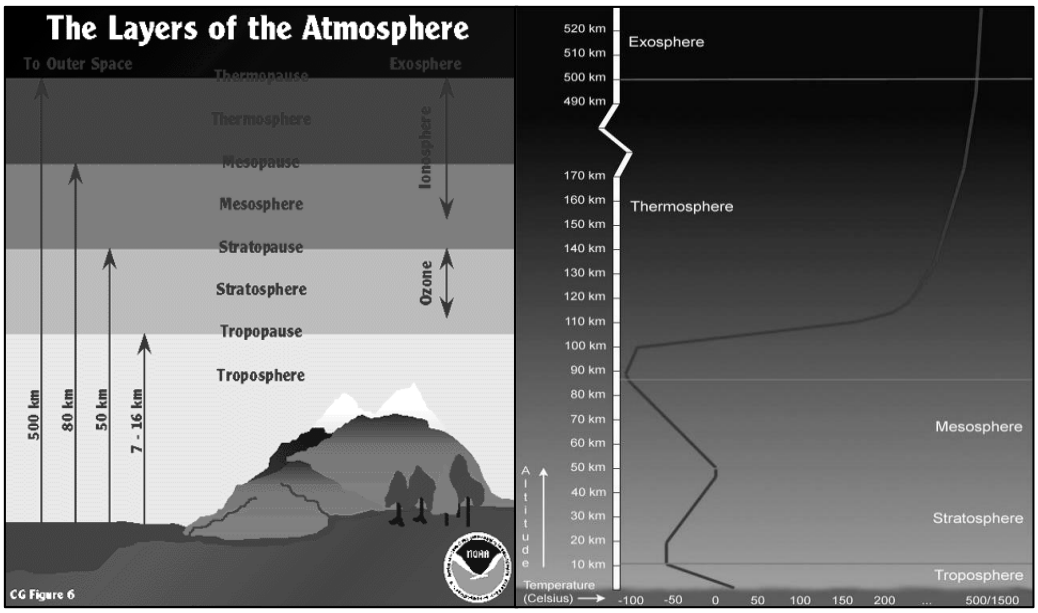

a. Source: Team ESRL Web, 2008) b. (Source: "Layers of Earth's Atmosphere", n.d.)

Figure 2.9 - Layers and Temperature profile of the earth's atmosphere

The troposphere is the lowest layer of the atmosphere and its thickness varies with the latitude and season. The troposphere begins at the earth's surface and extends up to 17 km at equator and 7 km at poles. Temperature decreases within the troposphere with altitude at 6.5 °C gradient for 1 km altitude. The troposphere contains most of the water vapour and wind motion which influence significantly weather occurrences. The tropopause is the transition layer between the troposphere and stratosphere. Temperature of the thin tropopause layer remain constant with the altitude and it act as the upper limit of weather occurrences. The stratosphere extends up to 48 km from the tropopause and temperature keep constant at lower part. Temperature increases with altitude in upper part of the stratosphere, finally reaches up to 7 °C at the top the

stratosphere. The atmospheric ozone layer is concentrated between 19 km and 30 km in the stratosphere. The stratopause is a thin transition layer between stratosphere and mesosphere. The mesosphere extends up to 80 km from stratopause and temperature decrease with altitude within the mesosphere finally reduces to -100 °C. Radio waves reflected concentrated electron layer (Dlayer) could be found at 70 km altitude. Mesopause is the transition layer between mesosphere and thermosphere. Thermosphere extends up to 500-1000 km altitude depend on location session from mesopause. Temperature remains constant in this layer up to 90 km and then increases with altitude finally reach up to 1800 °C. The ionosphere is located within the thermosphere. Thermopause is the transition layer between thermosphere and exosphere. Exosphere is the upper most layer of the earth's atmosphere and it gradually fades to space with altitude. The average pressure and temperature at mean sea level are 101325 Pa and 15 °C respectively. Total atmospheric mass is about 5.148×10^{18} and density at mean sea level is 1.2 kg/m^3.

2.4.4 Atmospheric attenuation

The atmospheric attenuation of solar radiation occurs due to scattering and absorption from gas molecules and other substances contain in the earth's atmosphere. Solar radiation that passed through earth's atmosphere undergoes some degree of absorption by gasses, water vapour and other substances particles. There are two mechanism of absorption. One type occurs due to absorption by electrons in molecules which caused narrow absorption lines. Other type occurs due to rotational-vibrations transition of molecules which caused broad absorption band.

Absorption phenomena depend on the wave length λ of the solar rays. Gasses in ionosphere like nitrogen (N_2) and oxygen (O_2) absorbs most amounts of x-rays and ultraviolet radiation contain in solar rays. Ozone (O_3) and water vapour (H_2O) absorbs ultraviolet ($\lambda < 0.40$ μm) radiations and infrared radiations ($\lambda > 2.3$ μm). In addition to that there is complete absorption of radiation below 0.29 μm wave lengths. Therefore, solar radiation received at earth's surface is almost between 0.29 μm and 2.3 μm. Figure 2.10 (a) shows the total atmospheric absorption at sea level and figure 2.10 (b) describes absorption from different type of gas molecules.

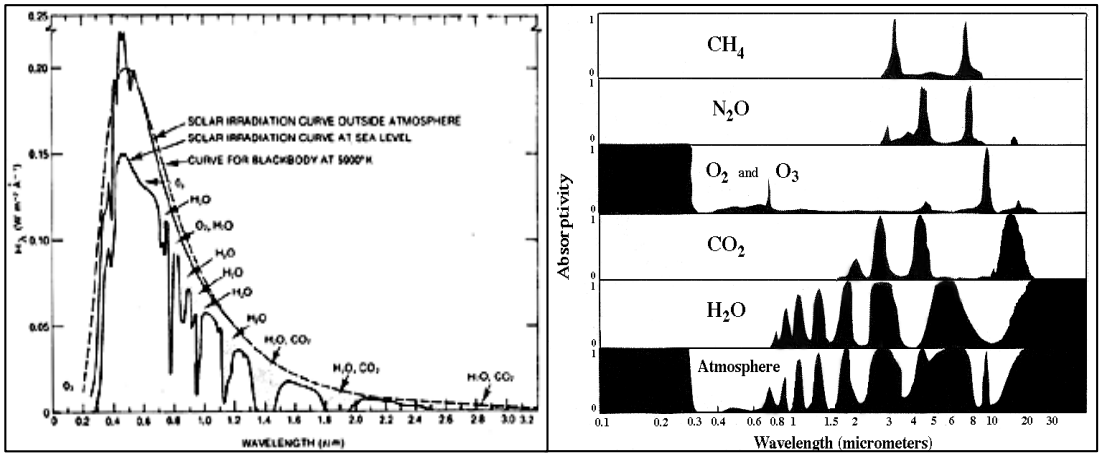

a. (Source: "Geo Appendix A", n.d.) b. (Source: "ATMS 101 Summer 2003", n.d.)

Figure 2.10 - Total atmospheric absorption at sea level

Redirection of solar rays from its original direction of propagation due to interactions with molecules and substance particles is known as solar radiation scattering. The atmospheric scattering phenomenon is a function of wave length λ of the solar rays and size of the interactive particles. Redistribution pattern of the incident solar radiation depends on the ratio between particle size and wave length. The scattering pattern is symmetrical along the propagation axis when particle is isotropic. Small particles compared to the wave length scatter almost equal to both forward and backward directions and forward direction percentage increases with the increasing of particle size compared to the wave length. Size of the scattering particle is expressed as non-dimensional parameter x shown in Equation 2.40.

$$x = \frac{2\pi r}{\lambda} \qquad 2.40$$

Where,

r : radius of the particle

λ : wave length

Scattering from the relatively smaller scatters ($x << 1$) is equally distributed in both forward and backward directions and phenomena is known as Rayleigh scattering. In Rayleigh scattering, scattered intensity is inversely proportional to the fourth power of wave length. Smaller particles cause scattering than larger particles do. The total scattered intensity of un-polarised solar radiation could be calculated using Equation 2.41.

$$G = \frac{G_o}{R^2}\alpha^2\left(\frac{2\pi}{\lambda}\right)^4 \frac{1+\cos^2\theta}{2} \qquad 2.41$$

Where,

G : Total scattered intensity of un-polarised solar radiation incident on a molecule in the direction θ

G_o : Incident intensity

α : Polarisability of the particle

R : Distance between the molecule and the point of observation

λ : Wave length of the incident radiation

A larger portion of the solar energy belonging to visible spectrum blue colour is highly scattered according to the theory of Rayleigh scattering. This higher scattering of blue light is caused to appear sky as blue when viewed from distance. For relatively larger particles, more energy is scattered in forward direction and phenomena is known as mie scattering. Mie scattering intensity is inversely proportional to the λ^4 to λ^0 depending upon the size of particles. Distribution pattern of both Rayleigh and Mie scattering are shown in Figure 2.11 (a) and relationship between the particle size and wavelength is shown in Figure 2.11 (b).

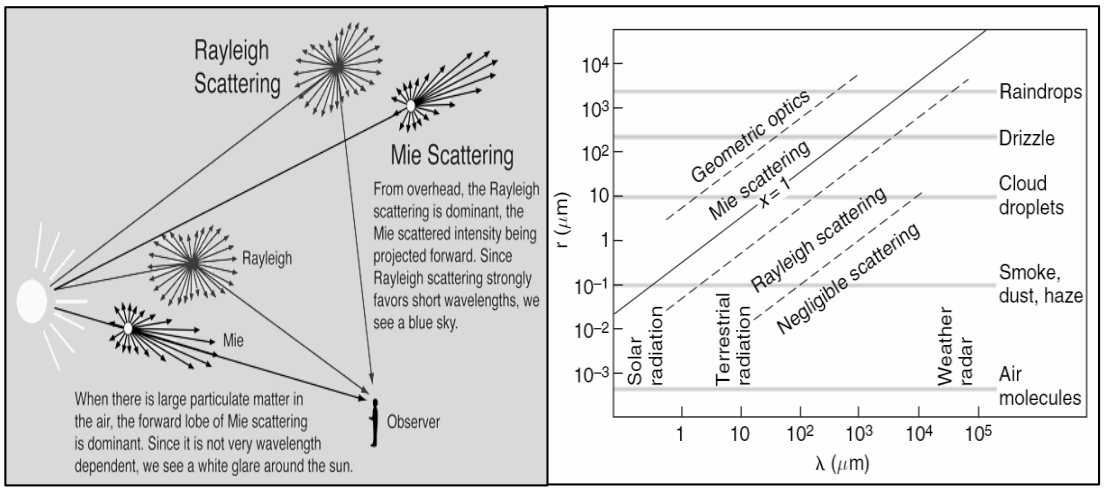

a. (Source: "Blue Sky", 2014) b. (Source: "Geo Appendix A", n.d.)

Figure 2.11 - Rayleigh and Mie Scattering

In both Rayleigh and Mie scattering, scattered radiation has same wave length as incident wave length and that type of scattering is known as elastic scatter. Almost half of the scattered radiation is emitted back to the space and other part is directed to earth's surface from all around the sky. Scattering of radiation due to dust particles and

water vapour varies location to location. Part of the received solar energy is absorbed by the atmosphere while another part is scattered and remaining part is received to earth's surface as beam radiation. Therefore, earth's surface receives two components of radiation as beam radiation and diffuse radiation. Part of the received radiation reflects back to the atmospheric by earth's surface. In the cloudy atmosphere, clouds also reflect part of the radiation back to the space. Fraction sum of these reflected parts to space and total scattered radiation to space is known as albedo of the earth. Earths atmospheric albedo could be considered as 0.3 when consider earth as a whole.

Thickness of the atmosphere which solar radiation passes through is another important parameter in the attenuation. Ratio between the vertical path and optical path length is known as Air mass m_h. Equation 2.42 could be used to calculate Air mass m_h using zenith angle θ_z.

$$m_h = \frac{1}{\cos\theta_z} \tag{2.42}$$

Equation 2.39 is reasonably accurate up to 70° zenith angles. Kasten and Young (1989) introduced more accurate model to predict air mass towards horizon. Equation 2.43 is the model introduced by Kasten and Young.

$$m_h = \frac{1}{\cos\theta_z + 0.50572(96.07995 - \theta_z)^{-1.6364}} \tag{2.43}$$

Diminution of solar radiation intensity within the solar radiation could be explained using Bouger's law. Bouger's law assumes the attenuation is proportional to the local intensity of transferring media. Equation 2.44 represents the bouger's law mathematically.

$$-dG_\lambda = G_\lambda(x)K_\lambda dx \tag{2.44}$$

Where,

$G_\lambda(x)$: monochromatic intensity

K_λ : monochromatic extinction co-efficient of the medium

Equation 2.38 could be integrated to find out intensity G_λ (L) after traveling through L in the medium and results is expressed in Equation 2.45

$$G_\lambda(L) = G_{\lambda,o}e^{-K_\lambda L} \tag{2.45}$$

Where,

$G_{\lambda,0}$: monochromatic intensity at x = 0

Monochromatic transmittance τ_λ is defined as ratio of the intensities after traveling though the medium and before entering the medium. The mathematical expression is given by Equation 2.46.

$$\tau_\lambda = \frac{G_\lambda(L)}{G_{\lambda,o}} = e^{-K_\lambda L} \quad 2.46$$

The extinction coefficient K_λ is a property of the atmosphere and depends on the absorption, emission, scattering and diffraction of the molecules and substances particles of the medium.

2.4.5 Terrestrial Solar Radiation

Solar radiation received on earth's surface is known as terrestrial irradiance. The term irradiance refers to process that surface is radiated by any radiant body. The solar radiation received by earth's surface could be divided into three main components called beam (direct) radiation, diffuse radiation and ground reflection component. Solar radiation received from the sun without having been scattered by the earth's atmosphere is known as beam radiation or direct radiation. The radiation received by the earth's surface whose direction has been changed by the reflection and scattering from the atmosphere is known as diffuse radiation. Terms sky radiation, skylight and diffuse skylight also refers to the diffuse radiation. The radiation received at a particular point resulting due to ground reflection is called as ground reflection radiation. Total radiation received at a particular point is known as global radiation or total radiation. The beam radiation received on a plane normal to the beam solar rays is known as beam normal radiation G_{bn}. The beam radiation received on horizontal plane is known as beam horizontal radiation G_b and could be expressed using Equation 2.47.

$$G_b = G_{bn} \cos\theta_z \quad 2.47$$

The diffuse radiation on horizontal plane is known as diffuse horizontal radiation G_d. The ground reflected component on horizontal plane is known as ground reflected horizontal radiation G_g. and could be assumed as negligible for most of the cases. The

total radiation on horizontal surface is known as global horizontal radiation G and mathematical expression is given in Equation 2.48.

$$G = G_b + G_d + G_g \quad 2.48$$

The ground reflected component on horizontal plane could be assumed as negligible for most of the cases. Therefore, equation 2.45 is reduced to Equation 2.49.

$$G = G_b + G_d \quad 2.49$$

When the beam solar radiation is considered in solar insolation terms in hourly, daily and monthly averaged daily irradiance equation 2.49 could be written as Equations shown in 2.50, 2.51 and 2.52 respectively.

$$I = I_b + I_d \quad 2.50$$

$$H = H_b + H_d \quad 2.51$$

$$\overline{H} = \overline{H_b} + \overline{H_d} \quad 2.52$$

2.4.6 Solar radiation on the tilted surface

Usually in most solar energy applications such as solar Photovoltaic panels and thermal collectors are not installed horizontally. Most of the net metering solar photovoltaic panels are mounted on existing roofs, hence mounting angle is equal to roof angle. Also amount of captured solar energy could be increased significantly using optimum mounting angles for the applications. Therefore, evaluation of solar radiation on tilted surface is also important. The beam radiation received on tilted plane is known as beam radiation on tilted surface G_{bt} and could be expressed using Equation 2.53.

$$G_{bt} = G_{bn} \cos\theta \quad 2.53$$

For horizontal surfaces Equation 2.53 reduce to Equation 2.47

It follows that,

$$r_b = \frac{G_{bt}}{G_b} = \frac{\cos\theta}{\cos\theta_z} \quad 2.54$$

The ratio r_b is called the beam radiation tilt factor. The original relationship for the beam radiation tilt factor is introduced by Hottel and Woertz in 1942 for the hourly periods based on midpoint of the hour. So the beam radiation component for any surface can be written as Equation 2.55.

$$G_{bt} = G_b r_b \quad 2.55$$

When the beam solar radiation is considered in solar insolation terms, it could be written as Equation 2.56.

$$H_{bt} = H_b R_b \tag{2.56}$$

The ratio R_b is known as daily beam radiation tilt factor and it could be evaluated by integrating Equation 2.54 over the periods of sun rise to sun set for horizontal and tilt surfaces.

$$R_b = \frac{\int_{\omega_{sr}}^{\omega_{ss}} \cos\theta}{\int_{\omega_{-s}}^{\omega_s} \cos\theta_z} \tag{2.57}$$

The resulting equation for the equator facing surface in northern hemisphere is given by Equation 2.58.

$$R_b = \frac{H_{bt}}{H_b} = \frac{\cos(L-\beta)\cos\delta\sin\omega_{ss} + \frac{\pi}{180}\omega_{ss}\sin(L-\beta)\sin\delta}{\cos L\cos\delta\sin\omega_s + \frac{\pi}{180}\omega_s\sin L\sin\delta} \tag{2.58}$$

The same equation could be applied to the averaged beam radiation tilt factor, so that Equation 2.59 can be written as follows,

$$\overline{R_b} = \frac{\overline{H_{bt}}}{\overline{H_b}} = \frac{\cos(L-\beta)\cos\delta\sin\omega_{ss} + \frac{\pi}{180}\omega_{ss}\sin(L-\beta)\sin\delta}{\cos L\cos\delta\sin\omega_s + \frac{\pi}{180}\omega_s\sin L\sin\delta} \tag{2.59}$$

The diffuse radiation on tilted plane is known as diffuse radiation on tilted surface G_{dt}. The ground reflected component of on tilted surface is known as ground reflected radiation on tilted surface G_{gt}. The total radiation on tilted surface is known as global radiation on tilted surface G_t and mathematical expression is given in Equation 2.60.

$$G_t = G_{bt} + G_{dt} + G_{gt} \tag{2.60}$$

When the beam solar radiation is considered in solar insolation terms in hourly, daily and monthly averaged daily irradiance equation 2.60 could be written as equations 2.61, 2.62 and 2.63 respectively.

$$I_t = I_{bt} + I_{dt} + I_{gt} \tag{2.61}$$

$$H_t = H_{bt} + H_{dt} + H_{gt} \tag{2.62}$$

$$\overline{H_t} = \overline{H_{bt}} + \overline{H_{dt}} + \overline{H_{gt}} \tag{2.63}$$

These components of radiation are shown in Figure 2.12.

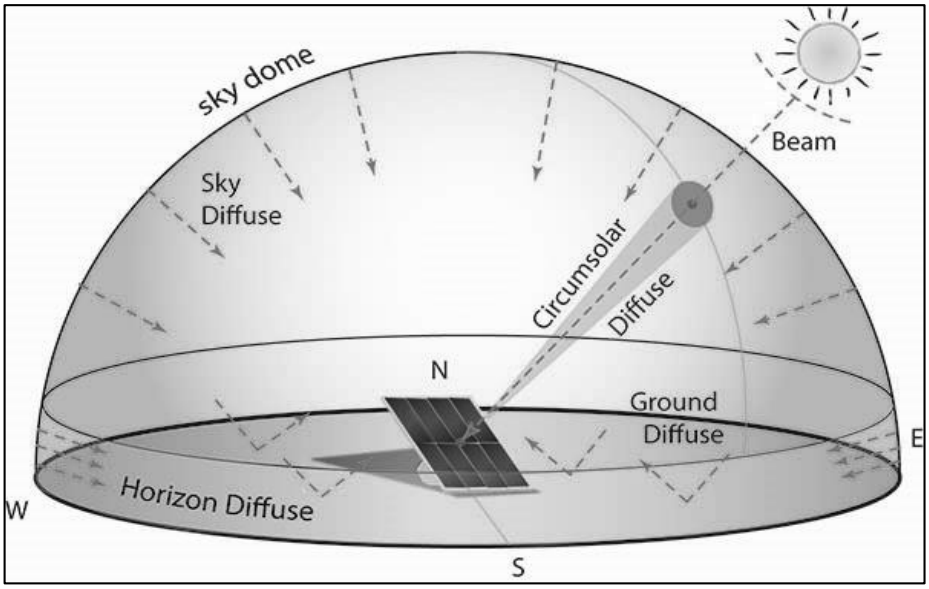

Figure 2.12 - Beam, diffuse and ground reflected solar radiation

(Source: "Empirical Correlation for Estimating Components of Light", n.d.)

2.5 Measuring of Solar Radiation

Accurate data of solar radiation is required in solar energy applications design, sizing, performance evaluations and solar energy researches. Mainly these data include global solar radiation, beam radiation, diffuse radiation and sunshine hours. Various type of equipment are available to measure instantaneous values and long term integrated values. Usually these equipment use thermoelectric and photovoltaic effects to measure solar radiation parameters. Mainly there are two types of solar radiation measuring instruments called pyranometers and pyrheliometers.

2.5.1 Pyranometers

The pyranometer is used to measure global (total) radiation within hemispherical field of horizontal view. Sensor of the pyranometer absorbs solar radiation from whole sky dome and transformed it to heat energy. Global solar radiation could be evaluated by measuring this heat energy. There are two types of pyranometers available in the field. Most widely used type is thermopile type pyranometers which use principles of the thermo couple. Other type is bimetallic pyranometers which use thermal expansion properties of metal strips. The pyranometers could be used to measure the diffuse solar radiation if the sensing element is shaded for the beam (direct) radiation. For this purpose, shading devise should be mounted with tracking system to shade the sensor

all over the time. Shading device also hide the considerable amount of diffuse radiation from the sensor. Therefore, corrections are required for the shading device.

2.5.2 Pyrheliometers

The pyrheliometer is used to measure beam (direct) solar radiation. The receiving surface of pyrheliometer should be normal to the direction of solar rays for the accurate measurements. Therefore, pyrheliometers usually mounted with a tracking mechanism. Mainly there are three types of pyrheliometers available. The Angstrom electrical compensation pyrheliometer uses effect of thermocouple to measure beam solar radiation. The silver disk pyrheliometer uses mercury bulb thermometer together with silver disk to measure beam solar radiation. Thermoelectric pyrheliometers use thermopile to measure beam solar radiation.

2.5.3 Sunshine recorders

The sunshine duration is an important parameter to estimate solar energy availability during a certain the period. The sunshine duration is defined as the time during which the sunshine is acute enough to cast a shadow. However, World Metrological Organization (WMO) has defined sunshine duration as time during which the beam solar irradiance exceeds the level of 120 W/m^2. Basically two types of sunshine recorders are used, i.e. focusing type and photoelectric type. The focusing type consists with a solid glass sphere mounted concentrically in a section of a spherical bowl. The bowl focuses sunrays into a paper placed in the bowl. The record card burns whenever the bright sunshine is available. The portion of the burn trace is proportional to the sunshine that exists. The photovoltaic sunshine recorders consist of two photovoltaic cells with one cell exposed to the whole sky dome and the other one is covered by shading ring to cover beam radiation. Thus, whenever the bright sunshine is not available, two readings are approximately equal and whenever the bright sunshine is available two readings are considerably different. Thus, difference of the two readings is a measure of a sunshine duration. In addition to above measuring equipment satellite images are also used to predict solar irradiance data.

The metrological department of Sri Lanka measures global solar radiation only at Colombo station (6° 54' N, 79° 51' E at 10 m MSL). In addition to that, metrological

department measures sunshine hours at four weather stations namely Colombo, Nuwara Eliya (6° 50' N, 80° 50' E at 1500 m MSL), Anuradhapura (8° 20' N, 80° 25' E at 25 m MSL) and Hambanthota (6° 10' N, 81° 15' E at 8 m MSL). The SLSEA recently started to measure global solar radiation and diffuse radiation at two stations namely Kilinochchi and Hambanthota. Methods of solar radiation estimation

2.6 Methods of solar radiation estimation

The global solar radiation received by the earth's surface depends on the location and the metrological condition of the location. Therefore, study of solar radiation under local climatic conditions is necessary. Solar radiation can be estimated using empirical models for locations where measured values are not available. Researchers have developed various methods to estimate solar radiation with reasonable accuracy. Basically these methods could be divided into two types as parametric models and decomposition models. Parametric models use detailed metrological data such as cloud cover data, sunshine hours, temperature, relative humidity, precipitation etc. Decomposition models are used to estimate beam and diffuse compunctions using global solar radiation data. Evaluation of long term performance of solar systems is very important rather than looking on instantaneous values. Therefore, models are developed to estimate long term monthly average daily insolation values, where insolation is the total amount of solar radiation received by a given surface in a given time duration.

2.6.1 Parametric Models

Estimation of monthly average daily solar radiation

One of the earliest methods of estimating solar radiation on a horizontal surface was proposed by Angstrom in 1924. Angstrom model was a simple linear model to estimate daily average horizontal radiation using sunshine hours and average clear day horizontal radiation. Equation 2.64 represents the Angstrom 1924 model.

$$\frac{\bar{H}}{\bar{H}_c} = \left(a + b\frac{\bar{S}}{\bar{S}_o}\right) \qquad 2.64$$

Where,

$\bar{H}$: Monthly averaged daily radiation on horizontal surface of terrestrial region

$\overline{H_c}$: Monthly averaged clear day radiation on horizontal surface terrestrial region

$\bar{S}$: Monthly averaged hours of sunshine

$\overline{S_o}$: Monthly averaged maximum possible hours of sunshine

a, b : Location specific constants

The location specific constants referred to as fractions of extra-terrestrial radiation on overcast days and average days respectively. The ratio $\bar{S}/\overline{S_o}$ is known as cloudless index and it explain about atmospheric characteristics and conditions of the location. Basic difficulty of the Angstrom (1924) models is calculating clear day radiation accurately. Prescott modified Angstrom (1924) model in 1940 to overcome the difficultness of calculating the clear day radiation. The modified model replaces the clear day radiation term by extra-terrestrial radiation. This new model is known as Angstrom-Prescott (1940) model and is given in Equation 2.65.

$$\frac{\bar{H}}{\overline{H_o}} = \left(a + b\frac{\bar{S}}{\overline{S_o}}\right) \qquad 2.65$$

Where,

$\bar{H}$: Monthly averaged daily radiation on horizontal surface of terrestrial region

$\overline{H_o}$: Monthly averaged daily radiation on horizontal surface of extra-terrestrial region

$\bar{S}$: Monthly averaged hours of sunshine

$\overline{S_o}$: Monthly averaged maximum possible hours of sunshine

a,b : Location specific constants

Ogelman et al (1984) presented second order model to predict monthly average daily radiation based on sunshine hours which expressed in Equation 2.66.

$$\frac{\bar{H}}{\overline{H_o}} = a + b\left(\frac{\bar{S}}{\overline{S_o}}\right) + c\left(\frac{\bar{S}}{\overline{S_o}}\right)^2 \qquad 2.66$$

Where,

a, b, c : Location specific constants

Samuel (1991) presented third order model to predict monthly average daily radiation based on sunshine hours which is expressed in Equation 2.67.

$$\frac{\overline{H}}{\overline{H_o}} = a + b\left(\frac{\overline{S}}{\overline{S_o}}\right) + c\left(\frac{\overline{S}}{\overline{S_o}}\right)^2 + d\left(\frac{\overline{S}}{\overline{S_o}}\right)^3 \quad 2.67$$

Where,

a, b, c, d : Location specific constants

El-Metwally developed another model for estimating global solar radiation which is expressed in Equation 2.68.

$$\frac{\overline{H}}{\overline{H_o}} = a^{\frac{1}{\left(\frac{\overline{S}}{\overline{S_o}}\right)}} \quad 2.68$$

Where,

a, b, c : Location specific constants

Bakirci (2009) developed the exponential model for global solar radiation prediction which is expressed in Equation 2.69.

$$\frac{\overline{H}}{\overline{H_o}} = a\left(\frac{\overline{S}}{\overline{S_o}}\right)^b \quad 2.69$$

Where,

a, b, : Location specific constants

Sen Z. (2007) introduced another non liner model to estimate monthly average global radiation which is expressed in Equation 2.70.

$$\frac{\overline{H}}{\overline{H_o}} = a + b\left(\frac{\overline{S}}{\overline{S_o}}\right)^c \quad 2.70$$

Where,

a, b, c : Location specific constants

Several other models based on other metrological data have been introduced by various scientists in addition to the above sunshine data based models.

Hargreaves and Samani (1982) developed the relationship given by Equation 2.71.

$$\frac{\overline{H}}{\overline{H_o}} = a(\overline{T_{max}} - \overline{T_{mın}})^{0.5} \quad 2.71$$

Where,

A : Location specific constants

$\overline{T_{max}}$: Monthly averaged daily maximum temperature

$\overline{T_{min}}$: Monthly averaged daily maximum temperature

Bristow and Campbell (1984) established an empirical equation for daily global irradiation using air temperature amplitude given in Equation 2.72.

$$\frac{\overline{H}}{\overline{H_o}} = a\left(1 - e^{-b(\overline{T_{max}} - \overline{T_{min}})^c}\right) \quad 2.72$$

Where,

a, b, c : Location specific constants

Hargreaves and Samani's (2000) introduced another model which is given in Equation 2.73.

$$\frac{\overline{H}}{\overline{H_o}} = [a + b(\overline{T_{max}} - \overline{T_{min}}) + c(\overline{T_{max}} - \overline{T_{min}})^2] \times (\overline{T_{max}} - \overline{T_{min}})^{0.5} \quad 2.73$$

Where,

a, b, c : Location specific constants

Chen et al (2004) introduced another model which is given in Equation 2.74.

$$\frac{\overline{H}}{\overline{H_o}} = a(\overline{T_{max}} - \overline{T_{min}})^{0.5} + b \quad 2.74$$

Where,

a, b, c : Location specific constants

In addition to above models following models are recommended by Duffie and Beckman (1991)

$$\frac{\overline{H}}{\overline{H_o}} = a + b\frac{\overline{S}}{\overline{S_o}} + c\overline{T} \quad 2.75$$

$$\frac{\overline{H}}{\overline{H_o}} = a + b\frac{\overline{S}}{\overline{S_o}} + c\overline{R_h} \quad 2.76$$

$$\frac{\overline{H}}{\overline{H_o}} = a + b\overline{T} + c\overline{R_h} \quad 2.77$$

$$\frac{\overline{H}}{\overline{H_o}} = a + b(\overline{T_{max}} - \overline{T_{min}}) + c\overline{c_\omega} \quad 2.78$$

$$\frac{\overline{H}}{\overline{H_o}} = a + b(\overline{T_{max}} - \overline{T_{min}})^{0.5} + c\overline{c_\omega} \quad 2.79$$

$$\frac{\overline{H}}{\overline{H_o}} = a + b\frac{\overline{S}}{\overline{S_o}} + c\overline{c_\omega} \quad 2.80$$

Where,

$\overline{T}$: Monthly averaged daily temperature

$\overline{R_h}$: Monthly averaged daily relative humidity

$\overline{c_\omega}$: Monthly averaged daily cloud cover index

Same type of correlations set could be used to estimate daily irradiance values.

Estimation of Clear Sky Radiation

The effects of the atmospheric attenuation vary with the time and atmospheric conditions and magnitude of the air mass. Therefore, methods for estimation of clear sky radiation in standard atmospheric conditions are important. Hottel (1976) introduced an Equation given in 2.81 to estimate atmospheric transmission for beam radiation for four climate regions based on zenith angle (altitude angle) and altitude.

$$\tau_b = \frac{G_{bn}}{G_{on}} = a_0 + a_1 e^{(-k \operatorname{cosec} \alpha)} \quad 2.81$$

Where,

$$a_0 = r_{0\times} a_0^* \quad 2.82$$

$$a_1 = r_{1\times} a_1^* \quad 2.83$$

$$k = r_{k\times} k^* \quad 2.84$$

Three correlation factors r_0, r_1, and r_k to allow changes in climate types are given in Table 2.2.

Table 2.2 - Hottlel correlations factors for different climate types

Climate type	r_0	r_1	r_k
Tropical	0.95	0.98	1.02
Mid latitude Summer	0.97	0.99	1.02
Subarctic Summer	0.99	0.99	1.01
Mid latitude winter	1.03	1.01	1.00

Constants a_0, a_1, and k for the standard atmosphere with 23 km visibility are found from a_0^*, a_1^*, and k^* for altitudes less than 2.5 km.

$$a_0^* = 0.4237 - 0.00821(6 - A)^2 \quad 2.85$$

$$a_1^* = 0.5055 + 0.00595(6.5 - A)^2 \quad 2.86$$

$$k^* = 0.2711 + 0.01858(2.5 - A)^2 \quad 2.87$$

Constants a_0, a_1, and k for the standard atmosphere with 5 km visibility are found from a_0^*, a_1^*, and k^* for altitudes less than 2.5 km.

$$a_0^* = 0.2538 - 0.0063(6 - A)^2 \quad 2.88$$

$$a_1^* = 0.7678 + 0.0010(6.5 - A)^2 \quad 2.89$$

$$k^* = 0.249 + 0.081(2.5 - A)^2 \quad 2.90$$

Where,

A : Altitude of the location in kilometres

Using equations 2.47 and 2.81 clear sky horizontal beam radiation cloud be expressed as equation 2.91.

$$G_b = G_{on}\left[a_0 + a_1 e^{(-k\,\mathrm{cosec}\,\alpha)}\right]\cos\theta_z \quad 2.91$$

The clear sky diffuse radiation could be estimated using Liu and Jordan (1960) given in Equation 2.92.

$$G_d = G_{on}\left\{0.2710 - 0.2939\left[a_0 + a_1 e^{(-k\,\mathrm{cosec}\,\alpha)}\right]\right\}\cos\theta_z \quad 2.92$$

American Society of Heating Refrigeration and Air-conditioning Engineers ASHRAE (2001) introduced equations given in 2.93 and 2.94 to predict clear sky beam and diffuse radiation respectively.

$$G_{bn} = Ae^{\left(\frac{-B}{\cos\theta_z}\right)} \quad 2.93$$

$$G_d = CG_{bn} \quad 2.94$$

Where,

A : apparent solar irradiation at zero air mass

B : atmospheric extinction coefficient

C : Diffuse radiation factor

The constants A, B, and C are given in Table 2.3 which is given in ASHRAE (1985) for the twenty first day of each month.

Table 2.3 - ASHRAE (1985) clear sky radiation model coefficients

Month	n	A (W/m^2)	B	C
January	21	1229.4750	0.142	0.058
February	52	1213.7125	0.144	0.060
March	80	1185.3400	0.156	0.071
April	11	1134.9000	0.180	0.097
May	141	1103.3750	0.196	0.121
June	172	1087.6125	0.205	0.134
July	202	1084.4600	0.207	0.136
August	233	1106.5275	0.201	0.122
September	264	1150.6625	0.177	0.092
October	294	1191.6450	0.160	0.073
November	325	1220.0175	0.149	0.063
December	355	1232.6275	0.142	0.057

Various other correlations for clear sky radiations are found in the literature and some of these are given in Equations 2.95 to 2.99

Hourtwitz correlation

$$G = 1098 \cos\theta_z e^{\left(\frac{-0.057}{\cos\theta_z}\right)} \quad 2.95$$

Berger and Duffie correlation

$$G = 1350 \times 0.7 \times \cos\theta_z \quad 2.96$$

Adnot et al correlation

$$G = 951.39\cos^{1.15}\theta_z \quad 2.97$$

Kasten and Czeplak correlation

$$G = 910 \cos\theta_z - 30 \quad 2.98$$

Robledo and Soler correlation

$$G = 1159.24\cos^{1.179}\theta_z - e^{-0.00149\left(\frac{\pi}{2}-\theta_z\right)} \quad 2.99$$

2.6.2 Decomposition Models

When considering the solar engineering applications, it is essential to quantify the beam and diffuse radiation of a particular location of interest. The amount of global insolation on a terrestrial tilted surface is the sum of beam, diffuse and ground reflected insolation as discussed previously. There are some decomposition models available in literature which are capable of estimating diffuse insolation from hourly radiation, daily radiation and monthly average daily global solar radiation. The usual approach

of decomposition models is to correlate diffuse component and global component using clearness index. The clearness index is the ratio between terrestrial radiation and extra-terrestrial radiation. The clearness indices could be defined as hourly clearness index, daily clearness index and monthly average daily clearness index. Hourly clearness index k_T, daily clearness index K_T and monthly average daily clearness index $\overline{K_T}$ are given in Equations 2.100, 2.101 and 2.102 respectively.

$$k_T = \frac{I}{I_o} \tag{2.100}$$

$$K_T = \frac{H}{H_o} \tag{2.101}$$

$$\overline{K_T} = \frac{\bar{H}}{\overline{H_o}} \tag{2.102}$$

Since the clearness index is a direct measurement of cloudiness of the sky, Iqbal (1983) proposed the classification of sky given in Table 2.4 based on the clearness index.

Table 2.4 - Classification of the sky types according to the clearness index

Sky Type	Clearness index
Clear	$0.7 \leq$ clearness index ≤ 0.9
Partly Cloudy	$0.3 \leq$ clearness index ≤ 0.7
Cloudy	$0.0 \leq$ clearness index ≤ 0.3

Decomposition models based on hourly radiation

Liu and Jordan (1960) introduced decomposition model given in Equation 2.103 for hourly radiation using data of 98 Canadian and USA stations.

$$\frac{I_d}{I} = 0.384{k_T}^{-1} - 0.416 \tag{2.103}$$

Orgil and Hollands (1977) introduced decomposition model given in Equation 2.104 for hourly radiation using data of Canadian stations.

$$\frac{I_d}{I} = \begin{cases} 1.0 - 0.249k_T & \text{for } 0 \leq k_T \leq 0.35 \\ 1.557 - 1.84k_T & \text{for } 0.35 < k_T < 0.75 \\ 0.177 & \text{for } k_T > 0.75 \end{cases} \tag{2.104}$$

Bugler (1977) introduced decomposition model given in Equation 2.105 for hourly radiation using data of Australian stations.

$$\frac{I_d}{I} = \begin{cases} 0.94 & for\ 0 \le k_T \le 0.4 \\ \dfrac{1.29 - 1.19k_T}{1.0 - 0.334k_T} & for\ > 0.4 \end{cases} \quad 2.105$$

Erbs et al (1982) introduced decomposition model given in Equation 2.106 using data of US stations and one Australian station.

$$\frac{I_d}{I} = \begin{cases} 1.0 - 0.9k_T & \text{for } 0 \le k_T \le 0 \\ 0.9511 - 0.1604k_T + 4.388{k_T}^2 - 16.638{k_T}^3 + 12.336{k_T}^4 & \text{for } 0.22 < k_T < 0.80 \\ 0.165 & \text{for } k_T > 0.8 \end{cases} \quad 2.106$$

Hawlader (1984) introduced model given in Equation 2.107 using data of Singapore stations.

$$\frac{I_d}{I} = \begin{cases} 0.915 & \text{for } 0 \le k_T \le 0.225 \\ 1.135 - 0.9422k_T - 0.3878{k_T}^2 & \text{for } 0.0.225 < k_T < 0.775 \\ 0.215 & \text{for } k_T > 0.775 \end{cases} \quad 2.107$$

Reindl et al (1990) introduced model given in Equation 2.108 using data of US stations and European stations.

$$\frac{I_d}{I} = \begin{cases} 1.020 - 0.248k_T & \text{for } 0 \le k_T \le 0.30 \\ 1.450 - 1.670k_T & \text{for } 0.30 < k_T < 0.78 \\ 0.147 & \text{for } k_T > 0.78 \end{cases} \quad 2.108$$

Reindl et al (1990) introduced another model in terms of additional parameter solar altitude angle α using the data of same stations which is given in Equation 2.109.

$$\frac{I_d}{I} = \begin{cases} 1.020 - 0.254k_T + 0.0123\sin\alpha & \text{for } 0 \le k_T \le 0.30 \\ 1.400 - 1.749k_T + 0.177\sin\alpha & \text{for } 0.30 < k_T < 0.78 \\ 0.486k_T - 0.182\sin\alpha & \text{for } k_T > 0.78 \end{cases} \quad 2.109$$

Reindl et al (1990) introduced another model in terms of additional parameters solar altitude angle α, Outside temperature T and Relative Humidity R_h using the data of same stations which is given in Equation 2.110.

$$\frac{I_d}{I} = \begin{cases} 1 - 0.232k_T + 0.0239\sin\alpha - 0.000682T + 0.019R_h \\ \text{for } 0 \le k_T \le 0.30 \\ 1.329 - 1.716k_T + 0.267\sin\alpha - 0.00357T + 0.106R_h \\ \text{for } 0.30 < k_T \le 0.78 \\ 0.426k_T + 0.256\sin\alpha - 0.00349T + 0.0734RH \\ \text{for } k_T > 0.78 \end{cases} \quad 2.110$$

Where,

α : solar altitude angle

T : Outside air temperature

R_h : Relative humidity

Chandrasekaran and Kumar (1994) introduced another model using data of Indian stations which is given in Equation 2.111.

$$\frac{I_d}{I} = \begin{cases} 1.0086 - 0.178k_T & \text{for } 0 \le k_T \le 0.24 \\ 0.9686 + 0.1325k_T + 1.4183{k_T}^2 - 10.1862{k_T}^3 + 8.3733{k_T}^4 & \text{for } 0.24 < k_T < 0.80 \\ 0.197 & \text{for } k_T > 0.80 \end{cases} \quad 2.111$$

Lam and Li (1996) introduced another model based on data of Hong Kong stations which is given in Equation 2.112.

$$\frac{I_d}{I} = \begin{cases} 0.977 & \text{for } 0 \le k_T \le 0.1 \\ 1.237 - 1.36k_T & \text{for } 0.15 < k_T < 0.70 \\ 0.273 & \text{for } k_T > 0.70 \end{cases} \quad 2.112$$

Miguel et al (2001) introduced another model based on data of some European stations which is given in Equation 2.113.

$$\frac{I_d}{I} = \begin{cases} 0.995 - 0.081k_T & \text{for } 0 \le k_T \le 0.21 \\ 0.724 + 2.738k_T - 8.32{k_T}^2 + 1.4926{k_T}^3 & \text{for } 0.21 < k_T < 0.76 \\ 0.18 & \text{for } k_T > 0.76 \end{cases} \quad 2.113$$

Boland et al (2001) introduced another model in terms of additional parameter hour angle ω using the data of some Australian stations which is given in Equation 2.114.

$$\frac{I_d}{I} = -0.039 + \frac{1.039}{1 + e^{(-8.769 + 7325k_T + 0.377\omega)}} \quad 2.114$$

Karatasou et al (2003) introduced another model based on data of Athens which is given in Equation 2.115.

$$\frac{I_d}{I} = \begin{cases} 0.9995 - 0.05k_T - 2.4156{k_T}^2 + 1.4926{k_T}^3 & for\ 0 \le k_T \le 0.78 \\ 0.2 & for\ > 0.78 \end{cases} \quad 2.115$$

Soares et al (2004) introduced another model based on data of Sao Paolo which is given in Equation 2.116.

$$\frac{I_d}{I} = \begin{cases} 1 & \text{for } 0 \le k_T \le 0.17 \\ 0.9 + 1.1k_T - 4.5{k_T}^2 + 0.01{k_T}^3 + 3.14{k_T}^4 & \text{for } 0.17 < k_T < 0.75 \\ 0.17 & \text{for } k_T > 0.75 \end{cases} \quad 2.116$$

Zhou et al (2004) introduced another model based on data of 78 Chinese stations which is given in Equation 2.117.

$$\frac{I_d}{I} = \begin{cases} 0.987 & \text{for } 0 \le k_T \le 0.2 \\ 1.292 - 1.447k_T & \text{for } 0.17 < k_T < 0.75 \\ 0.209 & \text{for } k_T > 0.75 \end{cases} \quad 2.117$$

Jacovides et al (2006) introduced another model based on data of Athalassa which is given in Equation 2.118.

$$\frac{I_d}{I} = \begin{cases} 0.987 & \text{for } 0 \le k_T \le 0.1 \\ 0.94 + 0.937k_T - 5.01{k_T}^2 + 3.32{k_T}^3 & \text{for } 0.1 < k_T < 0.8 \\ 0.209 & \text{for } k_T > 0.8 \end{cases} \quad 2.118$$

Boland et al (2008) introduced another model using the data of some Australian stations which is given in Equation 2.116.

$$\frac{I_d}{I} = \frac{1}{1 + e^{(8.6k_T - 5)}} \quad 2.119$$

Ridley et al (2010) introduced another model using the data of some Australian stations which is given in Equation 2.120.

$$\frac{I_d}{I} = \frac{1}{1 + e^{(5.38 + 6.63k_T - 0.007\alpha + 0.006\omega + 1.75K_T + 1.31\psi)}} \quad 2.120$$

Where,

$$\psi = \begin{cases} \frac{k_{T-1} + k_{T+1}}{2} & for\ sunrise < T < sunset \\ k_{T+1} & for\ T = sunrise \\ k_{T-1} & for\ T = sunset \end{cases} \quad 2.121$$

Skartveit and Olesh (1987) estimated beam irradiance fraction from global irradiance using clearness index and solar altitude angle which is given in Equation 2.122.

$$\frac{I_b}{I} = \begin{cases} 0 & \text{for } 0 \le k_T < k_0 \\ \dfrac{(1-d_1)[ak^{0.5} + (1-a)k^2]}{\sin\alpha} & \text{for } k_0 \le k_T \le k_1 \\ \dfrac{1.09(1-\xi)}{k_T \sin\alpha} & \text{for } k_T > k_1 \end{cases} \quad 2.122$$

Where,

$$k_0 = 0.2 \quad 2.123$$

$$k_1 = 1.09(0.87 - 0.56e^{-0.06\alpha}) \quad 2.124$$

$$d_1 = 0.15 + 0.43e^{-0.06\alpha} \quad 2.125$$

$$a = 0.27 \quad 2.126$$

$$k = 0.5\left\{1 + \sin\left[\pi\left(\frac{a'}{b'} - 0.5\right)\right]\right\} \quad 2.127$$

$$a' = k_T - k_0 \quad 2.128$$

$$b' = k_1 - k_0 \quad 2.129$$

$$\xi = 1 - (1-d_1)[ak'^{0.5} + (1-a)k'^2] \quad 2.130$$

$$k' = 0.5\left\{1 + \sin\left[\pi\left(\frac{a''}{b'} - 0.5\right)\right]\right\} \quad 2.131$$

$$a'' = 1.09k_1 - k_0 \quad 2.132$$

Authors of this model have indicated that some of the constant may have to be adjusted for conditions deviating from their validation domain.

Maxwell (1987) introduced a model to predict beam irradiance using extra-terrestrial irradiance which is given in Equation 2.133.

$$\frac{I_b}{I_o} = \psi - (n_1 + n_2 e^{m_a n_3}) \quad 2.133$$

Where,

$$\psi = 0.866 - 0.122m_a + 0.0121{m_a}^2 - 0.000653{m_a}^3 + 0.000014{m_a}^4 \quad 2.134$$

if $k_t \le 0.6$

$$n_1 = 0.512 - 1.56k_T + 2.286{k_T}^2 - 2.222{k_T}^3 \quad 2.135$$

$$n_2 = 0.370 + 0.962k_T \quad 2.136$$

$$n_3 = -0.280 + 0.923k_T - 2.048{k_T}^2 \quad 2.137$$

if $k_t > 0.6$

$$n_1 = -5.743 + 21.77k_T - 27.49{k_T}^2 + 11.56{k_T}^3 \quad 2.138$$

$$n_2 = 41.40 - 118.5k_T + 66.05{k_T}^2 + 31.9{k_T}^3 \quad 2.139$$

$$n_3 = -47.01 + 184.2k_T - 222{k_T}^2 + 73.81{k_T}^3 \quad 2.140$$

Louche et all (1991) introduced a model to estimate beam fraction of global irradiance using data of France which is given in Equation 2.141.

$$\frac{I_b}{I} = -10.676{k_T}^5 + 15.307{k_T}^4 - 5.205{k_T}^3 0.994{k_T}^2 - 0.059k_T + 0.002 \quad 2.141$$

Vignola and Mc Daniels (1986) introduced model to estimate beam fraction of global irradiance using the data of USA stations which is given in Equation 2.142.

$$\frac{I_b}{I} = \begin{cases} 0.013 - 0.175k_T + 0.52{k_T}^2 + 1.08{k_T}^3 \\ +\left(0.038k_T - 0.13{k_T}^2\right)\sin\left[\frac{2\pi(n-20)}{365}\right] \\ \qquad \text{for } k_T \le 0.175 \\ 0.125{k_T}^2 \\ \qquad \text{for } k_T > 0.175 \end{cases} \quad 2.142$$

Decomposition models based on daily radiation

Ruth and chant (1976) introduced model a to estimate diffuse fraction of daily global irradiance using the data of Canadian stations which is given in Equation 2.143.

$$\frac{H_d}{H} = \begin{cases} 0.98 & \text{for } K_T \le 0.175 \\ 1.91 + 1.154K_T - 4.936{K_T}^2 - 2.848{K_T}^3 & \text{for } K_T > 0.175 \end{cases} \quad 2.143$$

Collares-Pereira and Rabl (1979) introduced a model to estimate diffuse fraction of daily global irradiance using the data of four USA stations which is given in Equation 2.144.

$$\frac{H_d}{H} = \begin{cases} 0.99 & \text{for } K_T \leq 0.17 \\ 1.188 - 2.272K_T + 9.473{K_T}^2 - 11.9514{K_T}^3 + 9.3879{K_T}^4 & \text{for } 0.17 < K_T \leq 0.75 \\ 0.632 - 0.54K_T & \text{for } 0.75 < K_T \leq 0.80 \\ 0.2 & \text{for } K_T \leq 0.80 \end{cases} \quad 2.144$$

Erbs et al (1982) introduced a model to estimate diffuse fraction of daily global irradiance using the data of US stations and one Australian station which is given in Equation 2.145.

$$\frac{H_d}{H} = \begin{cases} \text{for } \omega_s \leq 81.4 \begin{cases} 1 - 0.2727K_T + 2.4495{K_T}^2 - 11.9514{K_T}^3 \\ \quad +9.3879{K_T}^2 \quad \text{for } K_T < 0.715 \\ 0.143 \quad \text{for } K_T < 0.715 \end{cases} \\ \text{for } \omega_s > 81.4 \begin{cases} 1 + 0.2832K_T - 2.555{K_T}^2 + 0.8448{K_T}^3 \\ \quad \text{for } K_T < 0.722 \\ 0.175 \quad \text{for } K_T < 0.722 \end{cases} \end{cases} \quad 2.145$$

Decomposition models based on monthly average radiation

Liu and Jordan (1960) developed a graphical relationship between monthly averaged daily diffuse radiation fraction and monthly averaged daily clearness index which is expressed later by Klein (1977) which is given in Equation 2.146.

$$\frac{\overline{H_d}}{\overline{H}} = 1.39 - 4.027\overline{K_T} + 5.531{\overline{K_T}}^2 - 3.108{\overline{K_T}}^3 \text{ for } 0.3 < \overline{K_T} < 0.7 \quad 2.146$$

Page (1961) introduced another model which is given in Equation 2.147.

$$\frac{\overline{H_d}}{\overline{H}} = 1.0 - 1.13\overline{K_T} \quad 2.147$$

Collares-Pereira and Rabl (1979) introduced another model which is given in Equation 2.148.

$$\frac{\overline{H_d}}{\overline{H}} = 0.775 + 0.00606(\omega_s - 90) - [0.505 + 0.00455(\omega_s - 90)]\cos(\overline{K_T} - 103) \quad 2.148$$

Iqbal (1979) model introduced another model which is given in Equation 2.149.

$$\frac{\overline{H_d}}{\overline{H}} = 0.958 - 0.952\overline{K_T} \quad 2.149$$

Erbs et al (1982) model introduced another model which is given in Equation 2.150.

$$\frac{\overline{H_d}}{\overline{H}} = \begin{cases} 1.391 - 3.567\overline{K_T} + 4.189\overline{K_T}^2 - 2.137\overline{K_T}^3 \\ \quad \text{for } \omega_s \leq 81.4° \text{ and } 0.3 < \overline{K_T} < 0.8 \\ 1.311 - 3.022\overline{K_T} + 3.427\overline{K_T}^2 - 1.821\overline{K_T}^3 \\ \quad \text{for } \omega_s > 81.4° \textit{ and } 0.3 < \overline{K_T} < 0.8 \end{cases} \quad 2.150$$

In addition to above clearness index based model some other authors have introduced decomposition models using sunshine duration data which are given in Equations 2.151 to 2.155.

Stanhill (1966),

$$\frac{\overline{H_d}}{\overline{H}} = 0.964 - 0.786\frac{\overline{S}}{\overline{S_0}} \quad 2.151$$

Iqbal 1 (1979),

$$\frac{\overline{H_d}}{\overline{H}} = 0.791 - 0.635\frac{\overline{S}}{\overline{S_0}} \quad 2.152$$

Iqbal 2 (1979),

$$\frac{\overline{H_d}}{\overline{H}} = 0.163 + 0.478\frac{\overline{S}}{\overline{S_0}} - 0.655\left(\frac{\overline{S}}{\overline{S_0}}\right)^2 \quad 2.153$$

Gopinathan and Soler 1 (1995),

$$\frac{\overline{H_d}}{\overline{H}} = 0.87813 - 0.3328\overline{K_T} - 0.53039\frac{\overline{S}}{\overline{S_0}} \quad 2.154$$

Gopinathan and Soler 2 (1995),

$$\frac{\overline{H_d}}{\overline{H}} = 1.01833 - 0.33029\overline{K_T} - 0.5311\frac{\overline{S}}{\overline{S_0}} - 0.14696\left(\frac{\overline{S}}{\overline{S_0}}\right)^2 \quad 2.155$$

2.6.3 Estimation of Hourly Irradiance from Daily Irradiance Data

Accurate determination of the hourly solar radiation received during the day is important in different solar energy applications, particularly in design methods.

Whillier (1956) introduced the 'utilisability' method to predict analytically the performance of active solar collectors. This method used a simple formulation to estimate the mean hourly radiation during each hour of an average day of the month, based on the ratio of the hourly to daily irradiations received by a horizontal surface outside of the atmosphere. The ratio of the hourly global irradiance to the daily irradiance r_t in each hour could be expressed as a function of a day length and the midpoint of the relevant hour. Based on the work of Whillier (1956) and Hottel and Whiller (1958) Liu and Jordan (1960) introduced the mathematical model to estimate hourly radiation from daily radiation, is given by the Equation 2.156.

$$r_t = \frac{I}{H} = \frac{\pi}{24} \times \frac{\cos\omega - \cos\omega_s}{\sin\omega_s - \frac{\pi\omega_s}{180}\cos\omega_s} \qquad 2.156$$

Colars-pereira and Rabl (1979a) developed a model to integrate atmospheric effects to the Liu and Jordan (1960) model as shown in Equation 2.157.

$$r_t = \frac{\pi}{24} \times (a + b\cos\omega) \times \frac{\cos\omega - \cos\omega_s}{\sin\omega_s - \frac{\pi\omega_s}{180}\cos\omega_s} \qquad 2.157$$

Where,

$$a = 0.409 + 0.5016\sin(\omega_s - 60) \qquad 2.158$$

$$b = 0.6609 - 0.4767\sin(\omega_s - 60) \qquad 2.159$$

Gueymard (1986) modified Colars-pereira and Rabl (1979a) to ensure consistency of the equation with the same "a" and "b" constants. The modified equation is shown in Equation 2.160.

$$r_t = \frac{\pi}{24} \times (a + b\cos\omega) \times \frac{\cos\omega - \cos\omega_s}{a + b\left(\frac{\pi\omega_s}{180} - \sin\omega_s\cos\omega_s\right)} \qquad 2.160$$

Newell (1983) introduced simple parabolic model to estimate hourly irradiance using daily irradiance which is given in Equation 2.161.

.

$$r_t = \frac{45}{4\omega_s} \times \left(1 - \frac{225(t-12)^2}{{\omega_s}^2}\right) \qquad 2.161$$

Where,

t : midpoint of the hour

Jain (1984) introduced another model based on normal distribution introduced another model which is given in Equation 2.148.

$$r_t = \frac{1}{(0.461 + 0.0256\omega_s)\sqrt{2\pi}} \times e^{\left[-\frac{(t-12)^2}{2(0.461+0.0256\omega_s)}\right]} \quad 2.162$$

Baiget all (1991) modified Jain (1984) model for better performance around sunrise and sunset introduced another model which is given in Equation 2.148.

$$r_t = \frac{1}{2(0.26+0.028\omega_s)\sqrt{2\pi}} \times e^{\left\{\left[-\frac{(t-12)^2}{2(0.26+0.028\omega_s)}\right]+\cos\left[180\left(\frac{t-12}{\frac{2\omega_s}{15}-1}\right)\right]\right\}} \quad 2.163$$

Conversion ratio for the diffuse radiation could also be done from above models. But most widely used model is Liu and Jordan (1960) model introduced another model which is given in Equation 2.148.

$$r_d = \frac{I_d}{H_d} = \frac{\pi}{24} \times \frac{\cos\omega - \cos\omega_s}{\sin\omega_s - \frac{\pi\omega_s}{180}\cos\omega_s} \quad 2.164$$

2.7 Estimation of Radiation on Tilted Surfaces

Solar radiation received by the tilted surface consists of three components as described in section 2.3.6. Total radiation on tilted surface could be computed by computing these three components separately. Beam radiation component of tilted surface could be computed by multiplying the horizontal beam radiation and relevant beam radiation tilt factor. Therefore, hourly, daily and monthly averaged daily beam radiation on tilted surface could be expressed as in Equations 2.165, 2.166 and 2.167 respectively.

$$I_{bt} = I_b r_b \quad 2.165$$

$$H_{bt} = H_b R_b \quad 2.166$$

$$\overline{H_{bt}} = \overline{H_b R_b} \quad 2.167$$

Ground reflected component of the total radiation on tilted surface could be estimated using ground reflectance coefficient ρ_g (ground albedo) and view factor between the ground and the tilted surface. The view factor of the tilted surface to the ground could be expressed as shown in Equation 2.168.

$$F_{c-g} = \frac{1 - \cos\beta}{2} \qquad 2.168$$

Annual variations of ground albedo for various land types for china is shown in Figure 2.13. (ENF: evergreen needle-leaf forest; EBF: evergreen broad-leaf forest; DNF: deciduous needle-leaf forest; DBF: deciduous broad-leaf forest; MF: mixed forests)

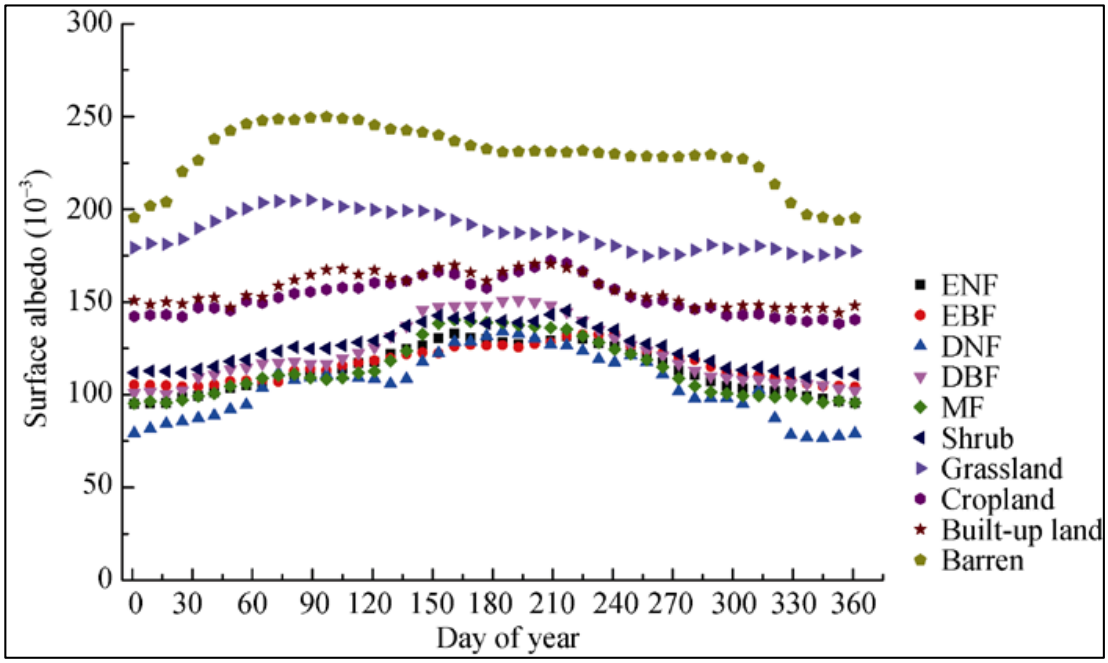

Figure 2.13 - Annual variations of Ground Albedo in China

(Source : Zhengjia LIU, 2015)

Therefore, hourly, daily and monthly averaged daily ground reflected radiation on tilted surface could be expressed as in Equations 2.169, 2.170 and 2.171 respectively.

$$I_{gt} = I\rho_g \frac{(1 - \cos\beta)}{2} \qquad 2.169$$

$$H_{gt} = H\rho_g \frac{(1 - \cos\beta)}{2} \qquad 2.170$$

$$\overline{H_{gt}} = \overline{H}\rho_g \frac{(1 - \cos\beta)}{2} \qquad 2.171$$

Estimation of the diffuse radiation is more complex than beam and ground reflected radiation due to the unpredictable behaviour of the sky. Two distinct types of solar radiation models developed to estimate diffuse radiation, called isotropic radiation models and anisotropic radiation models based on the behaviour of the diffuse solar radiation component of global solar radiation. The isotropic models have been developed by assuming that intensity of the sky diffuse radiation is uniform over the

entire sky dome. The assumption of isotropy of the sky provides a good fit to empirical data at low intensity conditions found during overcast skies. Isotropic models generally underestimate the amount of solar radiation falling on tilted surfaces at higher solar intensities and in clear or partly clear sky situations. In anisotropic sky models sky radiation has divided into three components as circumsolar, sky dome and horizon brightening components. The anisotropic models provide good estimates at clear sky condition and partly cloudy sky conditions and provide poor estimate at overcast sky conditions.

2.7.1 Isotropic sky hourly radiation models

The first isotropic sky model is developed by the Hottel and Woertz (1942) and latter refined by the Liu and Jordan (1960). This model estimates the diffuse radiation on tilted surface by multiplying the horizontal diffuse radiation from sky view factor of tilted surface. Sky view factor of tilted surface could be written as in Equation 2.172.

$$\mathrm{F_{c-s}} = \frac{1+\cos\beta}{2} = r_d \qquad 2.172$$

Where,

r_d, : Diffuse radiation tilt factor

Therefore, hourly diffuse radiation on tilted surface could be expressed as in Equation 2.173.

$$\mathrm{I_{dt}} = \mathrm{I}_d \frac{(1+\cos\beta)}{2} \qquad 2.173$$

Therefore, hourly total radiation on tilted surface could be expressed as in Equation 2.174.

$$\mathrm{I_t} = \mathrm{I_b r_b} + \mathrm{I}_d \frac{(1+\cos\beta)}{2} + \mathrm{I}\rho_g \frac{(1-\cos\beta)}{2} \qquad 2.174$$

Koronakis (1986) examined the Liu and Jordan model and they found that southern part of sky (in northern hemisphere) is more (63%) responsible for the total radiation. Based on that, Koronakis (1986) introduced a different equation to estimate diffuse radiation tilt factor which is given in Equation 2.175.

$$\mathrm{r_d} = \frac{(2+\cos\beta)}{3} \qquad 2.175$$

According to the Koronakis (1986) hourly total radiation on tilted surface could be expressed by the Equation 2.176.

$$I_t = I_b r_b + I_d \frac{(2+\cos\beta)}{3} + I\rho_g \frac{(1-\cos\beta)}{2} \quad 2.176$$

Tian et al. (2001) introduced another model to estimate diffuse radiation tilt factor which is given in Equation 2.177.

$$r_d = \left(1 - \frac{\beta}{180}\right) \quad 2.177$$

According to the Tian et al. (2001) hourly total radiation on tilted surface could be expressed as Equation 2.178.

$$I_t = I_b r_b + I_d \left(1 - \frac{\beta}{180}\right) + I\rho_g \frac{(1-\cos\beta)}{2} \quad 2.178$$

Badescu (2002) introduced another model to estimate diffuse radiation tilt factor which is given in Equation 2.179.

$$r_d = \left(\frac{3+\cos 2\beta}{4}\right) \quad 2.179$$

According to the Badescu (2002) total radiation on tilted surface could be expressed as Equation 2.180.

$$I_t = I_b r_b + I_d \left(\frac{3+\cos 2\beta}{4}\right) + I\rho_g \frac{(1-\cos\beta)}{2} \quad 2.180$$

2.7.2 Anisotropic sky hourly radiation models

Temps and Coulson (1977) suggested an anisotropic modification to the clear-sky diffuse radiance model. Temps and Coulson used clear sky measurements to explain the anisotropic nature of diffuse irradiation. In their study they observed increased intensity near the horizon and in the circumsolar region of the sky. Also they found that 40% greater intensity at horizons than at zenith. They introduced $(1+\sin^3\beta/2)$ factor to account for the effects of horizons brightness. Also they introduced $(1+\cos^2\theta\sin^3\theta_z)$ factor to account for the effects of circumsolar brightness. Hourly diffuse radiation tilt factor of Temps and Coulson (1977) is given in Equation 2.181.

$$r_d = \frac{(1+\cos\beta)}{2}[1+\cos^2\theta(\sin^3\theta_z)]\left[1+\sin^3\left(\frac{\beta}{2}\right)\right] \quad 2.181$$

Therefore, Temps and Coulson's anisotropic model (1977) for the estimation of hourly total radiation for a tilted surface could be expressed as Equation 2.182.

$$I_t = I_b r_b + I_d \frac{(1+\cos\beta)}{2}[1+\cos^2\theta(\sin^3\theta_z)]\left[1+\sin^3\left(\frac{\beta}{2}\right)\right] + \rho_g I \frac{(1-\cos\beta)}{2} \quad 2.182$$

Bugler (1977) introduced another equation to estimate hourly diffuse radiation tilt factor which is given in Equation 2.183.

$$r_d = \frac{(1+\cos\beta)}{2} + 0.05\frac{I_b r_b}{I_d}\left[\cos\theta - \frac{1}{\cos\theta_z}\left(\frac{(1+\cos\beta)}{2}\right)\right] \quad 2.183$$

Therefore, Bugler's anisotropic model (1977) for the estimation of hourly total radiation for a tilted surface could be expressed as Equation 2.184.

$$I_t = I_b r_b + I_d\left\{\frac{(1+\cos\beta)}{2} + 0.05\frac{I_b r_b}{I_d}\left[\cos\theta - \frac{1}{\cos\theta_z}\left(\frac{(1+\cos\beta)}{2}\right)\right]\right\} + \rho_g I\frac{(1-\cos\beta)}{2} \quad 2.184$$

Klucher (1979) further studied the models of Liu and Jordan (1960) and Temps and Coulson (1977) and found that Liu–Jordan isotropic model gives good results under overcast skies, but under estimates insolation under clear and part-overcast conditions. Klucher also noted that the Temps and Coulson model provides a good prediction for clear-sky conditions but overestimates overcast insolation. Klucher used hourly measured radiation values for New York for a 6-month period on surfaces tilted towards the equator at 37° and 60° angles. Klucher (1979) proposed new hourly diffuse radiation tilt factor based on the observations which is given in Equation 2.185.

$$r_d = \frac{(1+\cos\beta)}{2}\left[1 + F'\sin^3\left(\frac{\beta}{2}\right)\right](1 + F'\cos^2\theta\sin^3\theta_z) \quad 2.185$$

Where,

$$F' = 1 - \left(\frac{I_d}{I}\right)^2 \quad 2.186$$

The factor F' is called as the modified clearness index. The first modifying factor accounts for the horizons brightness and second modifying factor accounts for the circumsolar brightness. Klucher's equation (1979) reduced to Liu and Jordan's (1960) for the overcast sky and reduced to Temps and Coulson's (1977) for the clear sky conditions. Klucher's anisotropic model (1979) for the estimation of hourly total radiation for a tilted surface could be expressed as equation 2.187.

$$I_t = I_b r_b + I_d\frac{(1+\cos\beta)}{2}\left[1 + F'\sin^3\left(\frac{\beta}{2}\right)\right](1 + F'\cos^2\theta\sin^3\theta_z) + \rho_g I\frac{(1-\cos\beta)}{2} \quad 2.187$$

Hay (1979) (Hay and Davies 1980) proposed a diffuse radiation tilt factor considering only isotropic sky and circumsolar component, but horizon brightening is not taken into account. According to the Hay's equation (1979) hourly diffuse radiation tilt factor could be expressed as Equation 2.188.

$$r_d = Ar_b + (1 - A)\frac{(1 + \cos\beta)}{2} \quad 2.188$$

Where,

$$A = \frac{I_{bn}}{I_{on}} \quad 2.189$$

The factor A anisotropic index is used to quantify the portion of the diffuse radiation treated as circumsolar, with the remaining portion of diffuse radiation is assumed isotropic.

According to the Hay's model (1979) hourly total radiation on tilted surface could be expressed as Equation 2.190.

$$I_t = (I_b + AI_d)r_b + I_d(1 - A)\frac{(1 + \cos\beta)}{2} + \rho_g I\frac{(1 - \cos\beta)}{2} \quad 2.190$$

Willmot (1982) introduced new equations for the hourly diffuse radiation tilt factor using same anisotropic index which is given in Equation 2.191.

$$r_d = Ar_b + (1.0115 - 0.20293\beta - 0.080823\beta^2)(1 - A) \quad 2.191$$

According to the Willmot's model (1982) hourly total radiation on tilted surface could be expressed as Equation 2.192.

$$I_t = (I_b + AI_d)r_b + I_d(1.0115 - 0.20293\beta - 0.080823\beta^2)(1 - A) + \rho_g I\frac{(1 - \cos\beta)}{2} \quad 2.192$$

By using same anisotropic index and Latitude angle, Skartveit and Olseth (1986) introduced another hourly diffuse radiation tilt factor which is given in Equation 2.193.

$$r_d = Ar_b + \Omega\cos\beta + (1 - A - \Omega)\frac{(1 + \cos\beta)}{2} \quad 2.193$$

Where,

$$\Omega = \max\{0, (0.3 - 2A)\} \quad 2.194$$

According to the Skartveit and Olseth's model (1986) hourly total radiation on tilted surface could be expressed as Equation 2.195.

$$I_t = (I_b + AI_d)r_b + I_d\left\{\Omega\cos\beta + (1 - A - \Omega)\left[\frac{1+\cos\beta}{2}\right]\right\} + \rho_g I\frac{(1-\cos\beta)}{2} \quad 2.195$$

By using the same definition for anisotropy index, Reindl et al. (1990) proposed hourly diffuse solar radiation tilt factor given in Equation 2.196 which also accounts for the horizon brightening.

$$r_d = Ar_b + (1 - A)\left[\frac{1+\cos\beta}{2}\right]\left[1 + f\sin^3\left(\frac{\beta}{2}\right)\right] \quad 2.196$$

Where,

$$f = \sqrt{\frac{I_b}{I}} \quad 2.197$$

Reindl et al. (1990) has modified Hay and Davies (1980) model by adding factor like in Klucher's model (1979). Therefore, this model is called as HDKR model and is given in Equation 2.198.

$$I_t = (I_b + AI_d)r_b + I_D(1 - A)\frac{(1+\cos\beta)}{2}\left[1 + f\sin^3\left(\frac{\beta}{2}\right)\right] + \rho_g I\frac{(1-\cos\beta)}{2} \quad 2.198$$

Steven and Unswoth (1980) also proposed an anisotropic model which has the hourly diffuse radiation tilt factor explained in Equation 2.199.

$$r_d = 0.51r_b + \left(\frac{1+\cos\beta}{2}\right) - \frac{1.74}{1.26\pi}\left(\sin\beta - \frac{\pi\beta\cos\beta}{180} - \pi\sin^2\frac{\beta}{2}\right) \quad 2.199$$

According to the Steven and Unswoth's model (1980) hourly total radiation on tilted surface could be expressed as Equation 2.197.

$$I_t = (I_b + 0.51I_d)r_b + I_D\left[\left(\frac{1+\cos\beta}{2}\right) - \frac{1.74}{1.26\pi}\left(\sin\beta - \frac{\pi\beta\cos\beta}{180} - \pi\sin^2\frac{\beta}{2}\right)\right] + \rho_g I\frac{(1-\cos\beta)}{2} \quad 2.200$$

Iqbal (1983) introduced equations for the hourly diffuse radiation tilt factor using clearness index.

$$r_d = k_T r_b + (1 - k_T)\frac{(1+\cos\beta)}{2} \quad 2.201$$

According to the Iqbal's model (1983) hourly total radiation on tilted surface could be expressed as Equation 2.202.

$$I_t = (I_b + k_T I_d) r_b + I_D (1 - k_T) \frac{(1 + \cos \beta)}{2} + \rho_g I \frac{(1 - \cos \beta)}{2} \quad 2.202$$

Perez et al (1986) introduced more detailed model based on three diffuse components and later Perez et al (1990) introduced modification to the previous model. Perez (1990) modified hourly radiation tilt factor and the relationship is given in Equation 3.203.

$$r_d = (1 - F_1) \frac{(1 + \cos \beta)}{2} + F_1 \frac{a}{b} + F_2 \sin \beta \quad 2.203$$

Where,

F_1 : circumsolar brightness factor (given in Equation 2.208)

F_2 : horizon brightness factor (given in Equation 2.209)

a, b terms accounts for the angle of incident of the cone of circumsolar radiation (given in Equations 2.204 and 2.205).

$$a = \max(0, \cos \theta) \quad 2.204$$

$$b = \max(\cos 85 , \cos \theta_z) \quad 2.205$$

The brightness coefficients F_1 and F_2 are functions of the zenith angle θ_z, sky clearness ε (given in Equation 2.206) and brightness Δ (given in Equation 2.207).

$$\varepsilon = \frac{\frac{I_d + I_{bn}}{I_d} + 5.535 \times 10^{-6} {\theta_z}^3}{1 + 5.535 \times 10^{-6} {\theta_z}^3} \quad 2.206$$

$$\Delta = m_h \frac{I_d}{I_{on}} \quad 2.207$$

$$F_1 = \max \left[0, \left(f_{11} + f_{12} \Delta + \frac{\pi \theta_z}{180} f_{13} \right) \right] \quad 2.208$$

$$F_2 = \left(f_{21} + f_{22} \Delta + \frac{\pi \theta_z}{180} f_{23} \right) \quad 2.209$$

Coefficients f_{11}, f_{12}, f_{13}, f_{21}, f_{22} and f_{23} are given in Table 2.5.

Table 2.5 - Perez et al brightness coefficients

ε	f_{11}	f_{12}	f_{13}	f_{21}	f_{22}	f_{23}
1.000 -1.065	-0.008	0.588	-0.062	-0.060	0.072	-0.022
1.065 - 1.230	0.130	0.683	-0.151	-0.019	0.066	-0.029
1.230 - 1.500	0.330	0.487	-0.221	0.055	-0.064	-0.026
1.500 - 1.950	0.568	0.187	-0.295	0.109	-0.152	0.014
1.950 - 2.800	0.873	-0.392	-0.362	0.226	-0.462	0.001
2.800 - 4.500	1.132	-1.237	-0.412	0.288	-0.823	0.056
4.500 - 6.200	1.06	-1.600	-0.359	0.264	-1.127	0.131
6.200 - ∞	0.678	-0.327	-0.250	0.156	-1.377	0.251

According to the Perez (1990) model hourly total radiation on tilted surface could be expressed as Equation 2.210.

$$I_t = I_b r_b + I_D \left[(1 - F_1) \frac{(1 + \cos\beta)}{2} + F_1 \frac{a}{b} + F_2 \sin\beta \right] + \rho_g I \frac{(1 - \cos\beta)}{2} \quad 2.210$$

2.7.3 Daily radiation and averaged radiation models

Procedure for the calculation of the daily and averaged total radiation on a tilted surface is same as the hourly radiation. The developed calculation methods for the daily and averaged radiation on tilted surface are not satisfactory as hourly radiation models. The first model is introduced by Liu and Jordan (1962) which was later refined by Klein (1977) is widely used in literature.

As explained in section 3.4.1 this model estimates the diffuse radiation on tilted surface by multiplying the horizontal diffuse radiation from sky view factor of tilted surface. Sky view factor of tilted surface could be written as in Equation 2.211.

$$F_{c-s} = \frac{1 + \cos\beta}{2} = R_d = \overline{R_d} \quad 2.211$$

Where,

R_d, $\overline{R_d}$: Diffuse radiation tilt factors

Therefore, daily and monthly averaged daily diffuse radiation on tilted surface could be expressed as in equations 2.212, and 2.213 respectively.

$$H_{dt} = H_d \frac{(1 + \cos\beta)}{2} \quad 2.212$$

$$\overline{H_{dt}} = \overline{H_d} \frac{(1 + \cos\beta)}{2} \quad 2.213$$

Therefore, daily and monthly averaged daily total radiation on tilted surface could be expressed as in Equations 2.214 and 2.215 respectively using equations.

$$H_{bt} = H_b \frac{\cos(L - \beta)\cos\delta\sin\omega_{ss} + \frac{\pi}{180}\omega_{ss}\sin(L - \beta)\sin\delta}{\cos L\cos\delta\sin\omega_s + \frac{\pi}{180}\omega_s \sin L\sin\delta} + H_d \frac{(1 + \cos\beta)}{2} + H\rho_g \frac{(1 - \cos\beta)}{2} \quad 2.214$$

$$\overline{H_{bt}} = \overline{H_b} \frac{\cos(L - \beta)\cos\delta\sin\omega_{ss} + \frac{\pi}{180}\omega_{ss}\sin(L - \beta)\sin\delta}{\cos L\cos\delta\sin\omega_s + \frac{\pi}{180}\omega_s \sin L\sin\delta} + \overline{H_d} \frac{(1 + \cos\beta)}{2} + \overline{H}\rho_g \frac{(1 - \cos\beta)}{2} \quad 2.215$$

Klein and Theilacker (1981) introduced a model (KT model) given in Equation 2.216 to estimate daily and averaged total radiation of tilted surface facing the equator.

$$\overline{H_t} = \overline{H}\overline{R} \tag{2.216}$$

Where,

$$\overline{R} = \frac{\cos(L-\beta)}{\cos L}\left\{\left(a - \frac{\overline{H_d}}{\overline{H}}\right)\left(\sin\omega_{ss} - \frac{\pi\omega_{ss}}{180}\cos\omega'_{ss}\right) + \frac{b}{2}\left[\frac{\pi\omega_{ss}}{180} + \sin\omega_{ss}\left(\cos\omega_{ss} - 2\cos\omega'_{ss}\right)\right]\right\} + \frac{\overline{H_d}}{\overline{H}}\frac{(1+\cos\beta)}{2} + \rho_g\frac{(1-\cos\beta)}{2} \tag{2.217}$$

$$\omega'_{ss} = \cos^{-1}[-\tan(L-\beta)\tan\delta)] \tag{2.218}$$

$$d = \sin\omega_s - \frac{\pi\omega_s}{180}\cos\omega_s \tag{2.219}$$

Also a and b are same as the Equations given in 2.158 and 2.159.

Klein and Theilacker (1981) later modified the equation to be used for all surfaces. Modified equation is given in Equation 2.220

$$\overline{R} = D + \frac{\overline{H_d}}{\overline{H}}\frac{(1+\cos\beta)}{2} + \rho_g\frac{(1-\cos\beta)}{2} \tag{2.220}$$

Where,

$$D = \begin{cases}\max[0, G(\omega_{ss}, \omega_{sr})] & \text{if } \omega_{ss} \geq \omega_{sr} \\ \max[0, G(\omega_{ss}, -\omega_s) + G(\omega_s, \omega_{sr})] & \text{if } \omega_{ss} < \omega_{sr}\end{cases} \tag{2.221}$$

$$G(\omega_1, \omega_2) = \frac{1}{2d}\left[\left(\frac{bA}{2} - a'B\right)(\omega_1 - \omega_2)\frac{\pi}{180} + (a'A - bB)(\sin\omega_1 - \sin\omega_2) - a'C(\cos\omega_1 - \cos\omega_2) + \frac{bA}{2}(\sin\omega_1\cos\omega_1 - \sin\omega_2\cos\omega_2) + \frac{bC}{2}(\sin^2\omega_1 - \sin^2\omega_2)\right] \tag{2.222}$$

$$a' = a - \frac{\overline{H_d}}{\overline{H}} \tag{2.223}$$

$$|\omega_{sr}| = \min\left(\omega_s, \cos^{-1}\frac{AB + C\sqrt{A^2 - B^2 + C^2}}{A^2 + B^2}\right) \tag{2.224}$$

$$\omega_{sr} = \begin{cases}-|\omega_{sr}| \text{ if } (A > B \text{ and } B > 0) \text{ or } A \geq B \\ |\omega_{sr}| \quad \text{otherwise}\end{cases} \tag{2.225}$$

$$|\omega_{ss}| = \min\left(\omega_s, \cos^{-1}\frac{AB - C\sqrt{A^2 - B^2 + C^2}}{A^2 + B^2}\right) \quad 2.226$$

$$\omega_{sr} = \begin{cases} -|\omega_{ss}| \text{ if } (A > B \; and \; B > 0) \text{ or } A \geq B \\ |\omega_{ss}| \quad \text{otherwise} \end{cases} \quad 2.227$$

$$A = \cos\beta + \tan L \cos\gamma_p \sin\beta \quad 2.228$$

$$B = \cos\omega_s \cos\beta + \tan\delta \cos\gamma_p \sin\beta \quad 2.229$$

$$C = \frac{\sin\gamma_p \sin\beta}{\cos L} \quad 2.230$$

In addition to the Liu and Jordan's model (1962) and KT's model (1981), most of the other models explained in sections 2.6.1 and 2.6.2 have been used by various other authors in their papers for calculating the daily radiation and averaged radiation with modification of diffuse tilt factor. Models given in equations 2.231 to 2.251 were originally developed to estimate hourly radiation but many authors have used them for the estimation of daily and averaged radiation. Due to the similarity of the equations, only daily radiation equations are presented. Monthly averaged radiation model could be obtained by replacing the daily radiation terms and tilt factors from monthly averaged daily radiation terms and tilt factors, as shown in below.

Koronakis (1986),

$$R_d = \overline{R_d} = \frac{(2 + \cos\beta)}{3} \quad 2.231$$

$$H_{bt} = H_b \frac{\cos(L - \beta)\cos\delta\sin\omega_{ss} + \frac{\pi}{180}\omega_{ss}\sin(L - \beta)\sin\delta}{\cos L\cos\delta\sin\omega_s + \frac{\pi}{180}\omega_s \sin L \sin\delta} + H_d\frac{(2 + \cos\beta)}{3} + H\rho_g\frac{(1 - \cos\beta)}{2} \quad 2.232$$

Tian et al. (2001),

$$R_d = \overline{R_d} = \left(1 - \frac{\beta}{180}\right) \quad 2.233$$

$$H_{bt} = H_b \frac{\cos(L - \beta)\cos\delta\sin\omega_{ss} + \frac{\pi}{180}\omega_{ss}\sin(L - \beta)\sin\delta}{\cos L\cos\delta\sin\omega_{ss} + \frac{\pi}{180}\omega_s \sin L \sin\delta} + H_d\left(1 - \frac{\beta}{180}\right) + H\rho_g\frac{(1 - \cos\beta)}{2} \quad 2.234$$

Badescu (2002),

$$R_d = \overline{R_d} = \frac{(3 + \cos 2\beta)}{4} \quad 2.235$$

$$H_{bt} = H_b \frac{\cos(L - \beta)\cos\delta \sin\omega_{ss} + \frac{\pi}{180}\omega_{ss}\sin(L - \beta)\sin\delta}{\cos L \cos\delta \sin\omega_{ss} + \frac{\pi}{180}\omega_s \sin L \sin\delta} + H_d \frac{(3 + \cos 2\beta)}{4} + H\rho_g \frac{(1 - \cos\beta)}{2} \quad 2.236$$

Hay (1979) and (Hay and Davies 1980),

$$R_d = AR_b + (1 - A)\frac{(1 + \cos\beta)}{2} \quad 2.237$$

Where,

$$A = \frac{H_{bn}}{H_{on}} \quad 2.238$$

$$H_t = (H_b + AH_d)R_b + H_d(1 - A)\frac{(1 + \cos\beta)}{2} + \rho_g H\frac{(1 - \cos\beta)}{2} \quad 2.239$$

Willmot (1982),

$$R_d = AR_b + (1.0115 - 0.20293\beta - 0.080823\beta^2)(1 - A) \quad 2.240$$

$$H_t = (H_b + AH_d)R_b + H_d(1.0115 - 0.20293\beta - 0.080823\beta^2)(1 - A) + \rho_g H\frac{(1 - \cos\beta)}{2} \quad 2.241$$

Skartveit and Olseth (1986),

$$R_d = AR_b + \Omega\cos\beta + (1 - A - \Omega)\frac{(1 + \cos\beta)}{2} \quad 2.242$$

Where,

$$\Omega = \max\{0, (0.3 - 2A)\} \quad 2.243$$

$$H_t = (H_b + AH_d)R_b + H_d\left[\Omega\cos\beta + (1 - A - \Omega)\frac{(1 + \cos\beta)}{2}\right] + \rho_g H\left[\frac{1 - \cos\beta}{2}\right] \quad 2.244$$

Reindl et al. (1990),

$$R_d = AR_b + (1 - A)\frac{(1 + \cos\beta)}{2}\left[1 + f\sin^3\left(\frac{\beta}{2}\right)\right] \quad 2.245$$

Where,

$$f = \sqrt{\frac{H_b}{H}} \quad 2.246$$

$$H_t = (H_b + AH_d)R_b + H_D(1 - A)\frac{(1 + \cos\beta)}{2}\left[1 + f\sin^3\left(\frac{\beta}{2}\right)\right] + \rho_g H\frac{(1 - \cos\beta)}{2} \quad 2.247$$

Steven and Unswoth (1980),

$$R_d = 0.51R_b + \frac{(1 + \cos\beta)}{2} - \frac{1.74}{1.26\pi}\left(\sin\beta - \frac{\pi\beta\cos\beta}{180} - \pi\sin^2\frac{\beta}{2}\right) \quad 2.248$$

$$H_t = (H_b + 0.51H_d)R_b + H_D\left[\frac{(1 + \cos\beta)}{2} - \frac{1.74}{1.26\pi}\left(\sin\beta - \frac{\pi\beta\cos\beta}{180} - \pi\sin^2\frac{\beta}{2}\right)\right] + \rho_g H\frac{(1 - \cos\beta)}{2} \quad 2.249$$

Iqbal (1983),

$$R_d = K_T r_b + (1 - K_T)\frac{(1 + \cos\beta)}{2} \quad 2.250$$

$$H_t = (H_b + K_T H_d)R_b + H_D(1 - K_T)\frac{(1 + \cos\beta)}{2} + \rho_g H\frac{(1 - \cos\beta)}{2} \quad 2.251$$

3 RESEARCH METHODOLOGY

3.1 Analysis of existing diffuse radiation models

Hourly diffuse radiation models described in Equations 2.172 to 2.210 was analysed and compared with actual measured data from August 2011 to December 2012 at Hambathota (6.23° N, 81.08° E) solar park owned to SLSEA. The data has been recorded hourly basis according to the Local Standard Time (LST). LST was converted to Apparent Solar Time (AST) using Equation 2.32. Actual diffuse radiation at 7° tilt about east west axis in due south orientation was calculated using Equation 2.61 by substituting measured total tilted radiation, calculated tilted beam radiation and assumed ground reflected radiation. Tilted beam radiation was calculated using Equation 2.165 by substituting beam radiation tilt factor using Equation 2.54 and horizontal beam radiation from Equation 2.50. Horizontal beam radiation was calculated by subtracting the measured horizontal diffuse radiation from measured global horizontal radiation assuming that zero ground reflectance radiation at horizontal surface. Ground reflected diffuse radiation was calculated using Equation 2.170 assuming that 0.11 uniform ground reflectance throughout the year.

Model comparison was carried out by using statistical parameters called Mean Bias Error (MBE), Mean Absolute Error (MAE), Root Mean Square Error (RMSE), Mean Percentage Error (MPE) and Mean Absolute Percentage Error (APE) which are given in Equations 3.1 to 3.5

$$\mathrm{MBE} = \frac{\sum(\mathrm{C_i} - \mathrm{M_i})}{\mathrm{n}} \tag{3.1}$$

$$\mathrm{MAE} = \frac{\sum|\mathrm{C_i} - \mathrm{M_i}|}{\mathrm{n}} \tag{3.2}$$

$$\mathrm{RMSE} = \sqrt{\frac{\sum(\mathrm{C_i} - \mathrm{M_i})^2}{\mathrm{n}}} \tag{3.3}$$

$$\mathrm{MPE} = \frac{\sum\left({}^{(\mathrm{C_i} - \mathrm{M_i})}/_{\mathrm{M_i}}\right) \times 100\%}{\mathrm{n}} \tag{3.4}$$

$$APE = \frac{\sum \left| {}^{(C_i - M_i)}/_{M_i} \right| \times 100\%}{n} \quad 3.5$$

Where,

C_i : i^{th} calculated value

M_i : i^{th} measured value

n : Sample size

3.2 Development of new model suitable for dry zone in Sri Lanka

Percentage errors of existing hourly diffuse radiation models were analysed with various parameters such as clearness index, declination angle, azimuth angle etc. It was found that declination angle and clearness index have correlation with percentage errors of models. Figure 3.1 described the variation of percentage variations of annual average hourly insolation with annual average hourly clearness index and Figure 3.2 described the variations of percentage variations of annual average daily insolation with annual average daily clearness index.

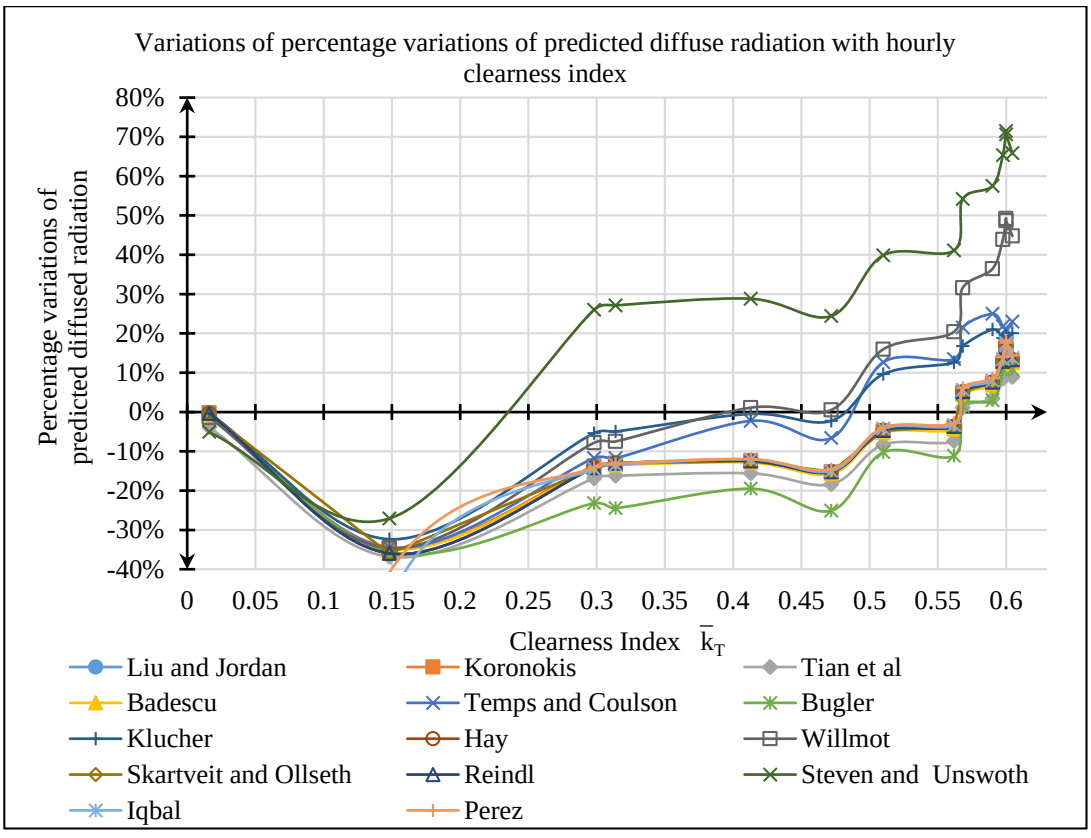

Figure 3.1 - Variations of percentage variations of predicted diffuse radiation with hourly clearness index

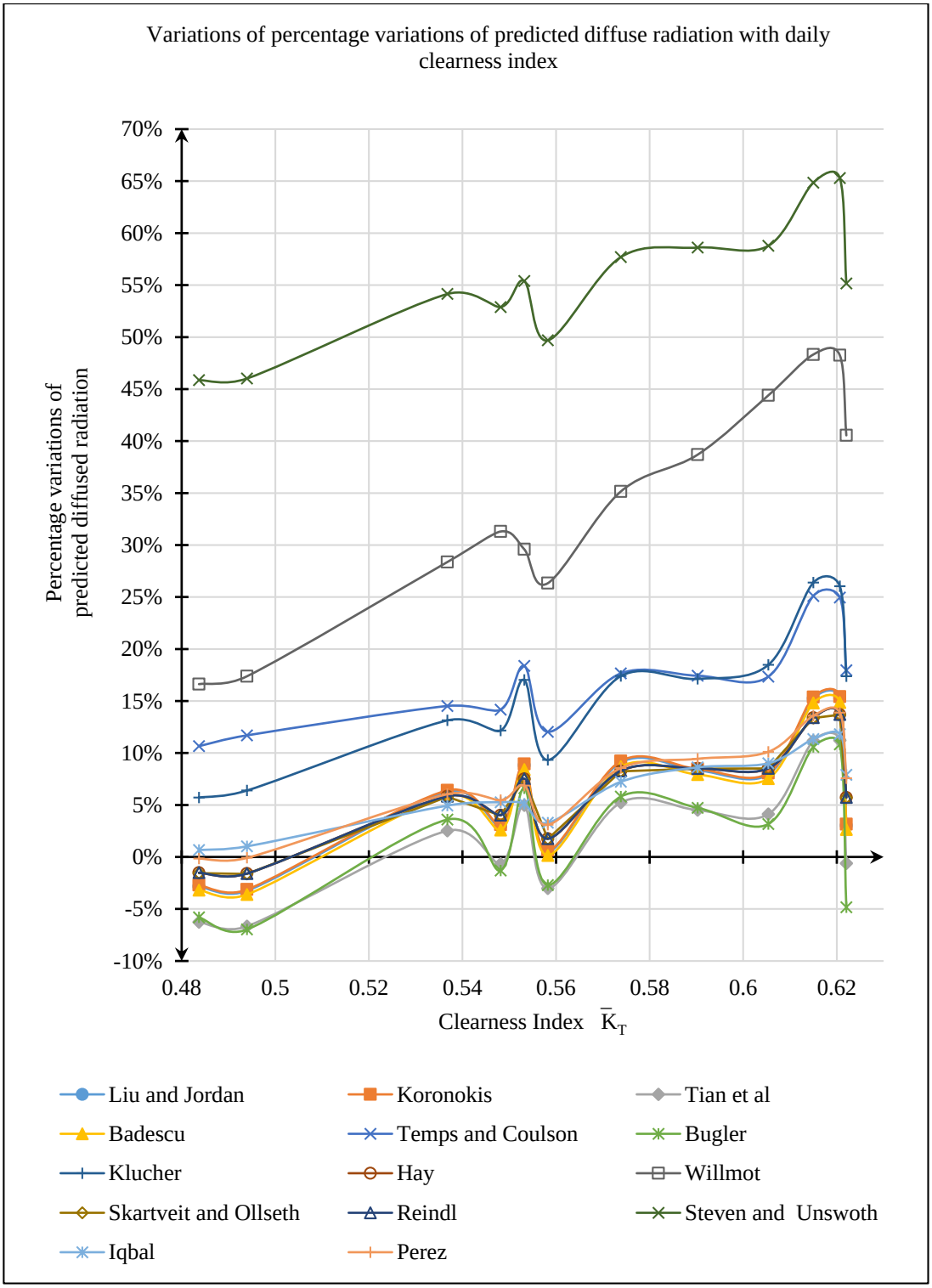

Figure 3.2 - Variations of percentage variations of predicted diffuse radiation with daily clearness index

Figure 3.1 and Figure 3.2 indicate that the significant relevance between the percentage variations of predicted diffuse radiation and clearness index. Figure 3.1 and Figure 3.2

also indicate that models under estimate the diffuse radiation for relatively cloudy sky conditions and overestimate for clear sky conditions. Figure 3.1 indicates that there exists exponential relationship between the percentage variations and hourly clearness index. Variations of percentage variations of monthly averaged daily diffuse insolation with declination angle are shown in Figure 3.3.

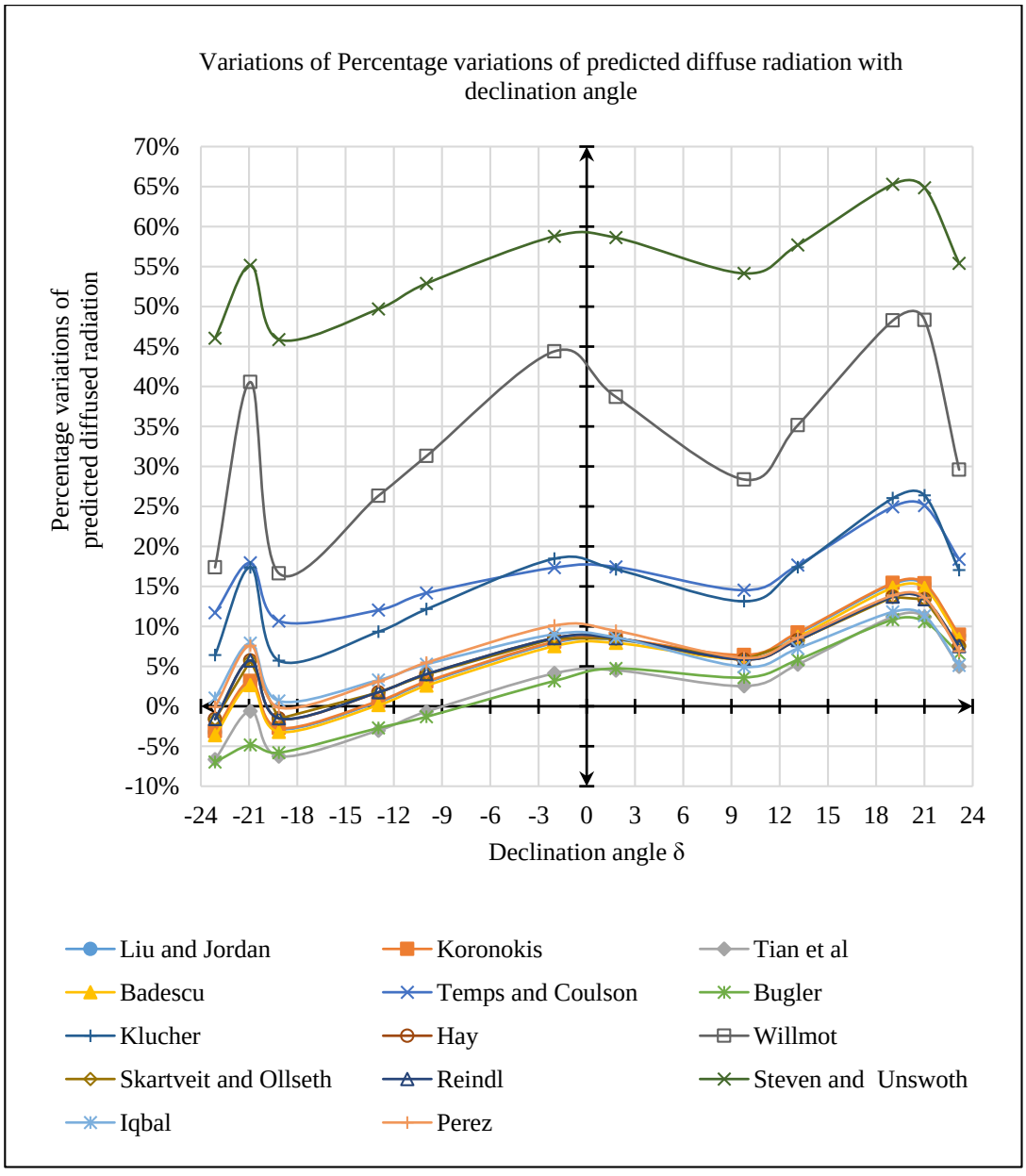

Figure 3.3 - Variations of Percentage variations of predicted diffuse radiation with declination angle

Figure 3.3 indicates that linear relationship between the percentage variations and declination angle. Hence various types of nonlinear regression were performed by modifying the models using clearness index and declination angle to find out suitable model for dry zone. In addition to that separate nonlinear regressions were performed for each sky clearness band of Perez et al (1990) model in order to find out new brightness coefficient for Perez et al (1990) model. Modified models were compared using statistical parameters to find out more accurate hourly diffuse solar radiation model to predict diffuse radiation for dry zone in Sir Lanka.

3.3 Estimation of solar radiation potential on horizontal surfaces in dry zone in Sri Lanka

Measured hourly global horizontal radiation, diffuse horizontal radiation and total tilted radiation from August 2011 to December 2012 at Hambanthota (6.23° N, 81.08° E) solar park were used for estimating of averaged daily and hourly insolation. Calculation of hourly horizontal beam radiation and time conversion were performed as described in section 3.1. Monthly averaged hourly and daily clearness indexes was calculated using Equations 2.100 and 2.102 respectively.

3.4 Estimation of solar radiation potential on tilted surfaces in dry zone in Sri Lanka

The diffuse radiation potential on due south and north faced inclined surfaces of dry zone was estimated by using modified Perez et al (1990) model and total radiation potential on tilted surfaces was estimated by adopting estimated diffuse radiation values. Tilt angles of 0° to 45° with 1° increment for both due south and due north faced was used for the assessment of radiation potential.

3.5 Estimation of optimum tilt angle for dry zone in Sri Lanka

Daily optimum tilt angles and monthly optimum tilt angles were obtained to maximise predicted daily and monthly averaged global radiation. Optimum tilt angles for daily tracking and monthly tracking systems about the east west axis were also calculated.

4 RESULTS AND DISCUSSION

4.1 Analysis of existing diffuse radiation models

4.1.1 Isotropic models

Four existing isotropic hourly diffuse radiation models namely Liu and Jordan (1960), Koronakis (1986), Tian et al (2001) and Badescu (2002) were analysed using hourly data from August, 2011 to December, 2012 of Hambanthota solar park which is owned by SLSEA. Predicted annual average hourly insolation from isotropic models and actual annual average insolation for 7° due south faced surfaces are shown in Figure 4.1 and percentage variations of predictions are shown in Figure 4.2. Percentage variations of annual average daily insolation predicted from isotropic models are also plotted in the Figure 4.2.

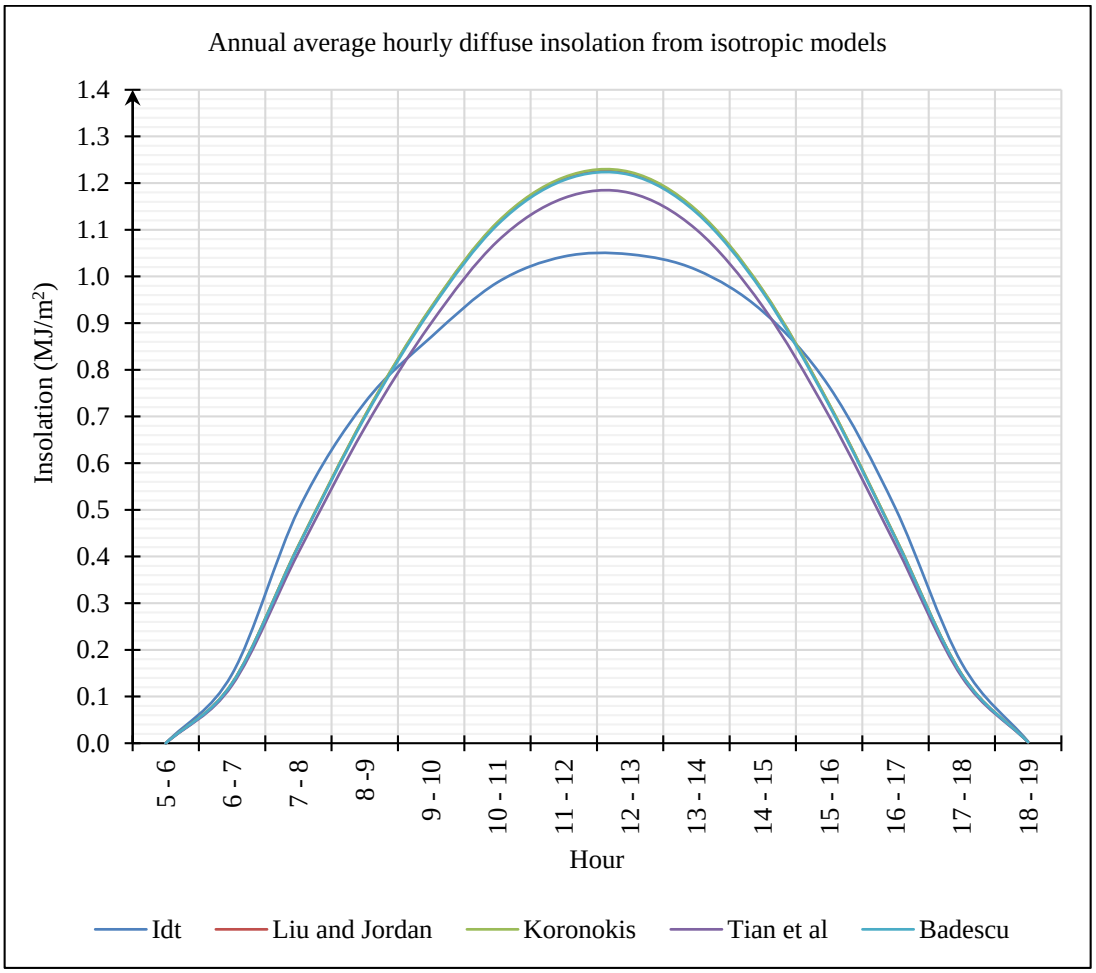

Figure 4.1 - Annual average hourly diffuse insolation from isotropic models

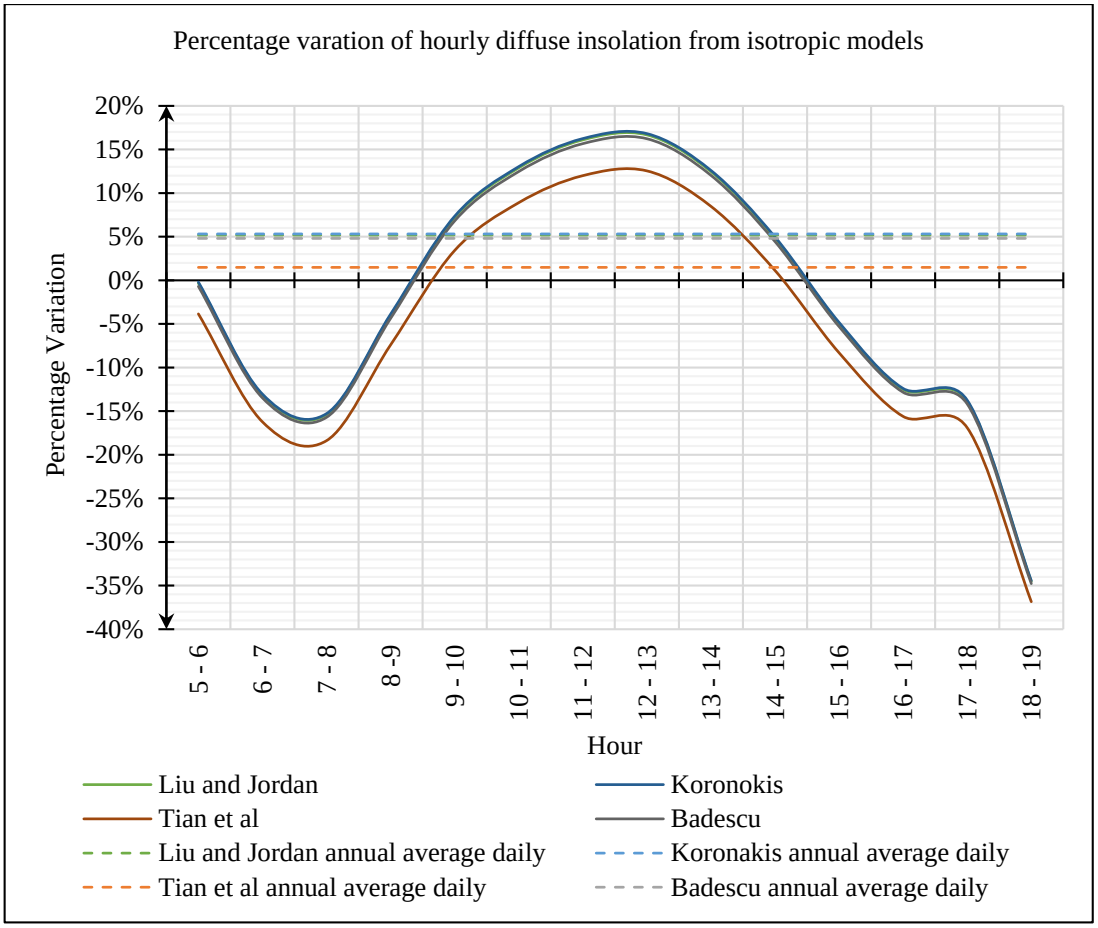

Figure 4.2 - Percentage variation of hourly diffuse insolation from isotropic models

All of the isotropic models overestimate the radiation from 0900 hour to 1500 hour while under estimating in rest of the morning hours and evening hours. Total annual average daily variation from four isotropic models Liu and Jordan, Koronakis, Tian et al and Badescu were 5.19%, 5.32%, 1.48% and 4.8% respectively. Comparison among the models were performed using statistical parameters MBE, MAE, RMSE, MPE and MAPE and results are illustrated in Table 4.1.

Table 4.1 - Comparison of isotropic models using statistical parameters

Model	MBE	MAE	RMSE	MPE	MAPE
Liu and Jordan	0.0373	0.0903	0.1295	10.64%	24.62%
Koronokis	0.0382	0.0905	0.1300	10.78%	24.63%
Tian et al	0.0106	0.0877	0.1192	6.74%	24.47%
Badescu	0.0345	0.0897	0.1281	10.23%	24.57%

Table 4.1 indicates that Tian et al (2001) model shows minimum values for all five statistical parameters among four isotropic models. Therefore, it can be concluded that Tian et al (2001) model predict the hourly diffuse radiation more accurately than other isotropic models.

4.1.2 Anisotropic models

Ten existing anisotropic hourly diffuse radiation models namely Temps and Coulson (1977), Bugler (1977), Klucher (1979), Hay (1979), Willmot (1982), Skartveit and Olseth (1986), Reindel (1990), Stevan and Unswoth (1980), Iqbal (1983) and Perez (1990) were analysed using same data set used in isotropic models. Predicted annual average hourly insolation from anisotropic models and actual annual average insolation for 7° due south faced surface are shown in Figure 4.3 and percentage variations of predictions are shown in Figure 4.4. Percentage variations of annual average daily insolation predicted from anisotropic models are also plotted in the Figure 4.4.

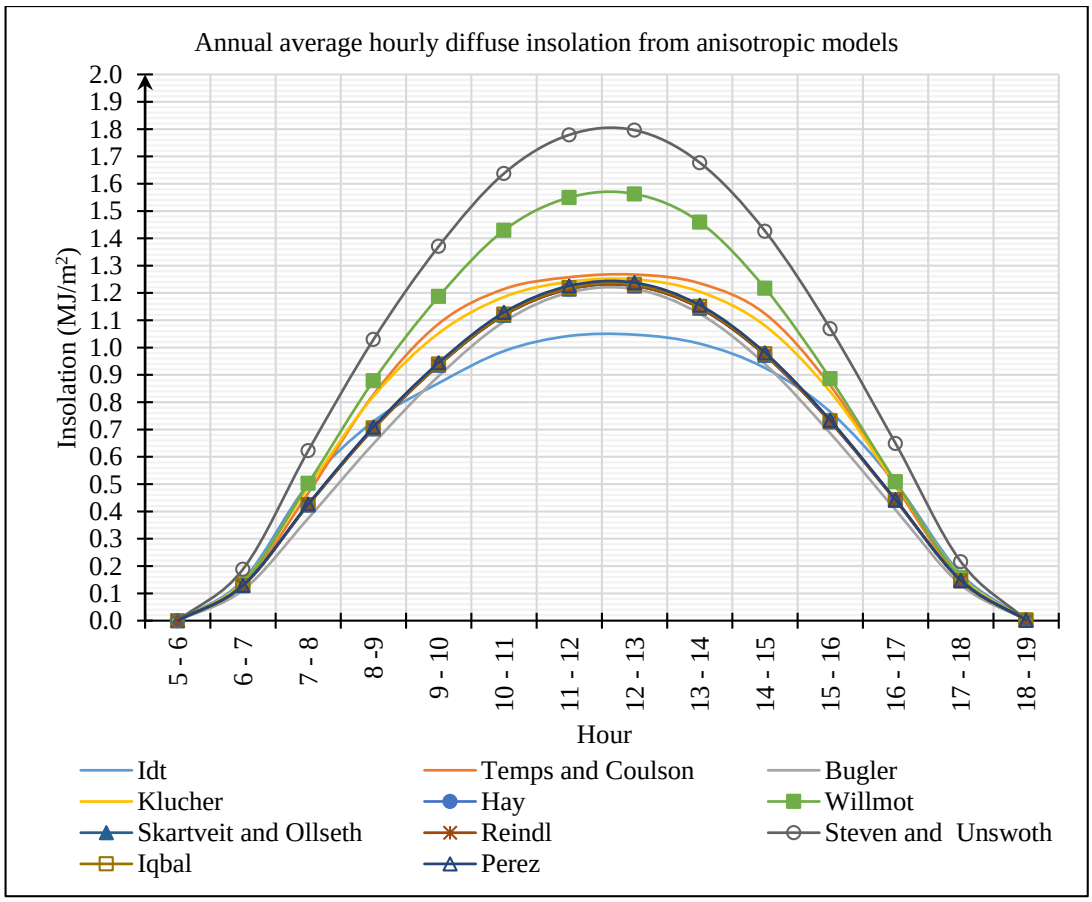

Figure 4.3 - Annual average hourly diffuse insolation from anisotropic models

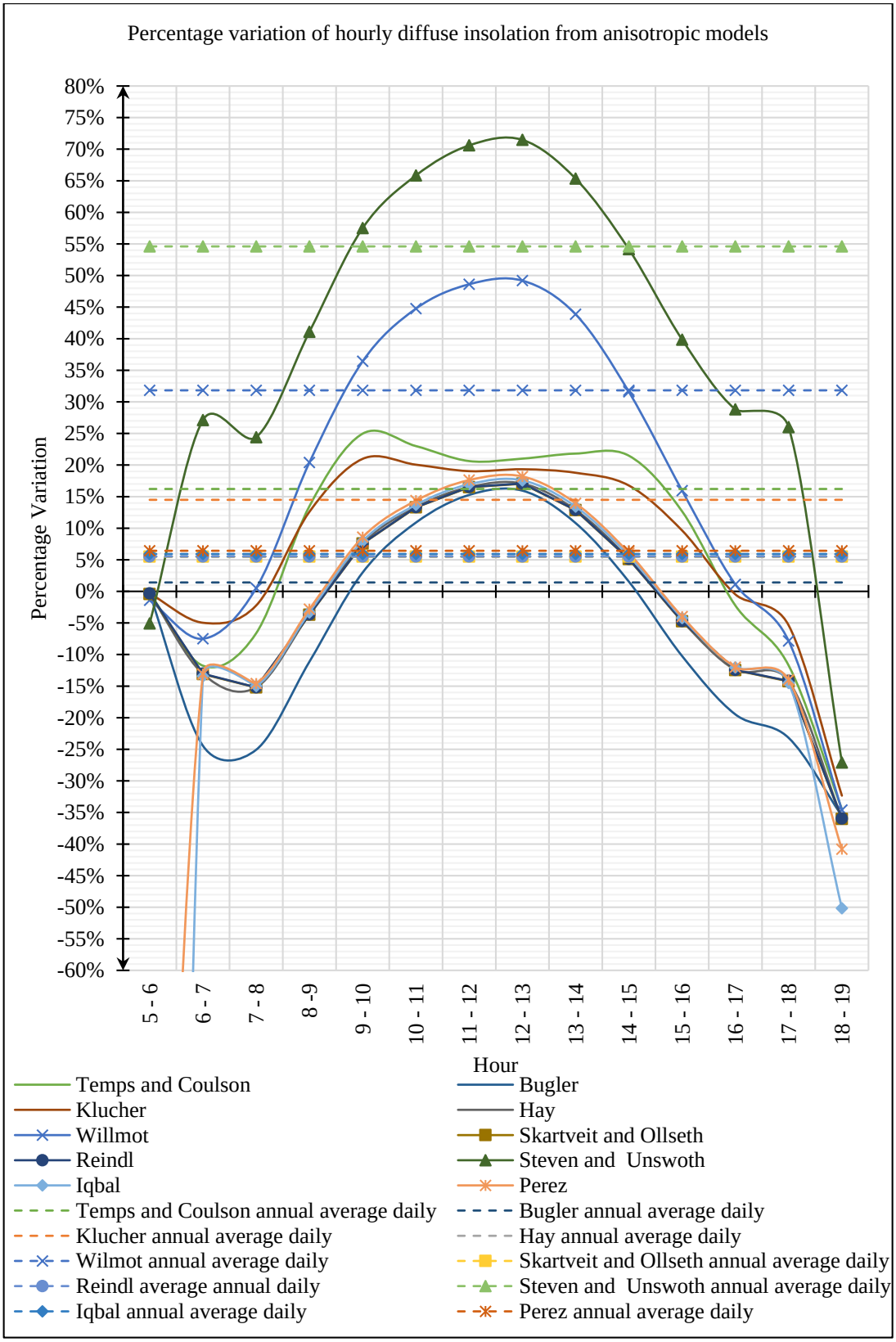

Figure 4.4 - Percentage variation of hourly insolation from anisotropic models

Wilmot (1982) and Steven and Unswoth (1980) models highly overestimate the hourly radiation among considered models having 31.82% and 54.60% variations of annual average diffuse insolation respectively. Temps and Coulson (1977) and Klucher (1979) models overestimate the radiation from 0800 hour to 1600 hour while under estimating the other hours resulting considerable overestimation of total daily diffuse radiation with variations of 16.21% and 14.49% of annual average daily diffuse insolation respectively. Behavior of the other anisotropic models Bugler (1979), Hay (1979), Skartveit and Ollseth (1986), Reindl (1990), Iqbal (1983) and Perez (1986) are same as the isotropic models having 1.42%, 5.52%, 5.49%, 5.52%, 5.91% and 6.42% annual average daily diffuse insolation respectively. Comparison among the models were performed using statistical parameters MBE, MAE, RMSE, MPE and MAPE and results are illustrated in Table 4.2.

Table 4.2 - Comparison of anisotropic models using statistical parameters

Model	MBE	MAE	RMSE	MPE	MAPE
Temps and Coulson	0.1164	0.1378	0.1781	20.98%	29.68%
Bugler	0.0102	0.0993	0.1355	3.83%	27.05%
Klucher	0.1040	0.1241	0.1684	21.43%	28.72%
Hay	0.0396	0.0898	0.1290	10.99%	24.61%
Willmot	0.2285	0.2483	0.3636	44.41%	51.92%
Skartveit and Ollseth	0.0394	0.0899	0.1290	10.96%	24.63%
Reindl	0.0397	0.0898	0.1290	11.00%	24.61%
Steven and Unswoth	0.3921	0.3949	0.4959	62.56%	64.35%
Iqbal	0.0424	0.0886	0.1283	11.15%	24.84%
Perez	0.0461	0.0928	0.1340	11.97%	25.26%

Table 4.2 indicates that Iqbal (1983) model shows minimum values for MAE and RMSE statistical parameters among ten anisotropic models. Therefore, it can be concluded that Iqbal (1983) model predict the hourly diffuse radiation more accurately than other anisotropic models.

4.1.3 Summary of Analysis of existing diffuse radiation models

Monthly averaged daily diffuse insolation for 7° due south faced surfaces were also predicted for each considered models and results are shown in Figure 4.5. Percentage variations of the predicted values are shown in the Figure 4.6.

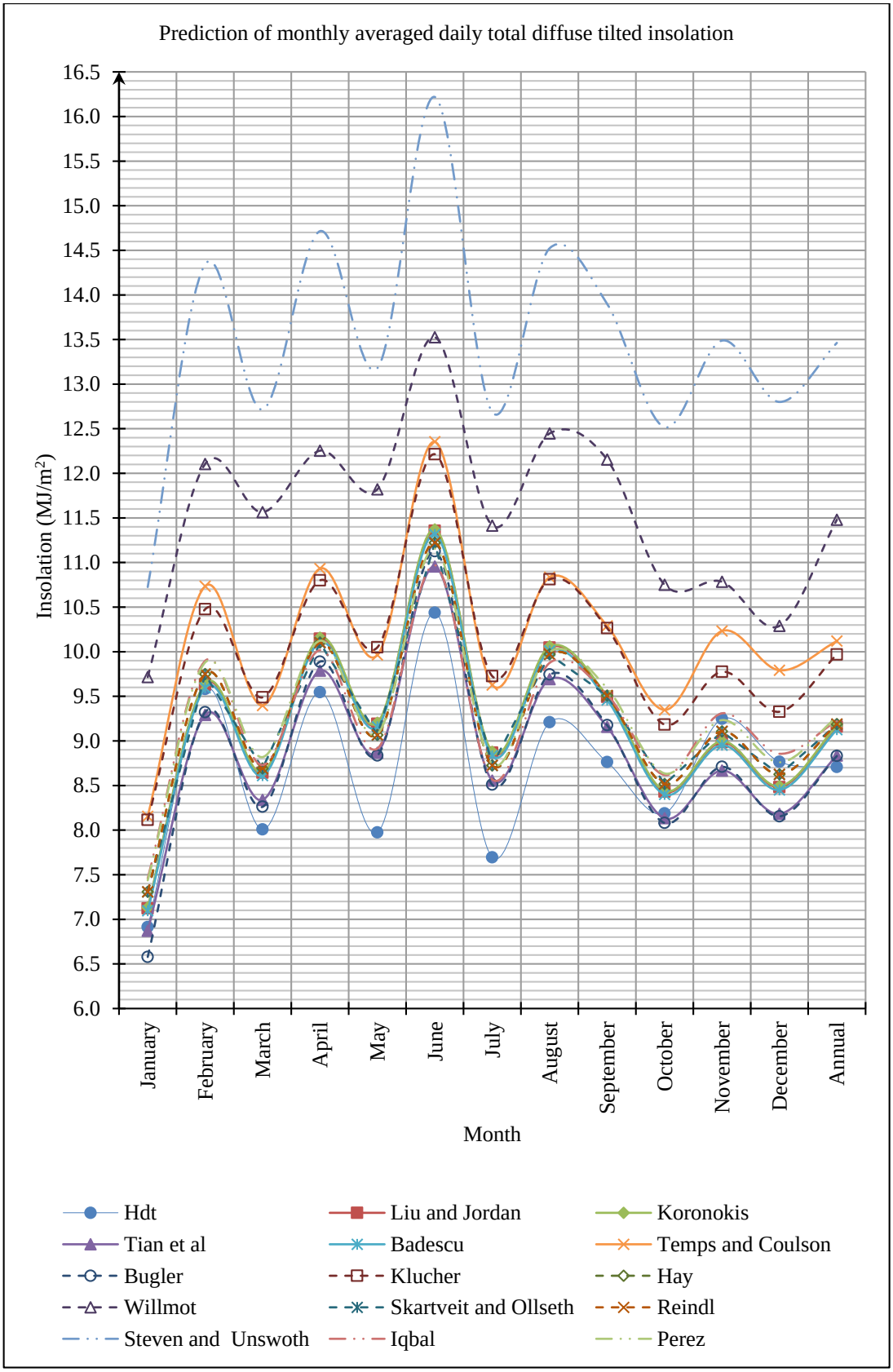

Figure 4.5 - Prediction of monthly averaged daily total diffuse tilted insolation

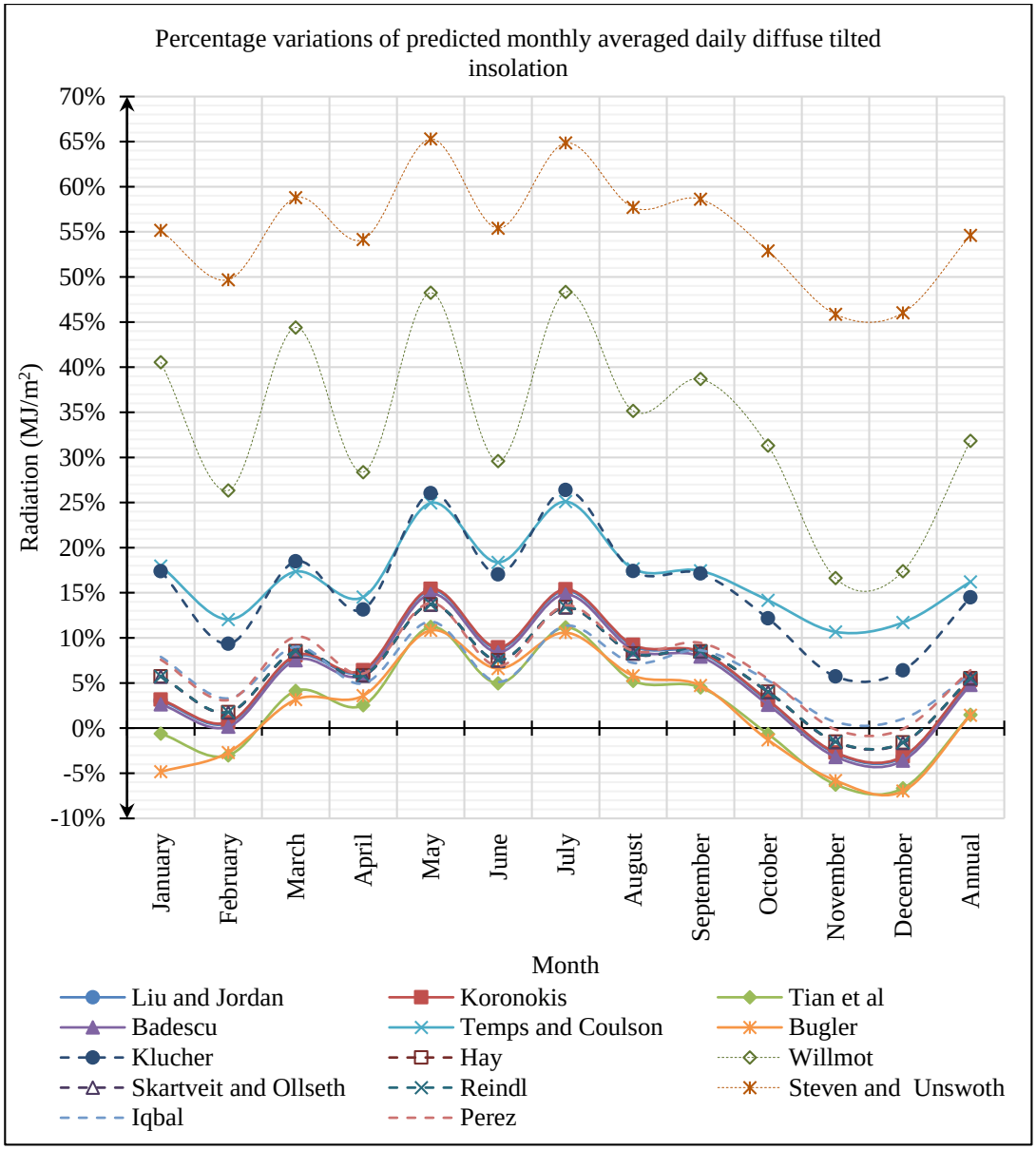

Figure 4.6 - Percentage variations of predicted monthly averaged daily diffuse tilted insolation

Figure 4.6 indicates that four anisotropic models Temps and Coulson (1979), Klucher (1979), Wilmot (1982) and Steven and Unswoth (1980) are overestimate the daily total diffuse radiation throughout the year. One isotropic model Tian et al and one anisotropic model Bugler overestimate the daily total diffuse radiation from vernal equinox to autumnal equinox while under estimating autumnal to vernal. Other models overestimate the daily total diffuse radiation around the year except months of November and December. Comparison among the models using statistical parameters MBE, MAE, RMSE, MPE and MAPE and results are illustrated in Figure 4.7.

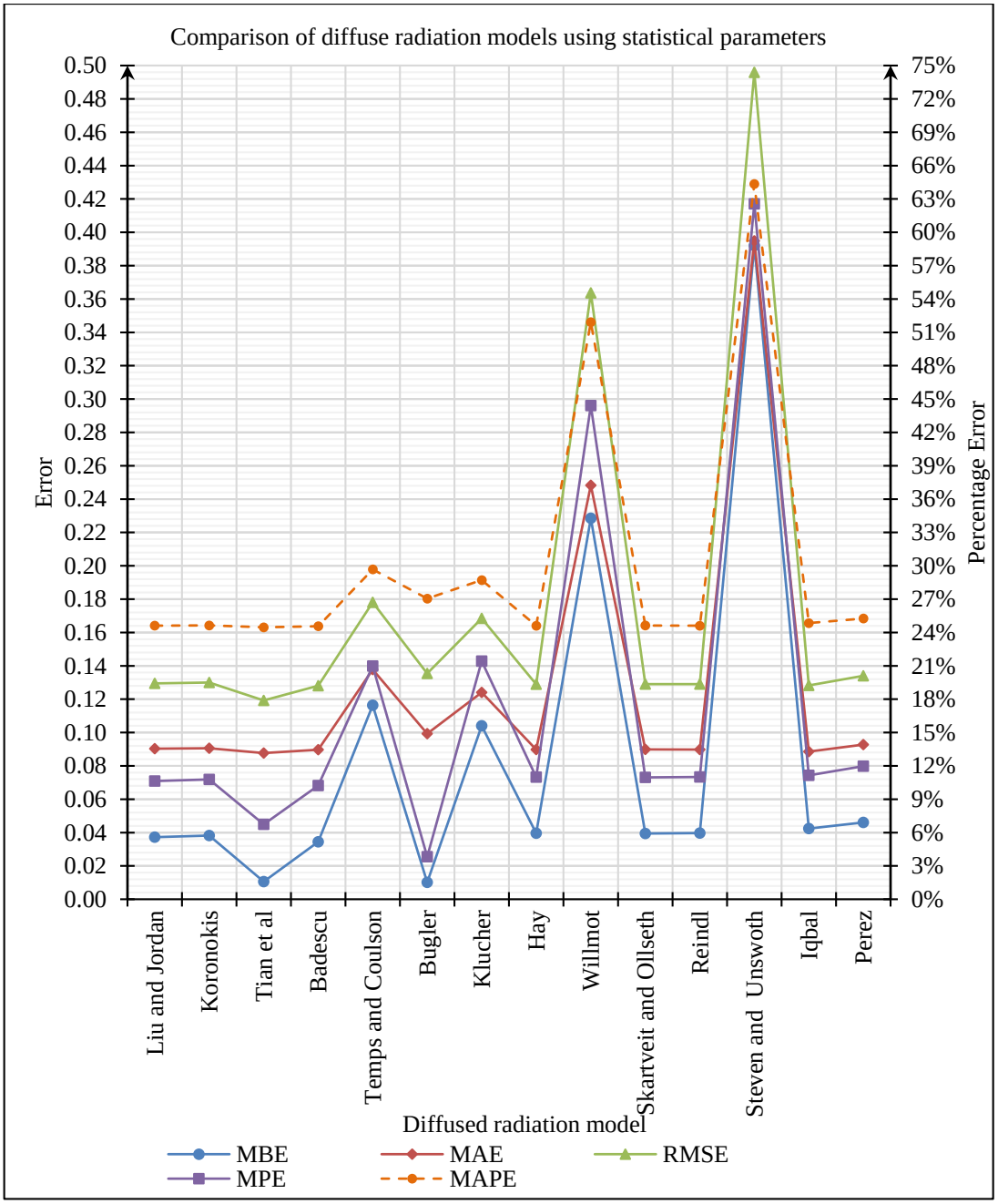

Figure 4.7 - Comparison of diffuse radiation models using statistical parameters

Figure 4.7 indicates that among all considered models, Bugler anisotropic model has comparatively high MAE, RMSE and MAPE even though it has least MBE and MPE values among considered models. Therefore, Bugler model cannot be considered as accurate model for prediction of diffuse radiation. Tian et al model has minimum RMSE, MAE and MAPE values. Hence, it can be concluded that among all considered

models Tian et al isotropic model predicts the diffuse radiation more accurately than other models.

4.2 Development of new diffuse radiation model suitable for dry zone in Sri Lanka

Existing hourly diffuse solar radiation models were modified and statistically compared as described in section 3.2. Modified Perez et al (1990) model shows the better statistical performance and comparison among Tian et al (2001), Bugler (1977), Iqbal (1983), Perez (1990) and modified model is shown in Table 4.3.

Table 4.3 - Comparison of modified Perez model using statistical parameters

Model	MBE	MAE	RMSE	MPE	MAPE
Tian et al	0.0106	0.0877	0.1192	6.74%	24.47%
Bugler	0.0102	0.0993	0.1355	3.83%	27.05%
Iqbal	0.0424	0.0886	0.1283	11.15%	24.84%
Perez	0.0461	0.0928	0.1340	11.97%	25.26%
Modified Perez	0.0209	0.0735	0.1021	5.67%	19.95%

Table 4.3 indicates that modified model has minimum values for MAE, RMSE and MAPE even though MBE and MPE not minimum. Therefore, it can be concluded that new model can predict the hourly diffuse solar radiation more accurately than previous hourly diffuse radiation models.

Modified Brightness coefficient of Perez et al (1990) hourly diffuse radiation model are shown in Table 4.4.

Table 4.4 - Modified Brightness coefficient of Perez et al

ε	f_{11}	f_{12}	f_{13}	f_{21}	f_{22}	f_{23}
1.000 – 1.065	-0.008	0.588	-0.062	0.055	-0.194	-0.011
1.065 – 1.230	0.130	0.683	-0.151	-0.032	-0.012	0.004
1.230 – 1.500	0.330	0.487	-0.221	-0.063	-0.187	0.106
1.500 – 1.950	0.568	0.187	-0.295	-0.204	-0.120	0.212
1.950 – 2.800	0.873	-0.392	-0.362	-0.517	0.295	0.358
2.800 – 4.500	1.132	-1.237	-0.412	-1.140	1.684	0.553
4.500 – 6.200	1.060	-1.600	-0.359	-1.732	3.224	0.923
6.200 - ∞	0.678	-0.327	-0.250	-3.910	16.730	1.275

Normal probability plot, residual plot, observation order plot and histogram of the modified model are shown in Figure 4.9, Figure 4.10, Figure 4.11 and Figure 4.12 respectively.

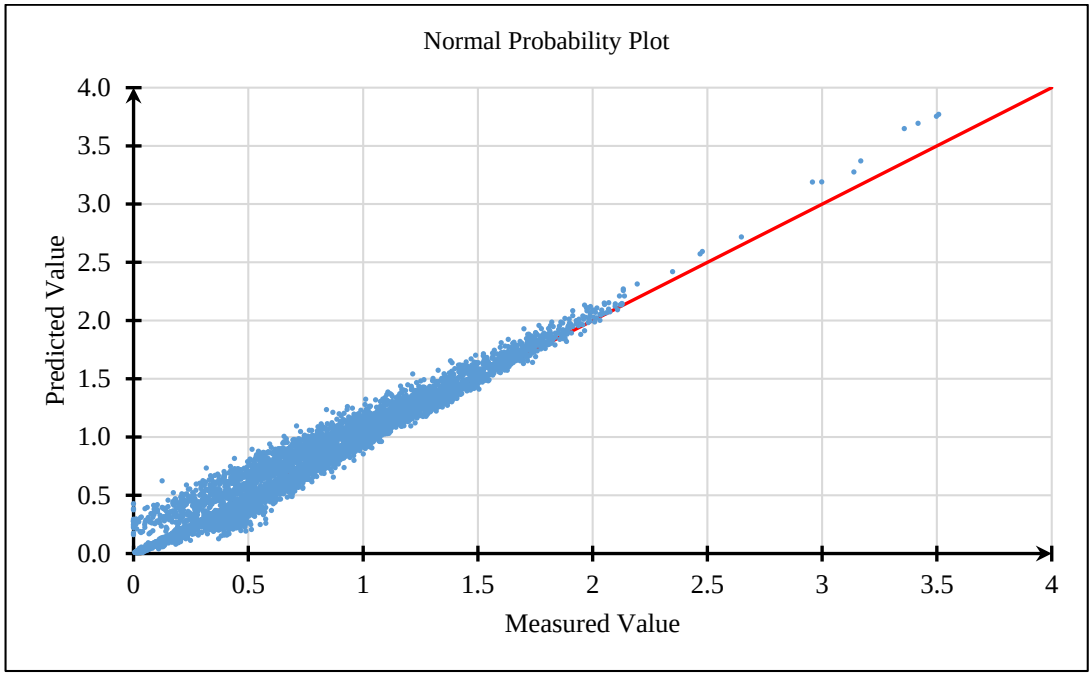

Figure 4.8 - Normal probability plot of modified Perez model

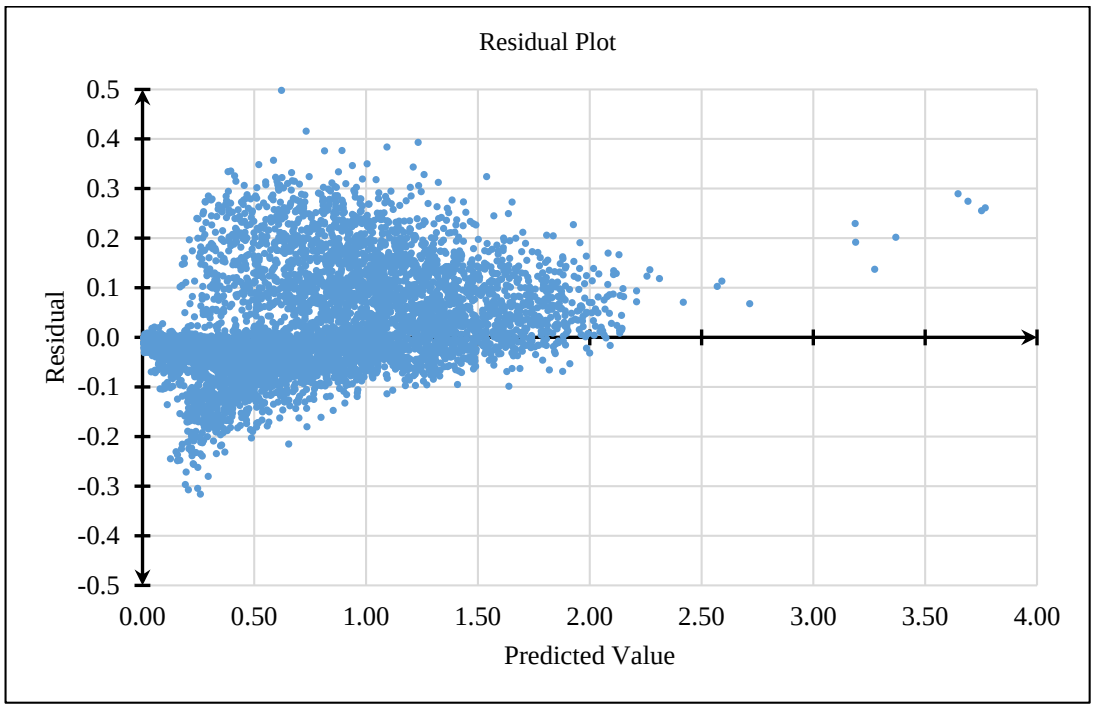

Figure 4.9 - Residual plot of modified Perez model

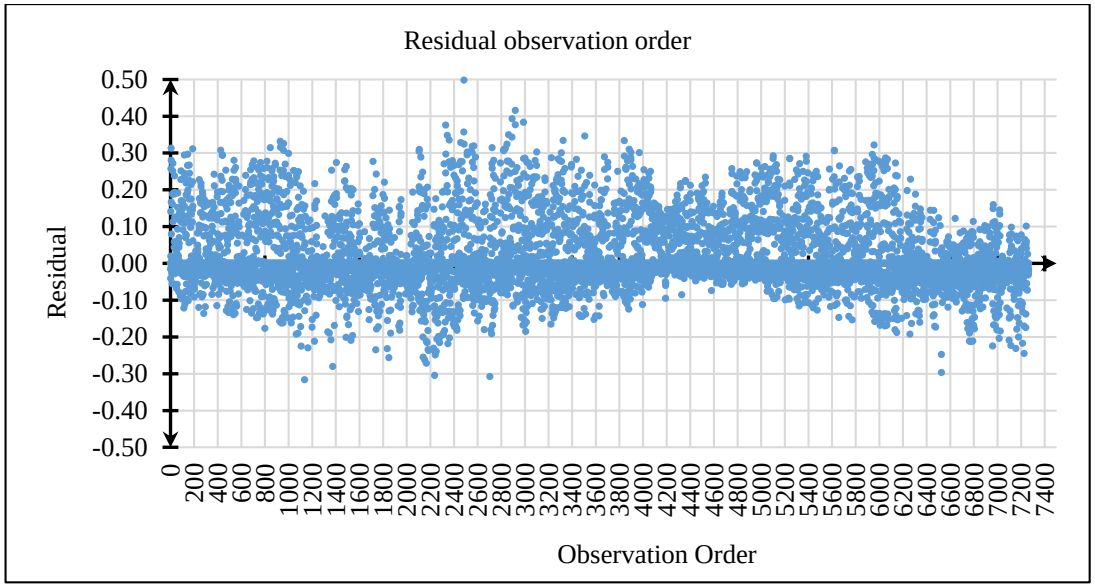

Figure 4.10 - Residual observation order of modified Perez model

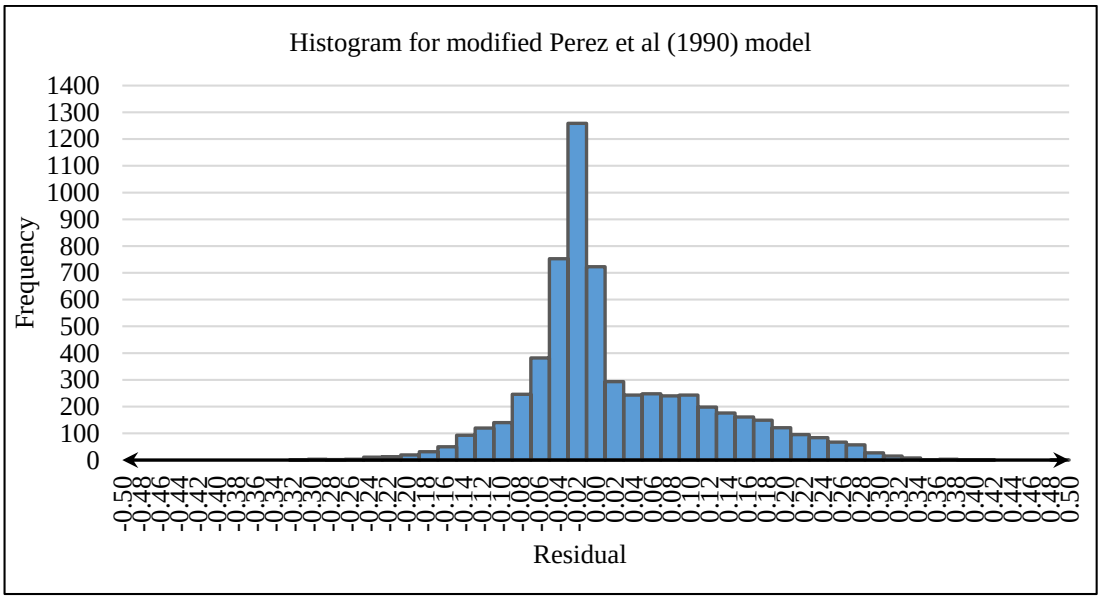

Figure 4.11 - Histogram for modified Perez et al (1990) model

Figure 4.8 described the normality of the model. Randomly distributed residuals in Figure 4.9 indicates the appropriateness of the model. Figure 4.10 describes that, there is no significance deviations of the prediction with considered time period. Therefore, model can be used for prediction of diffuse radiation throughout the year. Histogram of the model has symmetrically distributed with negative centre at -0.02 residual value indicating that approximate normal distribution.

4.3 Estimation of solar radiation potential on horizontal surfaces in dry zone in Sri Lanka

4.3.1 Estimation of Annually averaged hourly radiation

Annual hourly solar energy potential derived from actual measured data from August 2011 to December 2012 at Hambanthota are shown in Figure 4.12. annually averaged hourly beam normal radiation, beam tilted radiation at 7° tilt angle, diffuse tilted and diffuse total at same tilt angle and clearness index are also plotted in Figure 4.12 and same values are tabulated in Table 4.5.

Table 4.5 - Annually averaged hourly Insolation

Hour	Annually averaged hourly insolation						
	I	I_d	I_t	I_b	I_{bt} @ β=7°	I_{bn}	I_{dt} @ β=7°
	MJ/m^2	MJ/m^2	MJ/m^2	MJ/m^2	MJ/m^2	MJ/m^2	MJ/m^2
5-6	0.00	0.00	0.00	0.00	0.00	0.00	0.00
6-7	0.17	0.13	0.19	0.04	0.04	0.32	0.15
7-8	0.81	0.42	0.89	0.38	0.39	1.09	0.50
8-9	1.56	0.70	1.60	0.86	0.87	1.52	0.73
9-10	2.16	0.94	2.11	1.23	1.24	1.65	0.87
10-11	2.60	1.12	2.49	1.48	1.50	1.70	0.99
11-12	2.78	1.22	2.63	1.57	1.58	1.67	1.04
12-13	2.79	1.23	2.63	1.57	1.58	1.65	1.05
13-14	2.60	1.14	2.49	1.46	1.47	1.64	1.01
14-15	2.14	0.97	2.10	1.16	1.17	1.51	0.93
15-16	1.48	0.73	1.52	0.75	0.76	1.26	0.76
16-17	0.76	0.44	0.83	0.32	0.32	0.82	0.50
17-18	0.20	0.15	0.22	0.05	0.05	0.33	0.17
18-19	0.00	0.00	0.00	0.00	0.00	0.01	0.00
Total	20.07	9.19	19.69	10.87	10.98	15.17	8.71

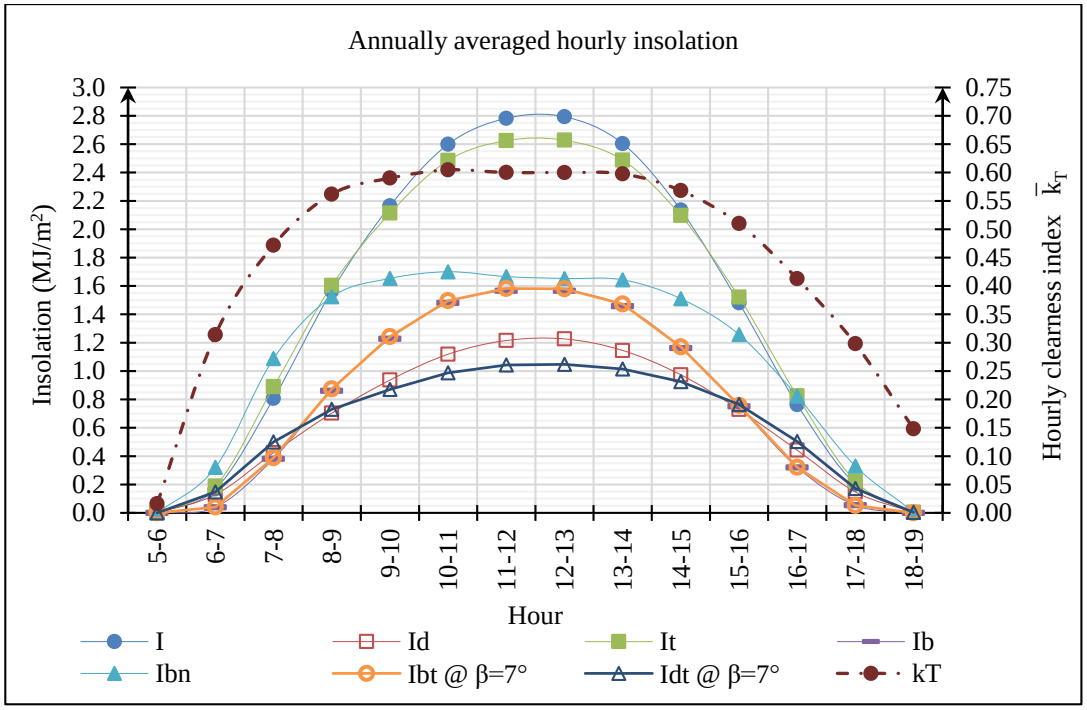

Figure 4.12 - Annually averaged hourly insolation

Figure 4.12 indicates that hourly global horizontal radiation is higher than the global tilted radiation 0900 hour to 1500 hour during the averaged day. It also indicates that difference between the global horizontal and global tilted radiation is almost equal to the difference between two diffuse components. There is no significant difference between the beam horizontal radiation and beam tilted radiation. Hence, it can be concluded that there is no significant advantage of tilting the surface towards due south by same angle equal to latitude for fixed axis systems. Figure 4.12 also indicates that variation of the beam normal radiation and clearness index is significantly low during the 0800 hour to 1500 hour illustrating that potential of maximising the energy generation by solar system using single axis hourly tracking system.

4.3.2 Estimation of monthly averaged hourly radiation

Monthly averaged hourly solar energy radiation also derived using the same data set at Hambanthota. Monthly averaged hourly global horizontal, beam horizontal, diffuse horizontal, global tilted, beam tilted, diffuse tilted and beam normal plots are shown in Figure 4.13 to 4.19 respectively. Tabulated values are given in appendix A to G respectively.

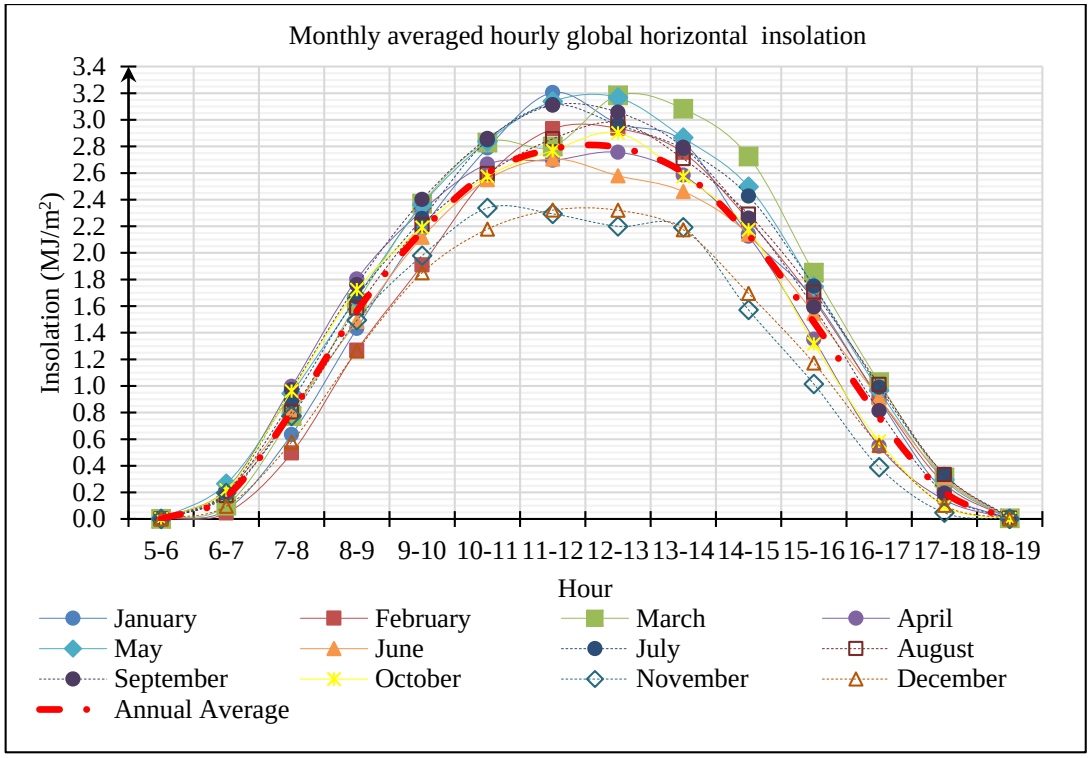

Figure 4.13 - Monthly averaged hourly global horizontal insolation

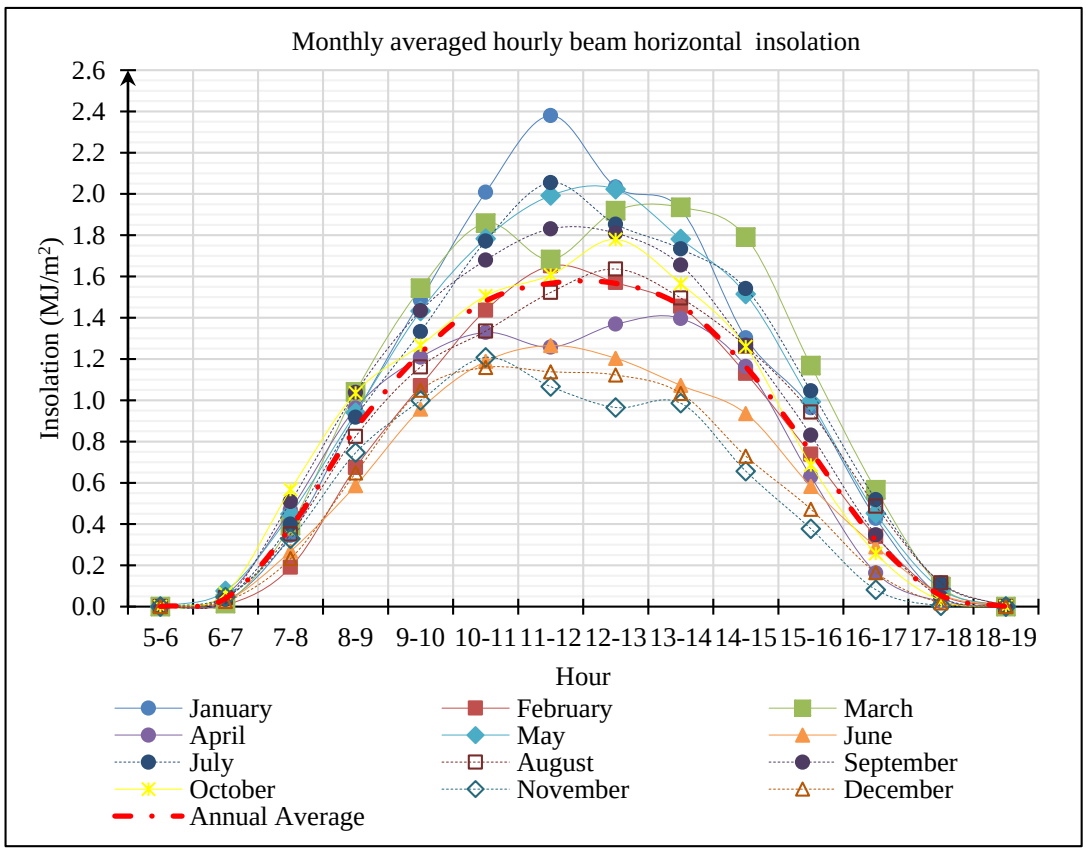

Figure 4.14 -Monthly averaged hourly beam horizontal insolation

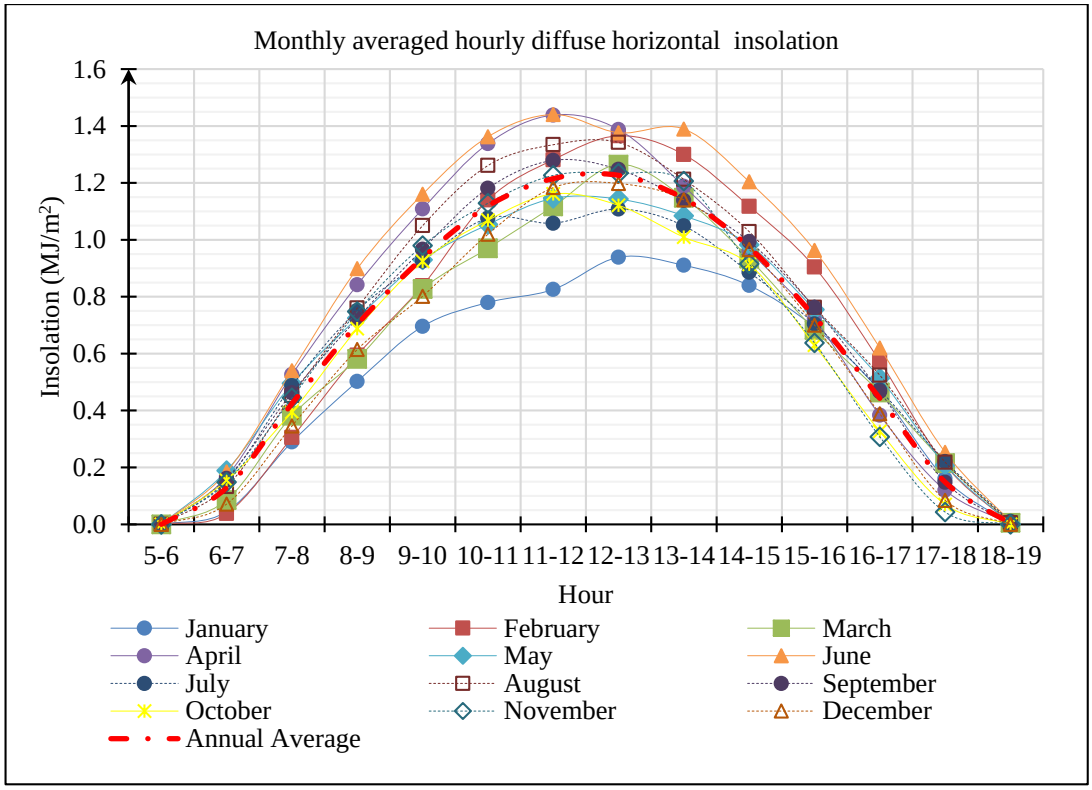

Figure 4.15 - Monthly averaged hourly diffuse horizontal insolation

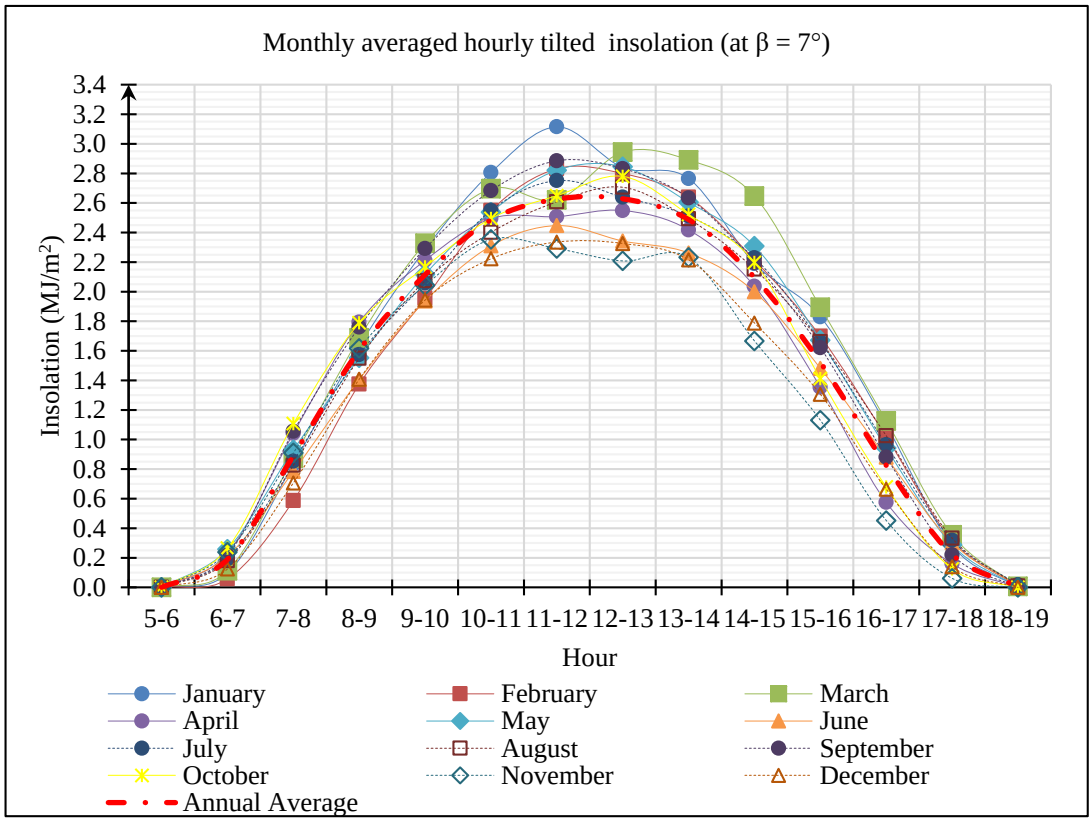

Figure 4.16 - Monthly averaged hourly tilted insolation (at β = 7°)

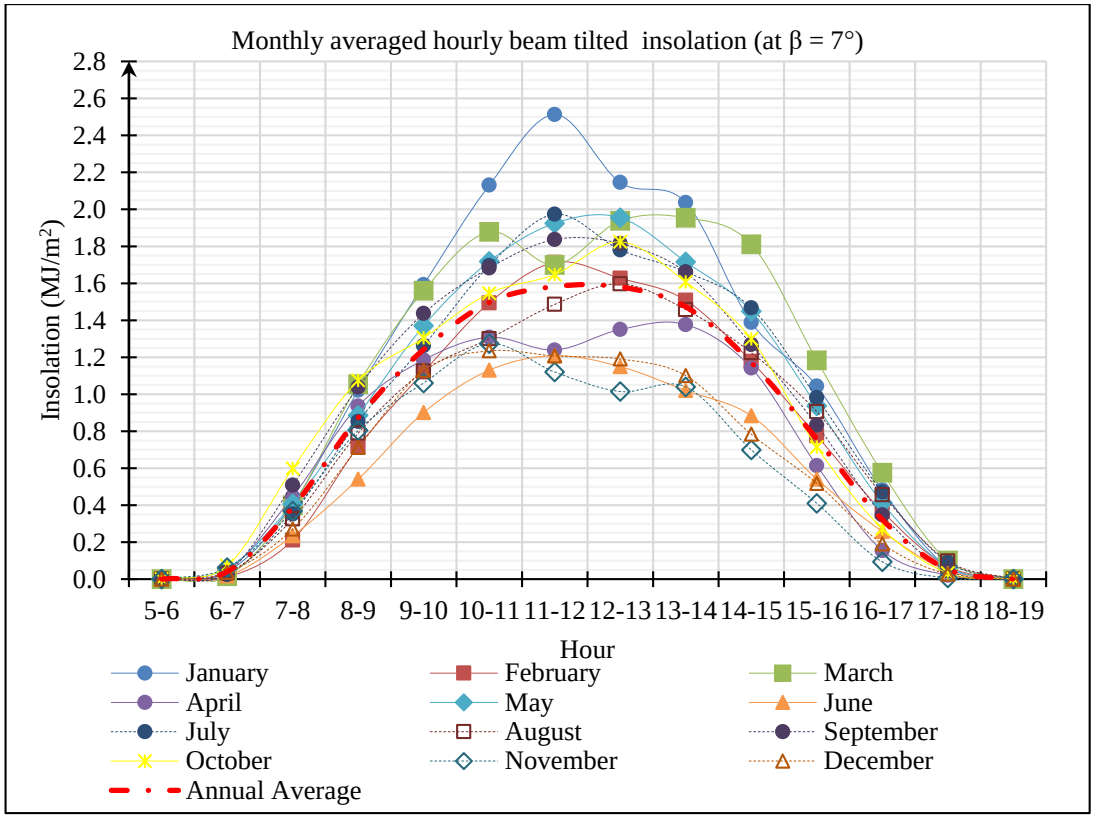

Figure 4.17 - Monthly averaged hourly beam tilted insolation (at β = 7°)

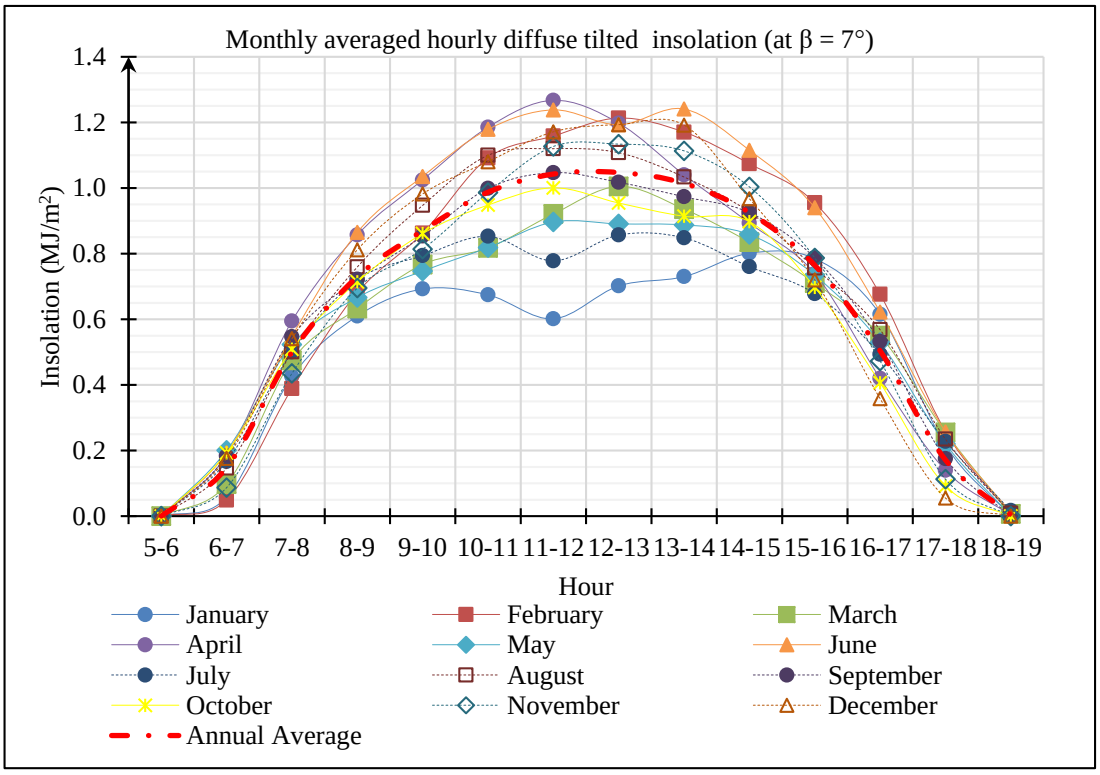

Figure 4.18 - Monthly averaged hourly diffuse tilted insolation (at β = 7°)

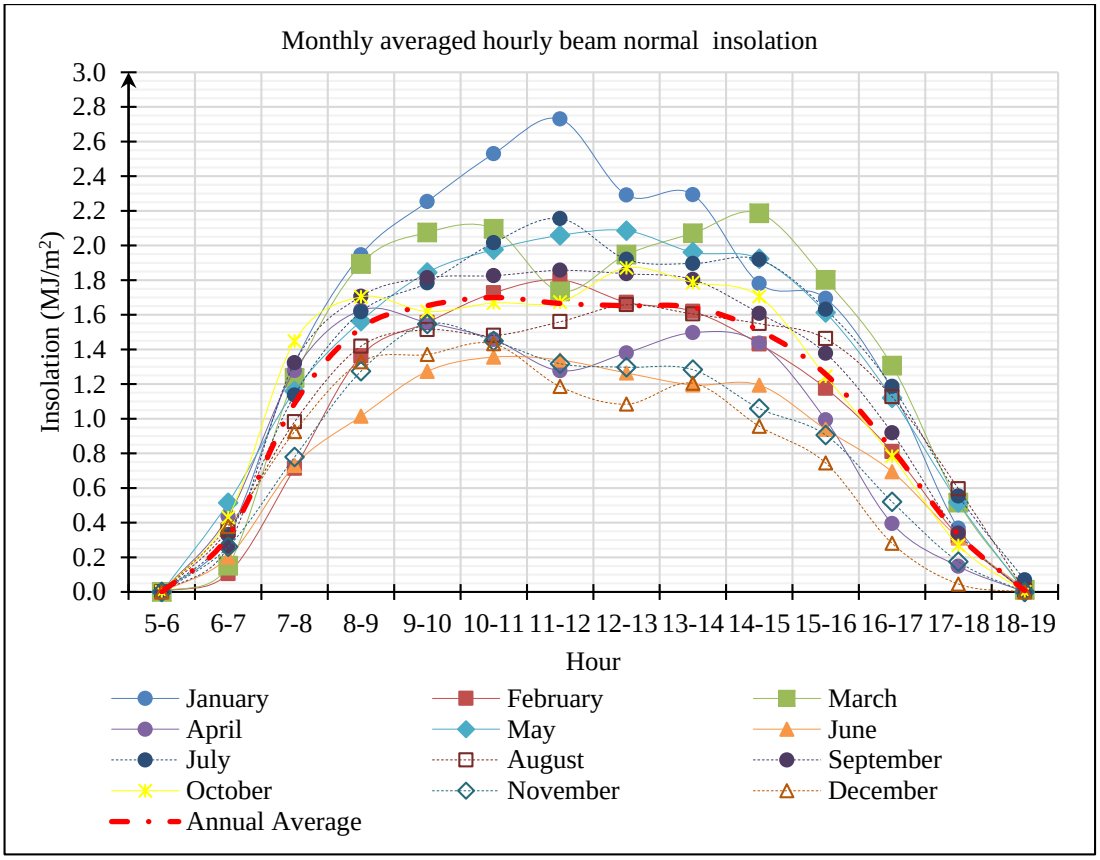

Figure 4.19 - Monthly averaged hourly beam normal insolation

Maximum global horizontal radiation occurs during the months of May and July while lowest occurs at months of November and December according to the Figure 4.13. In moths of November and December Sun is traveling on its lowest altitude path in south and fixed solar systems are tilted to latitude angle to capture energy equally during the highest and lowest path of Sun. Figure 4.19 also indicates that beam normal radiation has its lowest values during the month of November and December. Therefore, it implies that tilting to south by angle equal to latitude angle may not be the optimum tilted angle.

4.3.3 Estimation of monthly averaged clearness index

Monthly averaged hourly clearness index also calculated and values are tabulated in Table 4.6. and graphical presentation is given in Figure 4.20. Annually averaged clearness index and boundary lines between the clear sky conditions and partly cloudy sky condition also plotted in the Figure 4.20.

Table 4.6 - Monthly averaged hourly clearness index $\bar{K}_T$

Monthly averaged hourly clearness index $\bar{K}_T$													
Hour	January	February	March	April	May	June	July	August	September	October	November	December	Annual
5-6	0.00	0.00	0.00	0.00	0.00	0.00	0.00	0.00	0.00	0.00	0.00	0.00	0.02
6-7	0.32	0.22	0.28	0.37	0.37	0.32	0.35	0.32	0.30	0.29	0.26	0.32	0.31
7-8	0.48	0.37	0.49	0.55	0.51	0.46	0.53	0.47	0.52	0.49	0.38	0.43	0.47
8-9	0.59	0.51	0.60	0.62	0.58	0.54	0.62	0.57	0.59	0.56	0.49	0.53	0.56
9-10	0.65	0.55	0.64	0.61	0.63	0.59	0.63	0.60	0.62	0.56	0.54	0.54	0.59
10-11	0.69	0.61	0.64	0.60	0.66	0.61	0.68	0.60	0.64	0.57	0.54	0.55	0.60
11-12	0.72	0.63	0.58	0.56	0.68	0.60	0.69	0.61	0.65	0.57	0.53	0.51	0.60
12-13	0.66	0.62	0.65	0.57	0.68	0.57	0.64	0.63	0.63	0.61	0.53	0.49	0.60
13-14	0.66	0.61	0.66	0.57	0.66	0.58	0.64	0.60	0.62	0.59	0.53	0.53	0.60
14-15	0.58	0.56	0.67	0.54	0.66	0.57	0.64	0.58	0.59	0.59	0.49	0.45	0.57
15-16	0.57	0.52	0.58	0.44	0.59	0.52	0.57	0.55	0.54	0.48	0.44	0.40	0.51
16-17	0.47	0.43	0.48	0.27	0.50	0.46	0.48	0.49	0.44	0.36	0.35	0.27	0.41
17-18	0.29	0.29	0.33	0.17	0.37	0.35	0.34	0.37	0.30	0.25	0.23	0.15	0.30
18-19	0.09	0.08	0.16	0.11	0.06	0.20	0.19	0.15	0.00	0.00	0.00	0.00	0.15
Daily	0.62	0.56	0.61	0.54	0.62	0.55	0.61	0.57	0.59	0.55	0.48	0.49	0.56

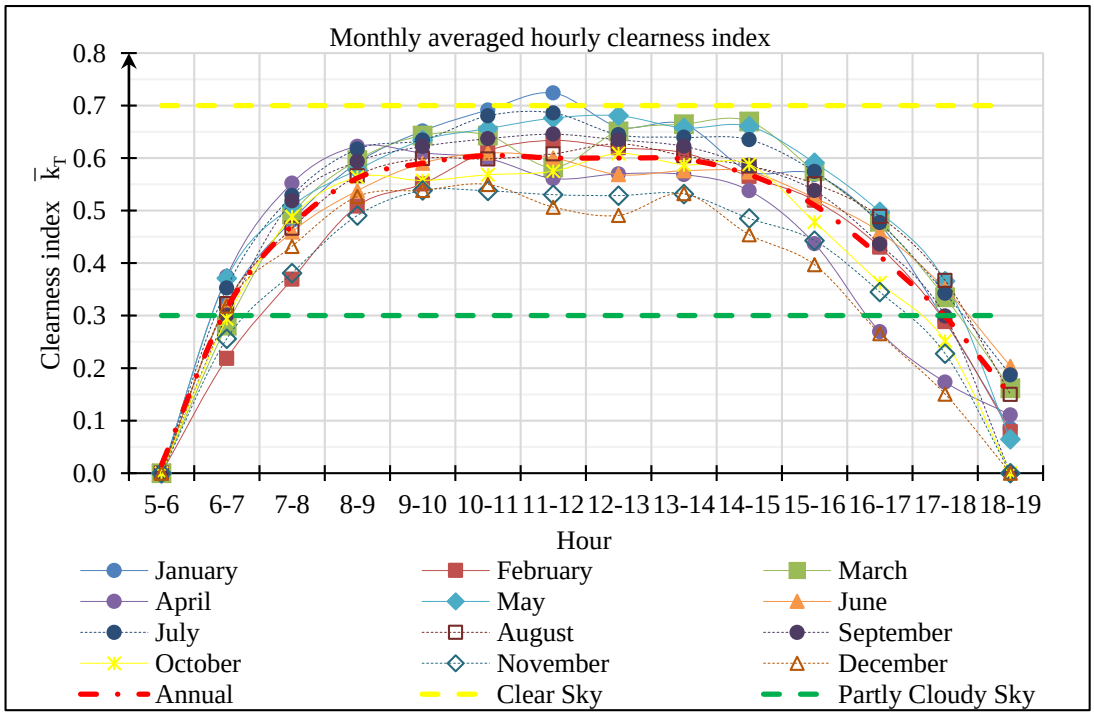

Figure 4.20 - Monthly averaged hourly clearness index

According to the Table 4.6 and Figure 4.20 November and December months are cloudier than other months and January, March, May and July months are lies in the upper part of the partly cloudy region. According the Figure 4.20 clear sky conditions occurs only in the 1100 hour to 1200 hour in January for whole year. Figure 4.20 also indicates that Sri Lanka has partly cloudy sky condition throughout year. Hence, it can be concluded that diffuse radiation component also has a significant impact on the global radiation and should be considered when selecting the suitable tilt angles for solar energy collecting systems.

4.3.4 Estimation of monthly averaged daily radiation

Monthly averaged daily insolation derived from actual measured data from August 2011 to December 2012 at Hambanthota are shown in Figure 4.21. Monthly averaged daily beam normal radiation, beam tilted radiation at 7° tilt about east west axis in due south orientation, diffuse tilted and diffuse total at same tilt angle and clearness index are also plotted in Figure 4.20 and same values are tabulated in Table 4.7.

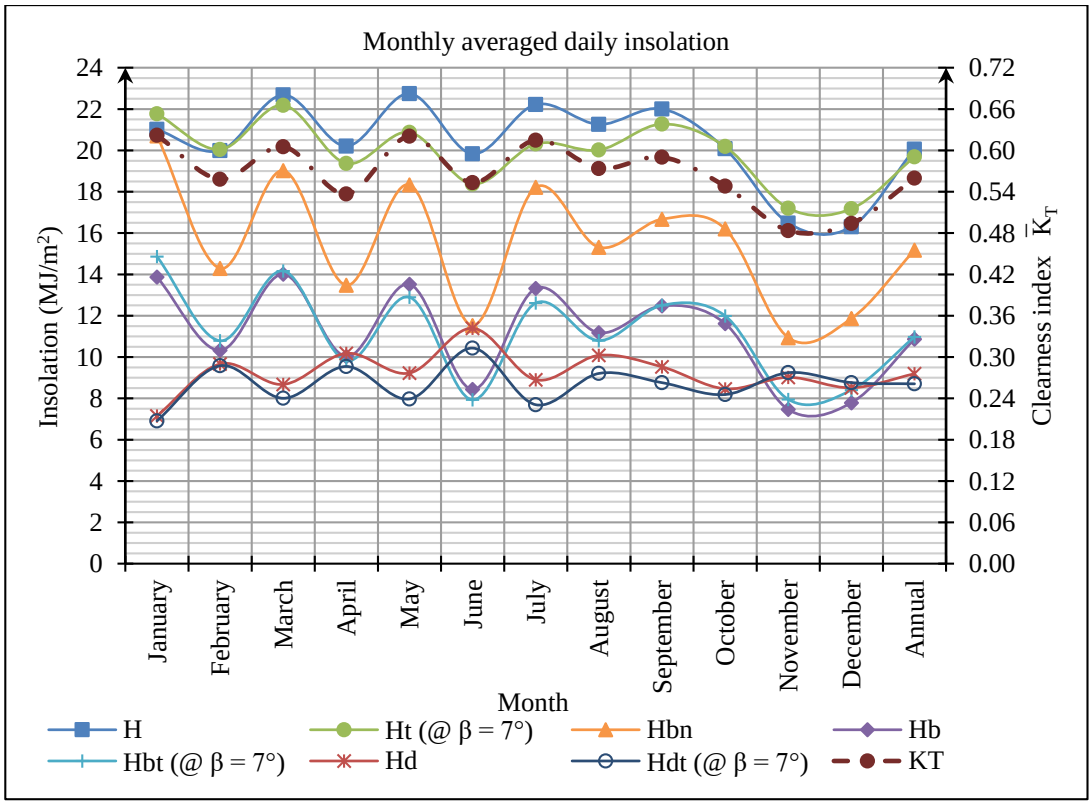

Figure 4.21 - Monthly averaged daily insolation

Table 4.7 - Monthly averaged daily insolation

Month	H	H_b	H_d	H_t (@ β = 7°)	H_{bt} (@ β = 7°)	H_{dt} (@ β = 7°)	H_{bn}
	MJ/m^2	MJ/m^2	MJ/m^2	MJ/m^2	MJ/m^2	MJ/m^2	MJ/m^2
January	21.02	13.87	7.15	21.78	14.87	6.91	20.70
February	19.99	10.32	9.67	20.05	10.79	9.58	14.29
March	22.69	14.01	8.68	22.19	14.17	8.01	19.03
April	20.21	10.03	10.18	19.37	9.82	9.55	13.48
May	22.75	13.52	9.23	20.88	12.90	7.97	18.34
June	19.83	8.44	11.40	18.38	7.93	10.44	11.53
July	22.22	13.32	8.90	20.32	12.62	7.70	18.22
August	21.26	11.18	10.08	20.02	10.80	9.21	15.32
September	22.01	12.48	9.53	21.28	12.51	8.76	16.67
October	20.09	11.62	8.46	20.19	12.00	8.19	16.20
November	16.48	7.47	9.02	17.21	7.95	9.25	10.94
December	16.30	7.79	8.51	17.18	8.40	8.77	11.87
Annual	20.07	10.87	9.19	19.69	10.98	8.71	15.17

According to the Figure 4.20 and Table 4.6 maximum global horizontal solar resource potential occurs in May which is 22.75 MJ/m^2/day (6.32 kWh/m^2/day) and minimum of 16.30 MJ/m^2/day (4.52 kWh/m^2/day) occurs in December. The annual average global horizontal solar insolation is 20.07 MJ/m^2/day (5.75 kWh/m^2/day). Figure 4.20 also indicates that seasonal variations of solar radiation potential is minimum except months of November and December which has 18% less potential than the annual average. According to the Figure 4.20 except Months of January, November and December all other months global horizontal radiation is higher than the global tilted radiation.

4.4 Estimation of solar radiation potential on tilted surfaces in dry zone in Sri Lanka

4.4.1 Annual averaged insolation on tilted surfaces

Predicted annual averaged daily insolation on due south faced surfaces from -45° to +45° are shown in Figure 4.22.

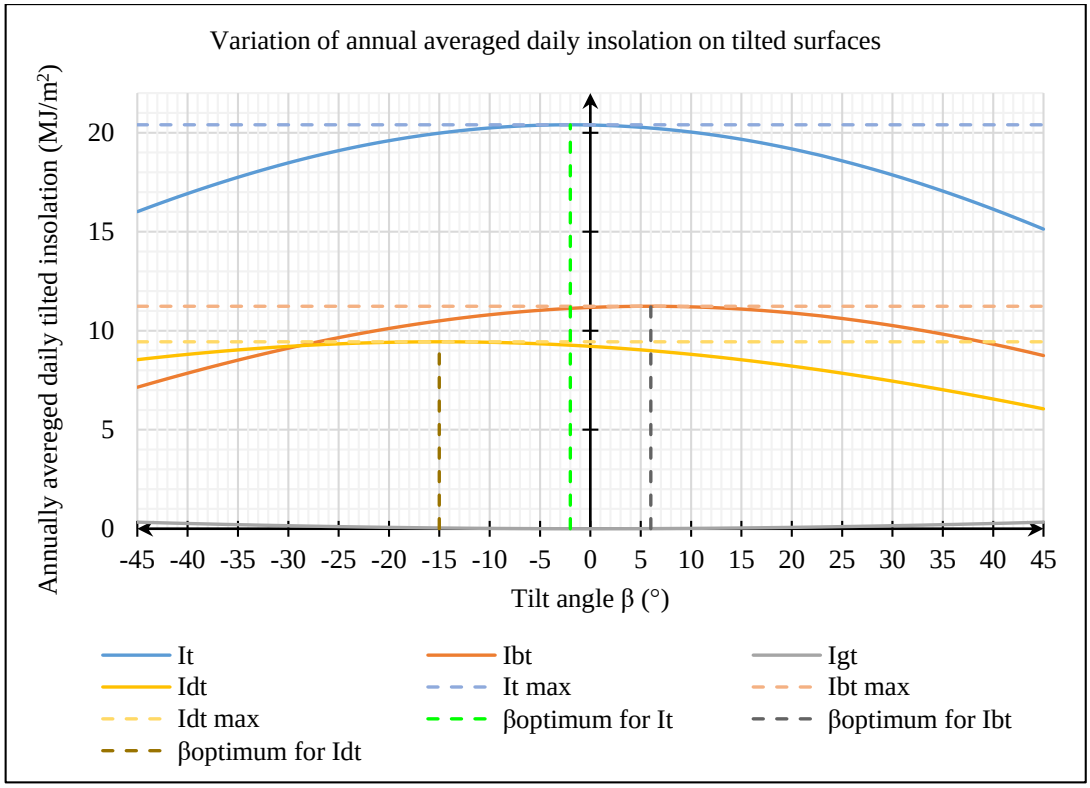

Figure 4.22 - Variation of annual averaged daily insolation on tilted surfaces

According to the Figure 4.22 maximum of 20.40 MJ/m^2/day (5.67 kWh/m^2/day) annually averaged daily global insolation occurs on due north faced 2° tilted surfaces and maximum of 11.24 MJ/m^2/day (3.12 kWh/m^2/day) annually averaged daily beam insolation occurs on due south faced 6° tilted surfaces. Therefore, it can be suggested that due north faced 2° tilt angle is suitable for fixed axis solar photovoltaic systems and parabolic collector systems. In addition to that, due south faced 6° tilt angle which is equal to latitude angle is more suitable for flat plate collector systems, where its intention is to utilised the beam radiation as much as possible.

4.4.2 Monthly averaged daily insolation on tilted surfaces

Predicted monthly averaged daily global insolation on due south faced and due north faced surfaces up to 45° are shown in Figure 4.23. Annually averaged daily values are also plotted on Figure 4.23 as reference line.

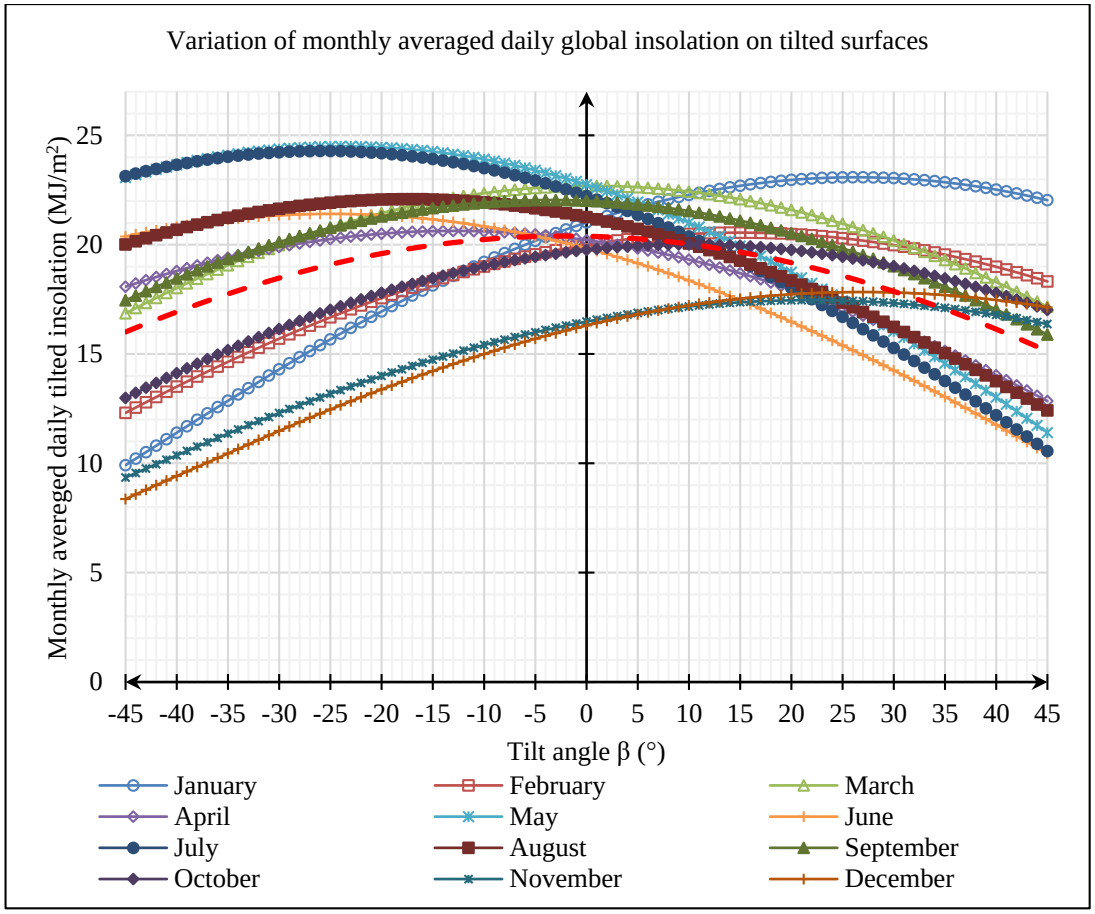

Figure 4.23 - Variation of monthly averaged daily global insolation on tilted surfaces

According to the Figure 4.23 optimum tilt angle for maximising the daily global insolation varies throughout the year and maximum for April to August occurs on due north faced surfaces while maximum for October to February occurs on due south faced surfaces and maximum for March and September occurs on nearly horizontal faced surfaces. Hence, it can be concluded that there exist potential to maximise energy collection by using east-west axis monthly tracking systems.

Monthly averaged daily global insolation, beam insolation, diffuse insolation and ground reflected insolation for January to December were calculated and graphical representation with optimum tilt angle and maximum global insolation are given in Figure 4.24 to Figure 4.35 respectively. Tabulated values for Monthly averaged daily global insolation, beam insolation and diffuse insolation are given in Appendix H to J respectively.

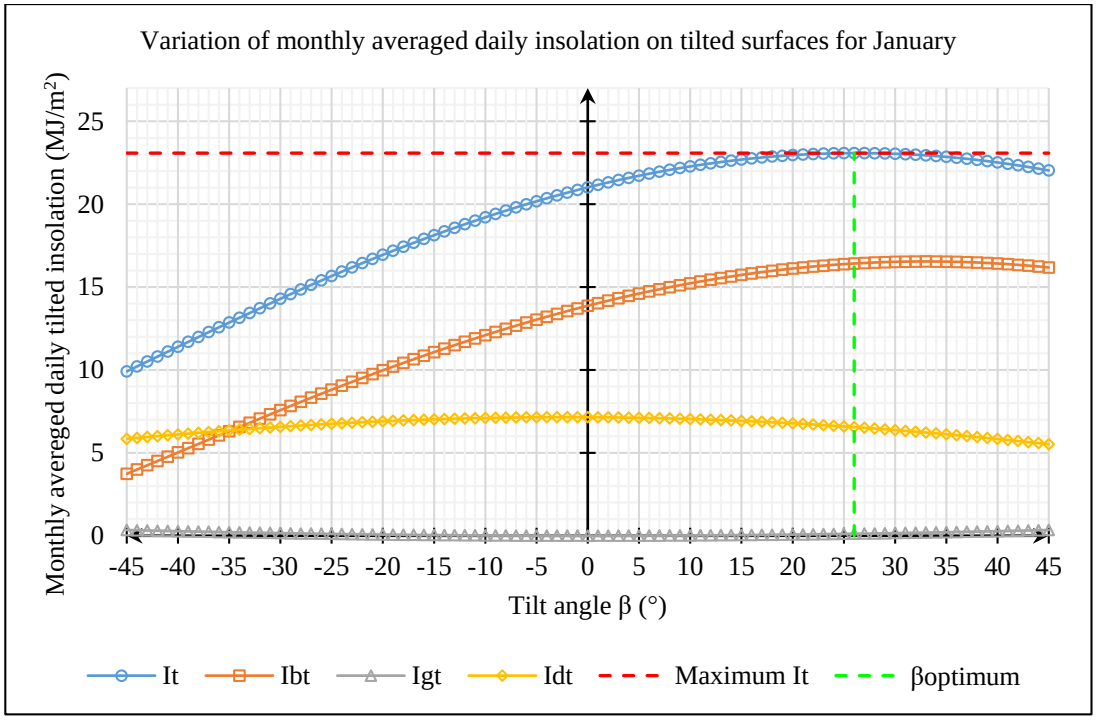

Figure 4.24 - Variation of monthly averaged daily insolation on tilted surfaces for January

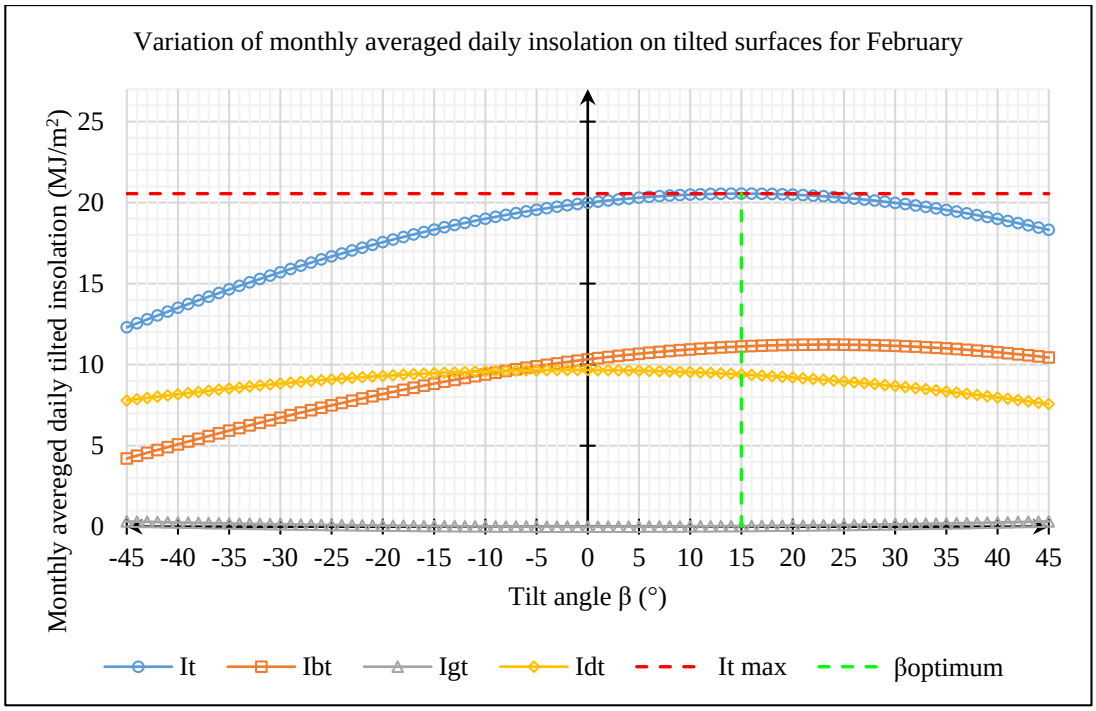

Figure 4.25 - Variation of monthly averaged daily insolation on tilted surfaces for February

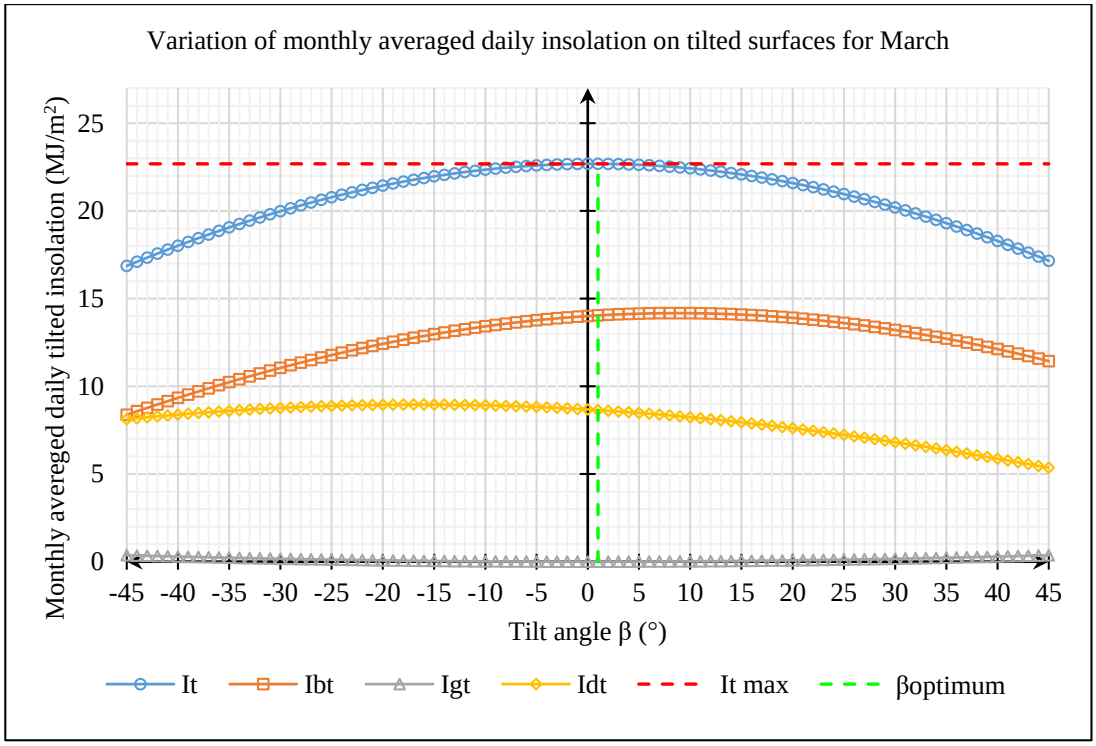

Figure 4.26 - Variation of monthly averaged daily insolation on tilted surfaces for March

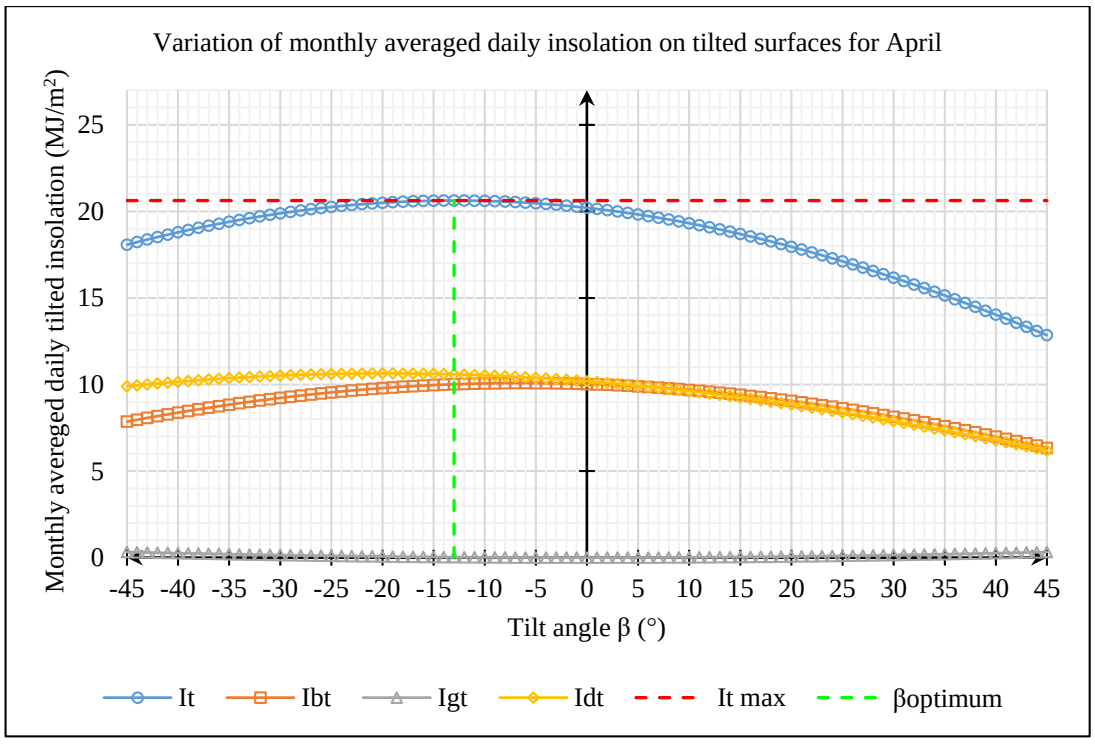

Figure 4.27 - Variation of monthly averaged daily insolation on tilted surfaces for April

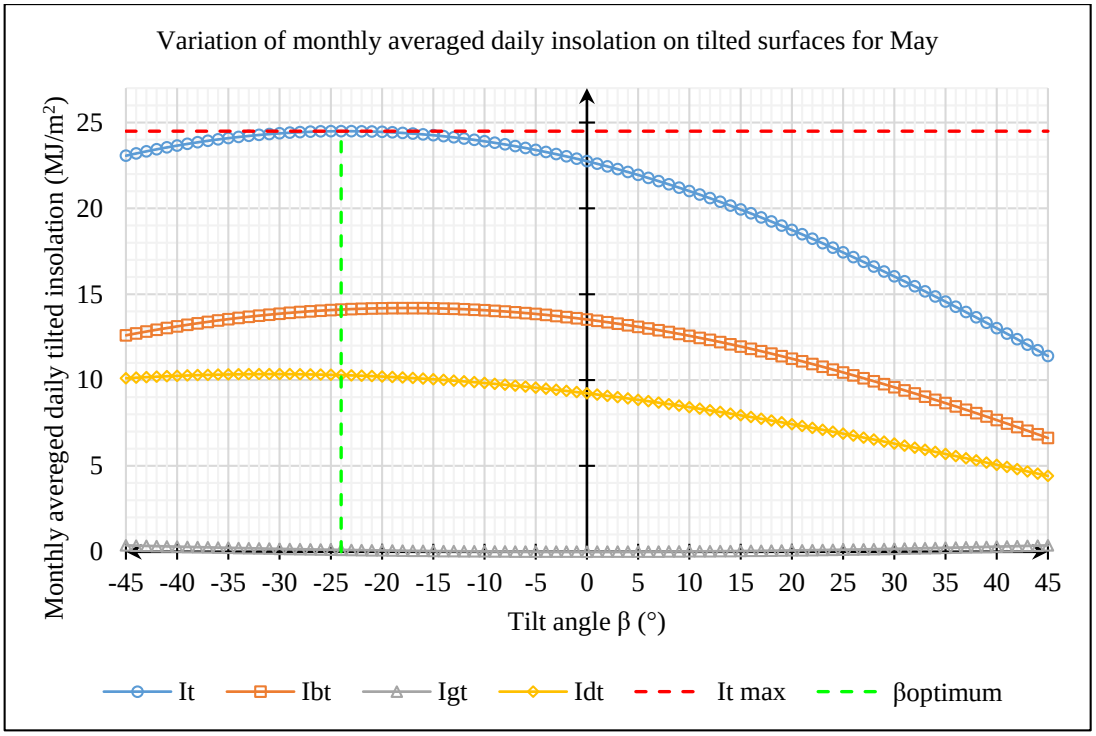

Figure 4.28 - Variation of monthly averaged daily insolation on tilted surfaces for May

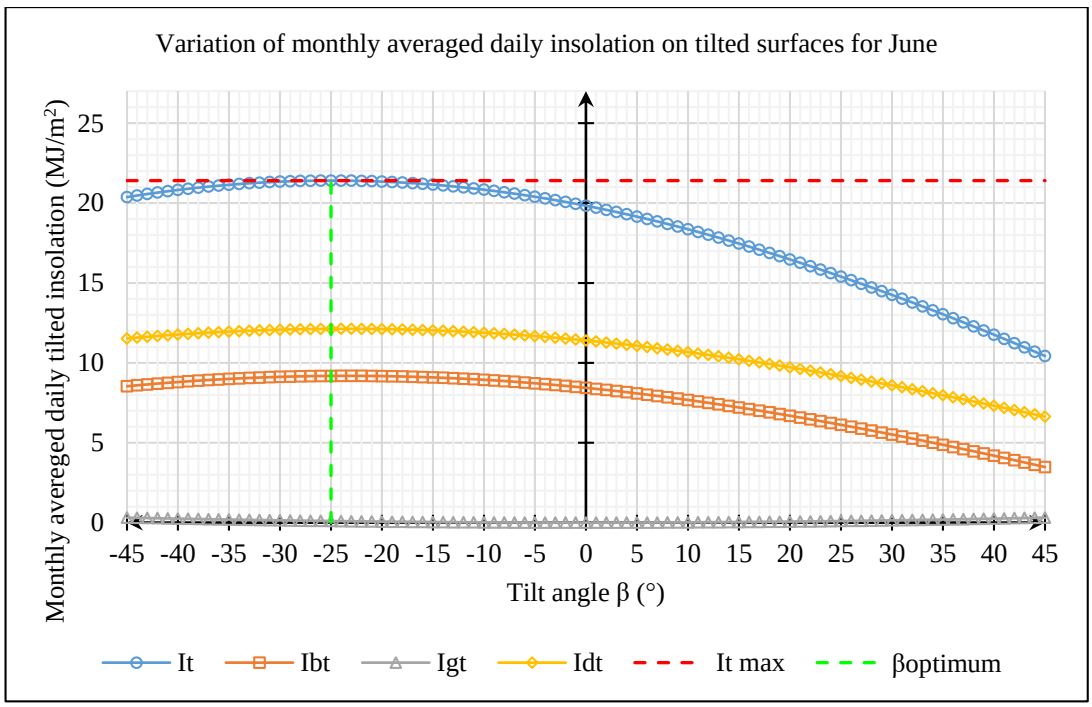

Figure 4.29 - Variation of monthly averaged daily insolation on tilted surfaces for June

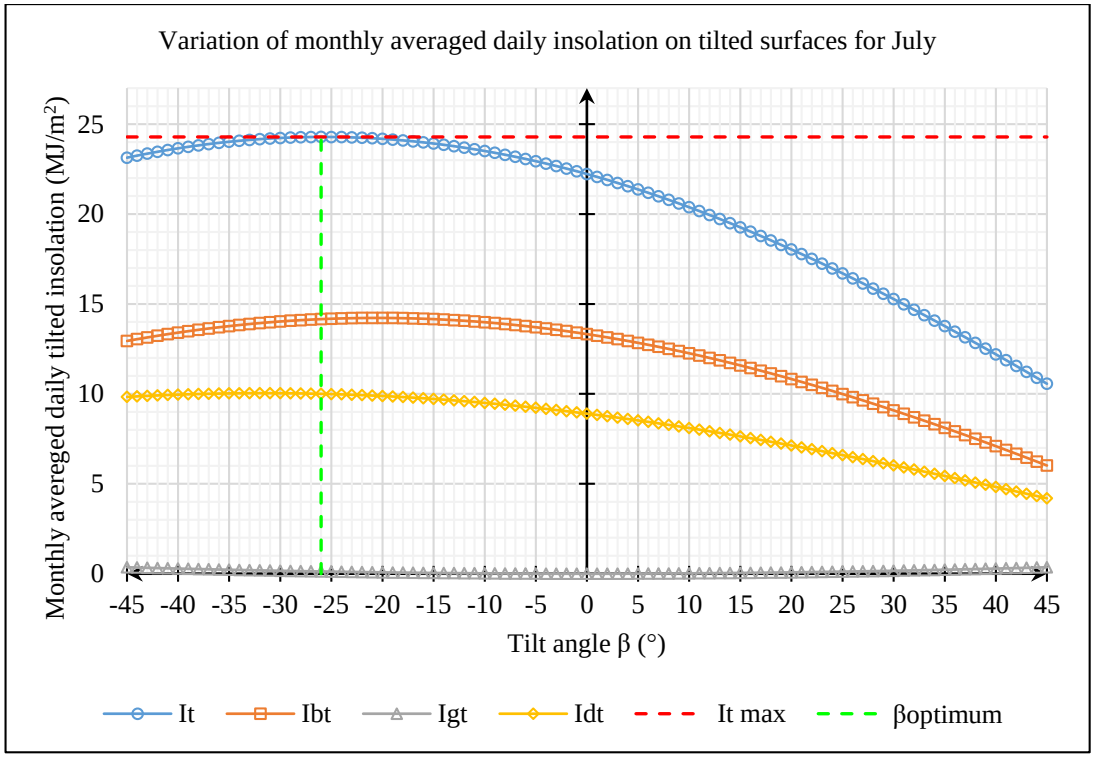

Figure 4.30 - Variation of monthly averaged daily insolation on tilted surfaces for July

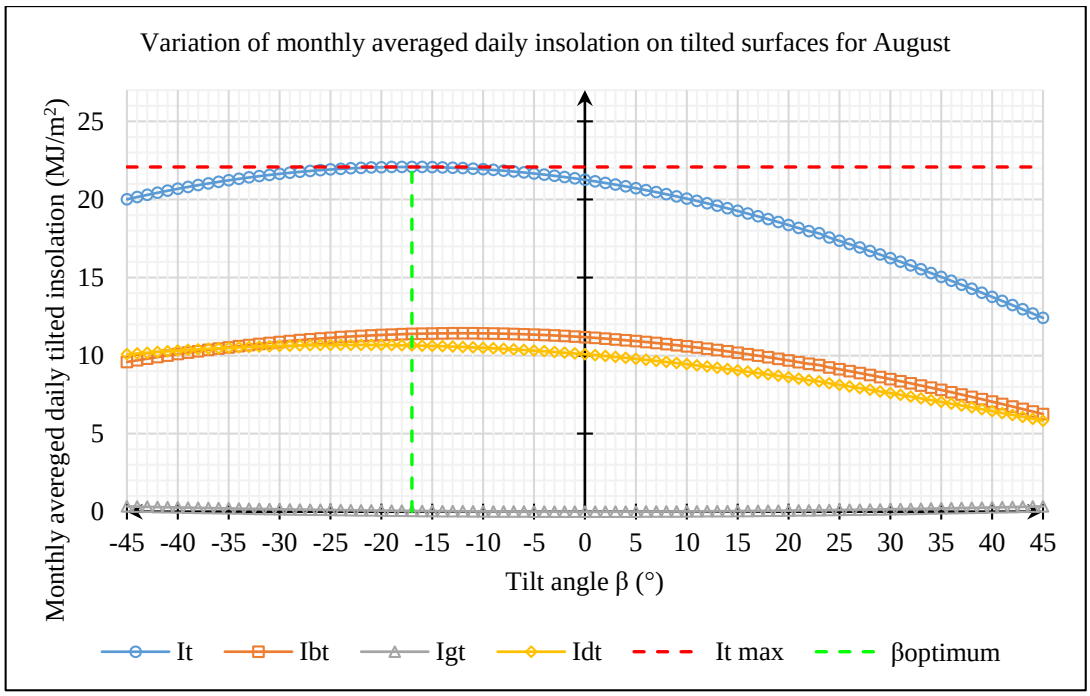

Figure 4.31 - Variation of monthly averaged daily insolation on tilted surfaces for August

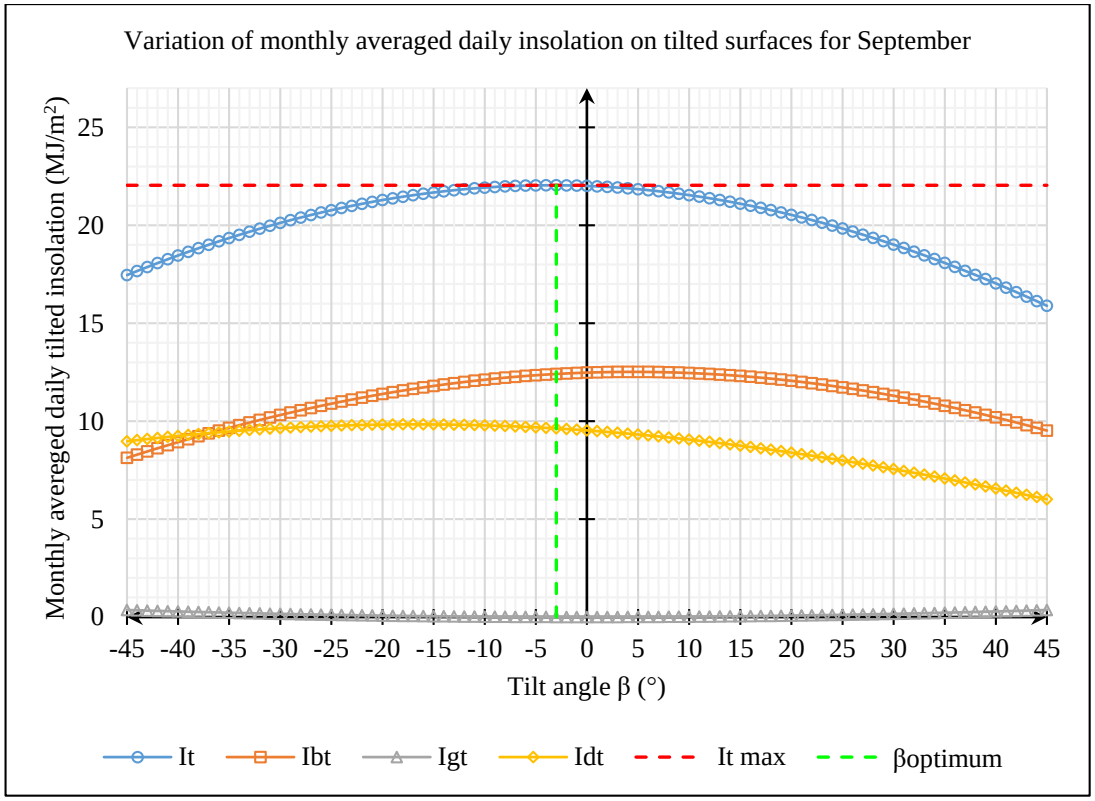

Figure 4.32 - Variation of monthly averaged daily insolation on tilted surfaces for September

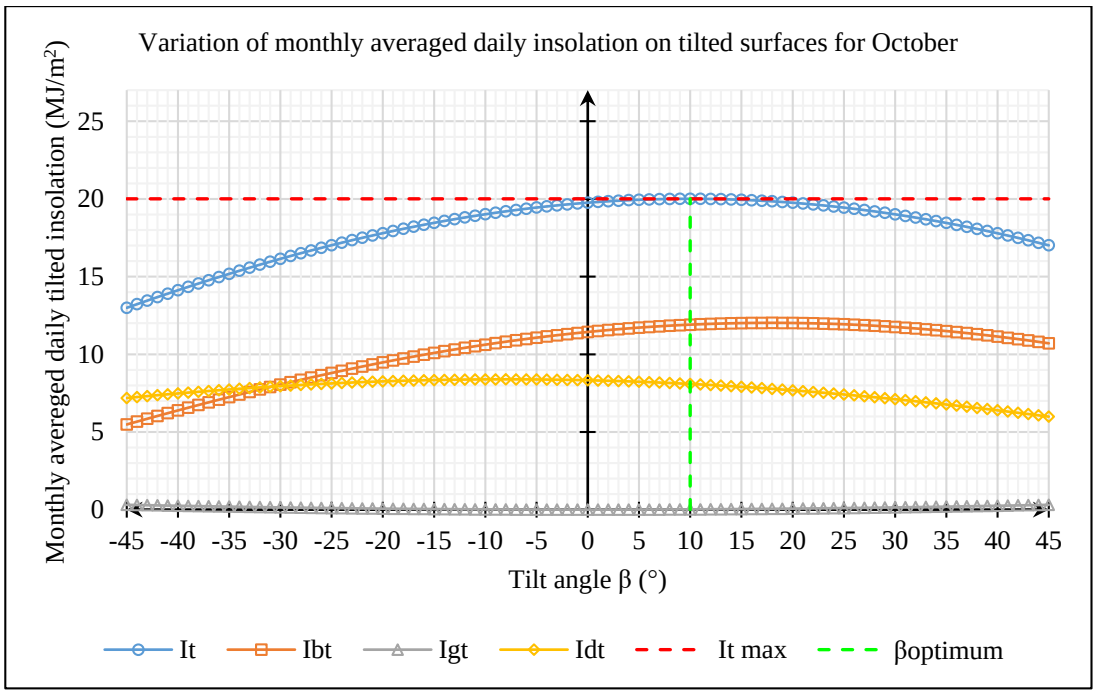

Figure 4.33 - Variation of monthly averaged daily insolation on tilted surfaces for October

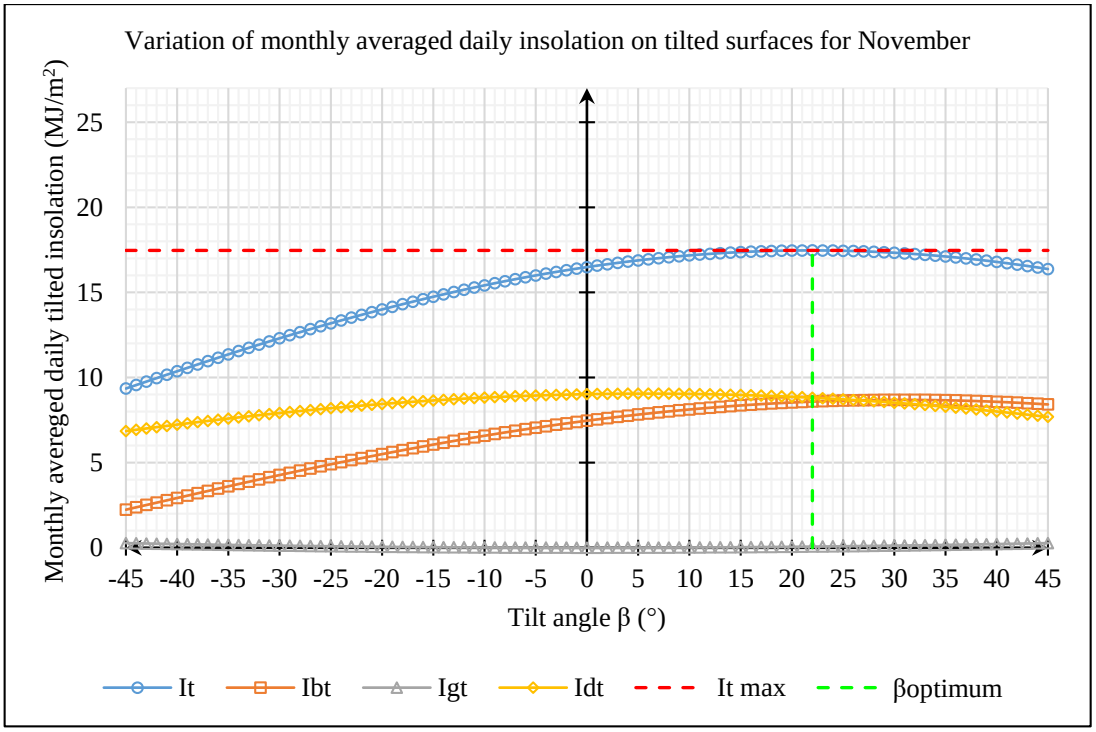

Figure 4.34 - Variation of monthly averaged daily insolation on tilted surfaces for November

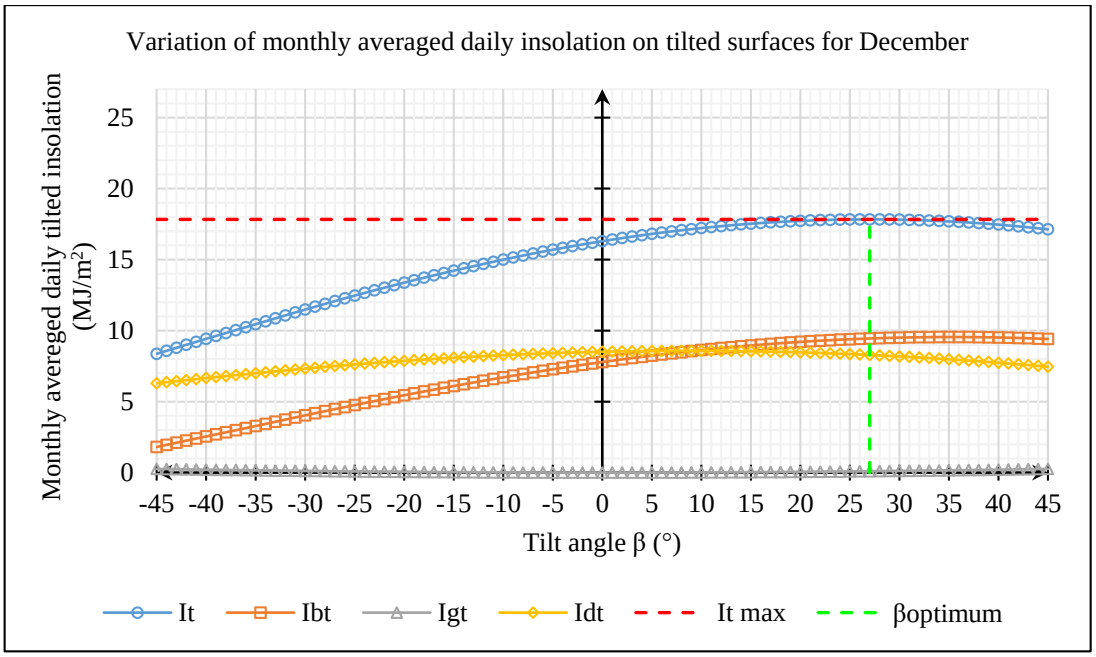

Figure 4.35 - Variation of monthly averaged daily insolation on tilted surfaces for December

Figure 4.24 to Figure 4.35 indicates that optimum tilt angle varies between -26° to +27° tilt angles and maximum global radiation varies between 24.50 MJ/m^2/day (6.8 kWh/m^2/day) to 17.46 MJ/m^2/day (4.85 kWh/m^2/day) throughout the year. Maximum monthly averaged global, beam and diffuse radiation for each month and optimum tilt angles are tabulated in Table 4.8.

Table 4.8 - Maximum monthly averaged insolation and optimum tilt angles

Month	$\bar{I}_t$		$\bar{I}_{bt}$		$\bar{I}_{dt}$		$\bar{k}_T$
	Maximum	$\beta_{optimum}$	Maximum	$\beta_{optimum}$	Maximum	$\beta_{optimum}$	
January	23.09	26.00	16.54	33.00	7.15	-2.00	0.62
February	20.55	15.00	11.24	23.00	9.67	-1.00	0.56
March	22.69	1.00	14.18	9.00	8.96	-16.00	0.61
April	20.63	-13.00	10.09	-6.00	10.64	-20.00	0.54
May	24.50	-24.00	14.19	-18.00	10.35	-31.00	0.62
June	21.41	-25.00	9.19	-23.00	12.13	-24.00	0.55
July	24.29	-26.00	14.22	-20.00	10.04	-32.00	0.61
August	22.08	-17.00	11.43	-12.00	10.69	-22.00	0.57
September	22.04	-3.00	12.52	5.00	9.84	-17.00	0.59
October	20.01	10.00	12.02	18.00	8.38	-8.00	0.55
November	17.46	22.00	8.69	31.00	9.05	6.00	0.48
December	17.83	27.00	9.55	35.00	8.58	9.00	0.49
Annual	20.40	-2.00	11.24	6.00	9.44	-15.00	0.57

4.5 Estimation of optimum tilt angle for dry zone in Sri Lanka

Daily optimum tilt angles were obtained by predicting daily global insolation on due south and north faced surfaces. The results were not varying consistently throughout the year to limited availability of measured data. Therefore, trend line was used to predict the daily optimum tilt angles and results are shown in Figure 4.36.

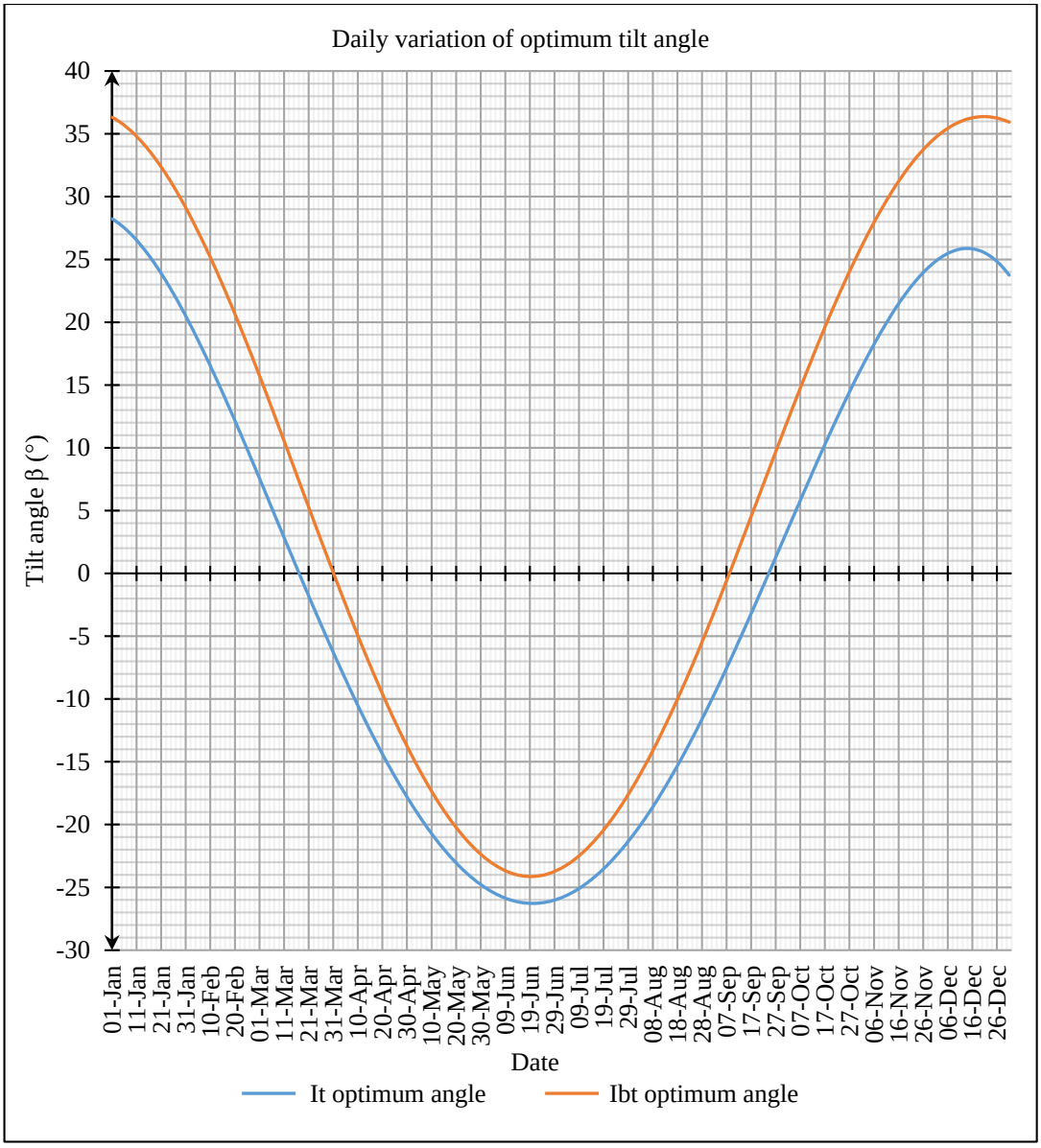

Figure 4.36 - Daily variation of optimum tilt angle

According to the Figure 4.36 it can be concluded that the daily optimum tilt angles are varying between +28° to -26° throughout the year.

Monthly averaged daily maximum global insolation with monthly tracking and daily tracking for each month are plotted in the Figure 4.37. Monthly averaged daily global horizontal, beam horizontal, diffuse horizontal, extra-terrestrial horizontal, global tilted at tilt angle 7° insulations and optimum monthly averaged daily tilt angle also plotted in Figure 4.37. Annual optimum fixed tilt angle (-2°) and daily insolation for same tilt angle are plotted in the Figure 4.37 as reference lines.

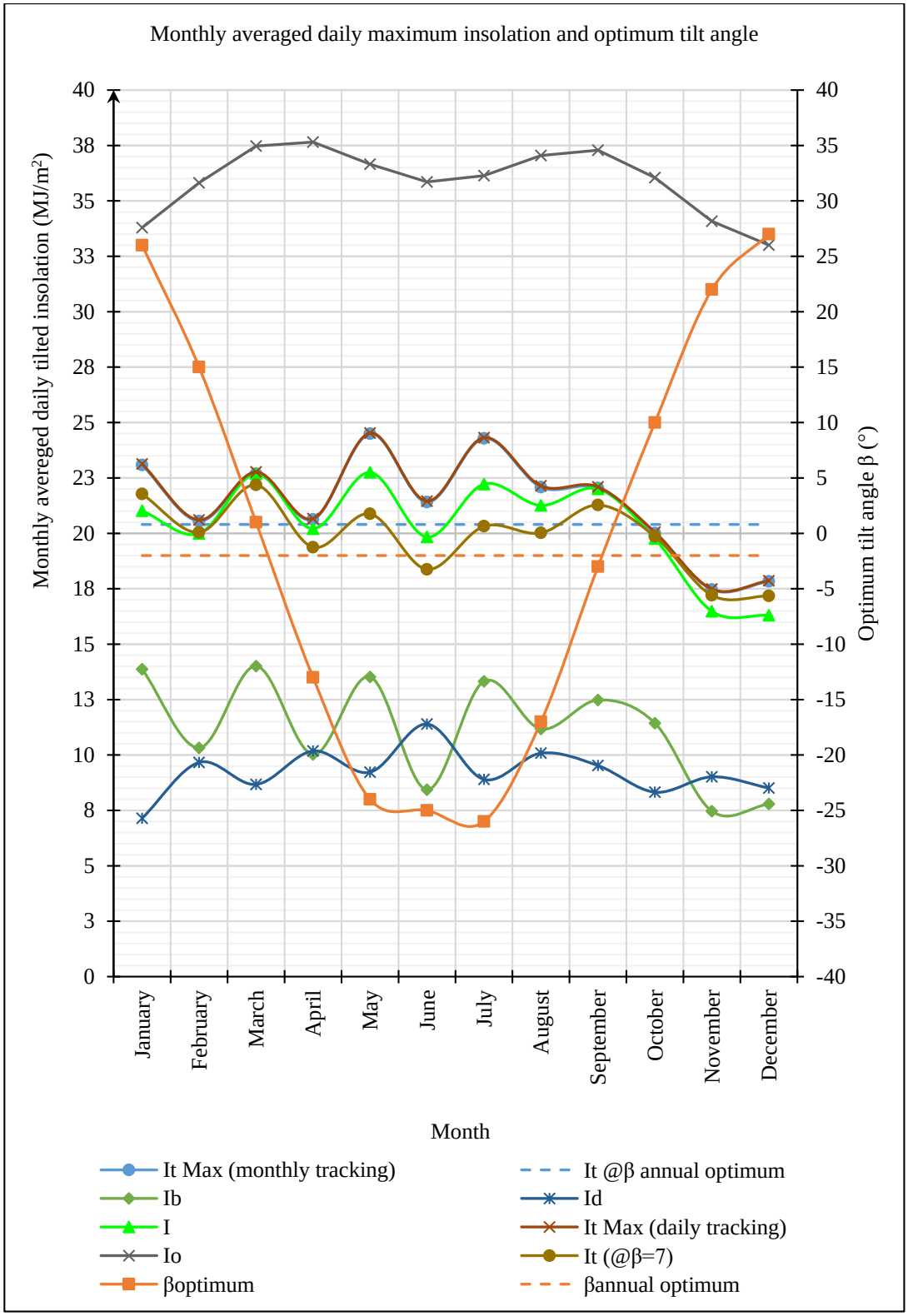

Figure 4.37 - Monthly averaged daily maximum insolation and optimum tilt angle

According to the Figure 4.37 monthly averaged daily global insolation for monthly tracking systems and daily tracking systems are higher than the monthly averaged

global horizontal insolation and global tilted insolation at 7° due south faced surfaces. It implies that energy maximising can be done using single axis tracking system about the east west axis. Figure 4.37 also indicates that there is no significance difference between the monthly tracking system and daily tracking systems. Percentage variations between the fixed systems and daily and monthly tracking systems were calculated and values are tabulated in Table 4.9 and graphical representations given in Figure 4.38.

Table 4.9 - Maximum solar resource potential with tracking (about E-W axis) systems

Month	$\bar{I}$	$\bar{I}_{t\ Max}$ (monthly tracking)		$\bar{I}_{t\ Max}$ (daily tracking)		$\bar{I}_{t\ (@\beta=7)}$		$\bar{I}_b$	As percentage of $\bar{I}$
	$MJ/m^2/day$	$MJ/m^2/day$		$MJ/m^2/day$		$MJ/m^2/day$		$MJ/m^2/day$	
January	21.02	23.09	9.83%	23.13	10.04%	21.78	3.59%	13.87	65.99%
February	19.99	20.55	2.81%	20.60	3.05%	20.05	0.28%	10.32	51.64%
March	22.69	22.69	0.00%	22.77	0.37%	22.19	-2.20%	14.01	61.76%
April	20.21	20.63	2.07%	20.66	2.24%	19.37	-4.14%	10.03	49.61%
May	22.75	24.50	7.69%	24.52	7.80%	20.88	-8.22%	13.52	59.44%
June	19.83	21.41	7.94%	21.45	8.15%	18.38	-7.36%	8.44	42.53%
July	22.22	24.29	9.28%	24.32	9.42%	20.32	-8.57%	13.32	59.95%
August	21.26	22.08	3.88%	22.14	4.15%	20.02	-5.83%	11.18	52.57%
September	22.01	22.04	0.15%	22.10	0.41%	21.28	-3.32%	12.48	56.71%
October	19.76	20.01	1.27%	20.05	1.48%	19.87	0.53%	11.44	57.87%
November	16.48	17.46	5.94%	17.49	6.10%	17.21	4.37%	7.47	45.29%
December	16.30	17.83	9.40%	17.87	9.58%	17.18	5.37%	7.79	47.78%
Annual	20.39	21.40	4.96%	21.44	5.16%	19.88	-2.48%	11.18	54.82%

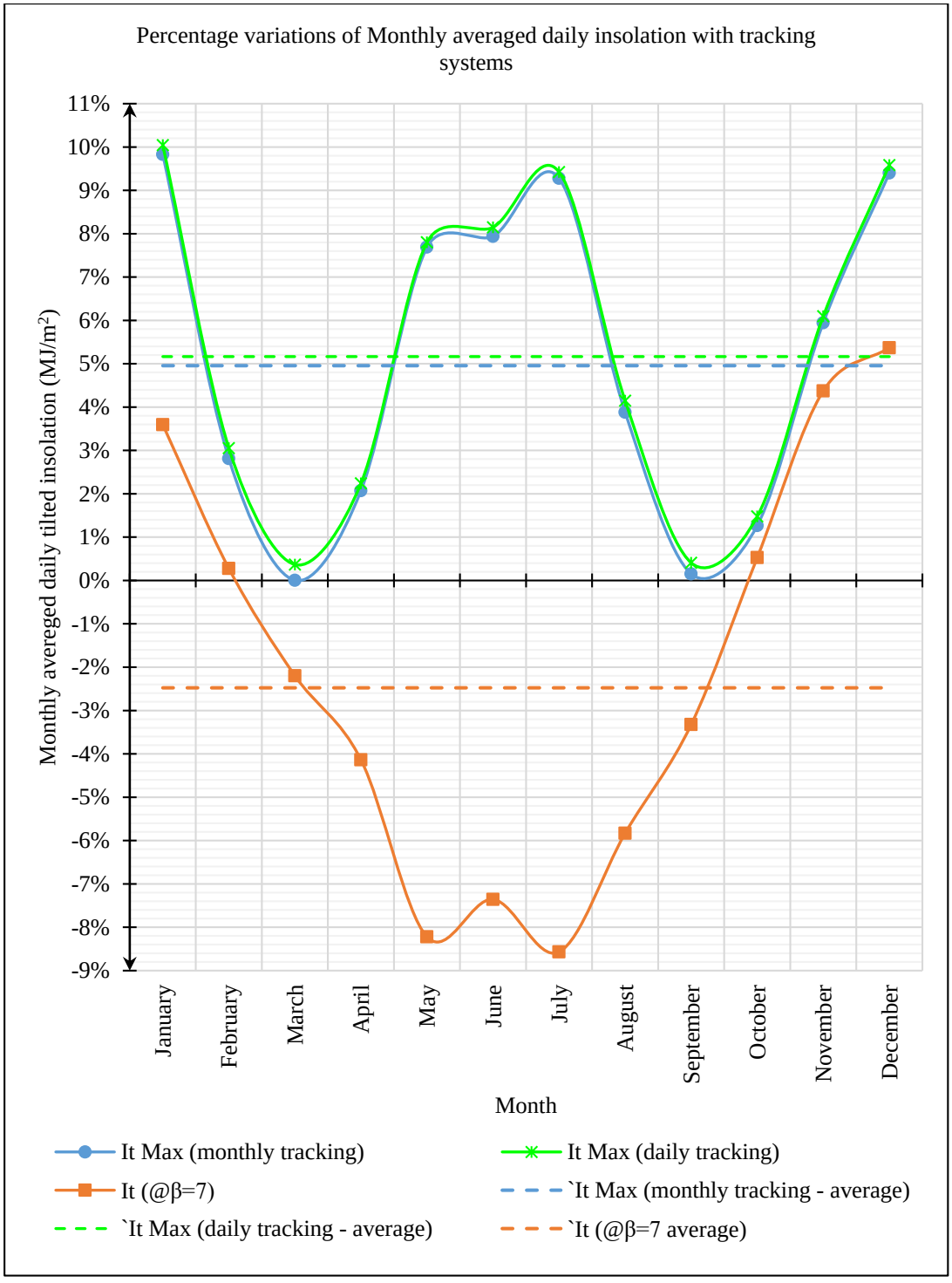

Figure 4.38 - Percentage variations of Monthly averaged daily insolation with tracking systems

Table 4.9 and Figure 4.38 clearly indicate that additional 4.96 % of annual energy can be harnessed by using very simple single axis monthly tracking system about the east

west axis. It also indicates that there is no significance increment of harnessed energy by using complex single axis daily tracking systems about the east west axis. Therefore, it can be suggested monthly single axis tracking systems about the east west axis is more suitable for the simple solar energy systems. In addition to that Table 4.9 and Figure 4.38 indicates that 2.48% decrement in 7° due south tilted surface than horizontal surfaces. Therefore, tilting towards due south for fixed systems not recommended.

$$\text{Annual averaged daily horizontal potential in dry zone} = 20.39\ \frac{\text{MJ}}{\text{m}^2 \times \text{day}}$$

$$= 5.66\ \frac{\text{kWh}}{\text{m}^2 \times \text{day}}$$

$$\text{Annual horizontal solar resource potential in dry zone} = 5.66 \times 365\ \frac{\text{kWh}}{\text{m}^2 \times \text{day}}$$

$$= 2067\ \frac{\text{kWh}}{\text{m}^2 \times \text{day}}$$

$$\left.\begin{array}{c}\text{Annual averaged daily solar resource potential in dry} \\ \text{zone with monthly tracking system}\end{array}\right\} = 21.40\ \frac{\text{MJ}}{\text{m}^2 \times \text{day}}$$

$$= 5.94\ \frac{\text{kWh}}{\text{m}^2 \times \text{day}}$$

$$\left.\begin{array}{c}\text{Annual solar resource potential in dry} \\ \text{zone with monthly tracking system}\end{array}\right\} = 5.94 \times 365\ \frac{\text{kWh}}{\text{m}^2 \times \text{day}}$$

$$= 2169\ \frac{\text{kWh}}{\text{m}^2 \times \text{day}}$$

5 CONCLUSIONS AND RECOMMENDATIONS

An analysis of existing diffuse radiation models was carried out in this thesis using ground level measured solar radiation data at Hambanthota obtained from Sri Lanka Sustainable Energy Authority SLSEA. Global, beam and diffuse solar radiation on horizontal and 7° tilted towards due south facing surfaces was used for analysing existing isotropic and anisotropic models. Four isotropic hourly diffuse radiation models namely Liu and Jordan (1960), Koronakis (1986), Tian et al (2001) and Badescu (2002) and ten anisotropic hourly diffuse radiation models namely Temps and Coulson (1977), Bugler (1977), Klucher (1979), Hay (1979), Willmot (1982), Skartveit and Olseth (1986), Reindel (1990), Stevan and Unswoth (1980), Iqbal (1983) and Perez (1990) were analysed. Tian et al (2001) isotropic model and Iqbal (1983) anisotropic model gave a better approximation for diffuse radiation among considered models. Horizon brightness coefficients of Perez et al (1990) was modified by using least square error method. Statistical test indicates that modified model gave a better approximation for the estimation of diffuse radiation than existing models.

Solar resource potential assessment for horizontal and zero azimuth tilted surfaces was also performed for the dry zone in Sri Lanka using measured hourly solar radiation data. The calculated monthly averaged daily insolation for dry zone in Sri Lanka varied between 16.30 MJ/m2/day to 22.75 MJ/m2/day with the annually averaged daily insolation of 20.07 MJ/m2/day. Seasonal variations of solar radiation potential are minimum except months of November and December where 18% less potential was observed than the annual average. Calculated annually averaged beam horizontal radiation was 10.87 MJ/m2/day and diffuse horizontal radiation was 9.19 MJ/m2/day. The calculated monthly averaged clearness index for dry zone in Sri Lanka varied between 0.48 to 0.62 in November and May, July respectively while having 0.56 annual average clearness index indicating partly cloudy sky conditions throughout the year.

Modified Perez et al (1990) model was used for estimation of titled radiation on due south and north faced surfaces. Diffuse tilted daily insolation and global tilted insolation for -45° to +45° inclined surfaces with 1° increments was estimated and

optimum tilt angle for each month and annual optimum tilt angle were derived. The calculated monthly optimum tilt angle varied between -26° to 27° while having annual optimum tilt angle of -2°. Monthly averaged daily maximum global insolation with monthly tracking and daily tracking was also calculated. It was found that there is no significant difference between the daily and monthly tracking performance about east west axis. Hence, it can be suggested that monthly single axis tracking systems about the east west axis is more suitable due to its simplicity in solar energy collecting systems. Optimum tilt angle for beam radiation was derived and it was found that annual optimum tilt angle for beam radiation is 6° towards due south. The derived maximum solar resource potential was 2068 kWh/m2 per annum for fixed system at -2° tilt angle and 2169 kWh/m2 per annum for monthly tracking system which is 4.96% higher than the horizontal potential.

It is required to validate modified Perez et al (1990) model using another yearly data set in future and it is not possible to validate model for another tilt angles except 7° due south due to the unavailability of data for other angles. It is proposed to assess the solar resource potential for tilted surfaces with different surface azimuth angle by using modified Perez et al (1990) model in future. It also required to calculate the global normal radiation for dry zone in order to find optimum tilt angles for hourly tracking systems. It is also proposed to modify the coefficients of circumsolar brightness components of Perez et al (1990) model.

References

Sri Lanka commissions 10MW solar power plant. (2017, 02 05). Retrieved from ECONOMYNEXT: http://www.economynext.com/Sri_Lanka_commissions_10MW_solar_power_plant-3-6916-8.html

Sri Lanka Energy Balence 2015. (2017, 02 02). Retrieved from Sri Lanka Sustainable Energy Authority: http://www.info.energy.gov.lk/

windforce. (2017, January 18). Retrieved from POWER PROJECTS: http://www.windforce.lk/power-projects/solar-one-ceylon.html

UC Santa Barbara Geography. (2010, April 22). Retrieved October 25, 2014, from Scattering and Absorption: http://www.geog.ucsb.edu/~joel/g266_s10/lecture_notes/chapt04/oh10_4_2/oh10_4_2.html

Blue Sky. (2014, August 19). Retrieved October 25, 2014, from HyperPhysics: http://hyperphysics.phy-astr.gsu.edu/hbase/atmos/blusky.html

Abdullah, Y. (2011). Investigation Of Applicability Of Ashrae Clear-Sky Model To Izmir, Turkey. *Isı Bilimi ve Tekniği Dergisi*, 25-32.

Aggarwa, K. (September 2012). Precise estimation of total solar radiation on tilted. *Environmental Science and Technology*, 365-370.

Ahmad, M. J., & Tiwari, G. (2008-2). Study of Models for Predicting the Mean Hourly Global Radiation from Daily Summations. *Open Environmental Sciences*, 6-14.

Al-Dabbas, & Ali, M. A. (2010). The analysis of the characteristics of the solar radiation climate of the daily global radiation and diffuse radiation in Amman, Jordan. *Renewable Energy*, 23-38.

Al-Rawahi, N. Z., Zurigat, Y. H., & Al-Azri, N. A. (2011). Prediction of Hourly Solar Radiation on Horizontal and Inclined Surfaces for Muscat/Oman. *Engineering Research*, 19-31.

Al-Rawahi, N. Z., Zurigat, Y. H., & Al-Azri, N. A. (2012). Prediction of global solar radiation using relativehumidity, maximum temperature and sunshine hours in Uyo, in the NigerDelta Region, Nigeria. *Advances in Applied Science Research* (pp. 1923-1937). Pelagia Research Library.

Anwar, S., Efstathiadis, H., & Qazi, S. (2013). *Handbook of Research on Solar Energy Systems and Technologies*. Hershey: IGI Global.

ATMS 101 Summer 2003. (n.d.). Retrieved October 29, 2014, from http://www.ems.psu.edu/~nese/f2_10.gif

Batlles, F., Rubio, M.A., Tovar, J., Olmo, F., & Alados-Arboledas, L. (2000). Empirical modeling of hourly direct irradiance by means of. *Energy*, 675-688.

Chandel, S. S., & Aggarwal, R. K. (2011). Estimation of Hourly Solar Radiation on Horizontal and Inclined Surfaces in Western Himalayas. *Smart Grid and Renewable Energy*, 45-55.

Cucumo, M., De Rosa, A., Ferraro, V., Kaliakatsos, D., & Marinelli, V. (n.d.). Experimental Validation Of Correlations For The Estimation Of Beam And Diffuse Components Of Hourly Radiation. *61st ATI National Congress – International Session "Solar Heating and Cooling".*

Dervishi, S., & Mahdavi, A. (2011). Comparison Of Models For The Derivation Of Diffuse Fraction Of Global Irradiance Data For Vienna, Austria. *12th Conference of International Building Performance Simulation Association* (pp. 765-771). Sydney: Building Performance Simulation Association.

Duffie, J. A., & Beckman, W. A. (2013). *Solar Engineering of Thermal Process.* Hoboken: John Wiley & Sons, Inc.

Edeoja, Okibe, A., Eloka-Eboka, & Andrew, C. (2013). Experimental Validation of Hottel's Transmittance Model for Estimating Beam Radiation In Makurdi Location. *Engineering Research*, 51-57.

El-Sebaii, A. A., Al-Hazmi, F., Al-Ghamdi, A. A., & Yaghmour, S. (2010). Global, direct and diffuse solar radiation on horizontal and tilted surfaces in Jeddah, Saudi Arabia. *Applied Energy*, 568-576.

Emanuele, C. (2012). The Disagreement between Anisotropic-Isotropic Diffuse Solar Radiation Models as a Function of Solar Declination: Computing the Optimum Tilt Angle of Solar Panels in the Area of Southern-Italy. *Smart Grid and Renewable Energy*, 253-259.

Empirical Correlation for Estimating Components of Light. (n.d.). Retrieved November 5, 2014, from John A. Dutton e-Education Institute: College of Earth and Mineral Sciences: https://www.e-education.psu.edu/eme810/node/543

Gana, N. N., & Akpootu, D. O. (2013). Angstrom Type Empirical Correlation for Estimating Global Solar Radiation in North-Eastern Nigeria. *Engineering And Science*, 58-78.

Geo Appendix A. (n.d.). Retrieved October 20, 2014, from Uniwersytet Im. Adama Mickiewicza w Poznaniu: http://geoinfo.amu.edu.pl/wpk/geos/GEO_APPENDIX_A.HTML

Gueymard, C. A. (1986). Monthly Averages of the Daily Effective Optical Air Mass and Solar Related Angles for Horizontal or Inclined Surfaces. *Solar Energy*, 320-324.

Gueymard, C. A. (2003). Direct solar transmittance and irradiance predictions with broadband models. Part I: detailed theoretical performance assessment. *Solar Energy*, 355-379.

Gueymard, C. A. (2008). From Global Horizontal To Global Tilted Irradiance: How Accurate Are Solar Energy Engineering Predictions In Practice? *Solar 2008 Conference.* San Diego: American Solar Energy Society.

Gulin, M., Vasak, M., & Baotic, M. (n.d.). *Estimation of the global solar irradiance on tilted surfaces.*

Hussein, T. A. (2012). Estimation of Hourly Global Solar Radiation in Egypt Using Mathematical Model. *Latest Trends in Agriculture & Food Sciences*, 74-82.

Idso, B., & Sherwood. (1969). Atmospheric Attenuation of Solar Radiation. *Atmospheric Sciences*, 1088-1095.

Ihya, B., Mechaqrane, A., Tadili, R., & Bargach, M. N. (2014). Optimal tilt angles for solar collectors facing south at Fez city (Morocco). *Natural Sciences Research*, 120-127.

Ineichen, P. (2008). Comparison and validation of three global-to-beam irradiance models against ground measurements. *Solar Energy*, 501-512.

Jakhrani, A. Q., Othman, K., Rigit, A. R., Samo, S. R., & Kamboh, S. A. (December 2012). Estimation of Incident Solar Radiation on Tilted Surface by Different Empirical Models. *Scientific and Research Publications*, 1-6.

Jakhrani, A. Q., Samo, S. R., Rigit, A. R., & Kamboh, S. A. (2013). Selection of Models for Calculation of Incident Solar Radiation on Tilted Surfaces. *World Applied Sciences*, 1334-1343.

Kasten, F., & Young, A. T. (1989). Revised Optical Air Mass Tables and Approximation Formula. *Applied Optics*, 4735-4738.

Keith, F., & Kreider, J. F. (2011). *Principles of Sustainable Energy*. Boca Raton: Taylor and Francis Group, LLC.

Khan, M. M., & Ahmad, M. J. (2012). Estimation of global solar radiation using clear sky radiation in Yemen. *Engineering Science and Technology Review*, 12-19.

Kuo, C., Chang, W., & Chang, K. (2014). Modeling the hourly solar diffuse fraction in Taiwan. *Renewable Energy*, 56-61.

Layers of Earth's Atmosphere . (n.d.). Retrieved October 15, 2014, from windows2universe:

http://www.windows2universe.org/earth/Atmosphere/layers_activity_print.html

Lealea, T., & Tchinda, R. (2013). Estimation of Diffuse Solar Radiation in the South of Cameroon. *Energy Technologies and Policy*, 32-42.

Liu, B. Y., & Jordan, R. C. (1960). The Interrelationship and Characteristic Distribution of Direct, Diffuse and Total Solar Radiation. *Solar Energy*, 1-9.

Loutzenhiser, P., Manz, H., Felsmann, C., Strachan, P., Frank, T., & Maxwell, G. (2006). Empirical validation of models to compute solar irradiance on inclined surfaces for building energy simulation. *Solar Energy*, 254-267.

Muneer, T., Gueymard, C., & Kambezidis, H. (2004). *Solar Radiation and Daylight Models.* Burlington: Elsevier Ltd.

Olayinka, S. (2011). Estimation of global and diffuse solar radiations for selected cities in Nigeria. *International Journal of Energy and Environmental Engineering*, 13-33.

Oliveira, A. P., Escobedo, J. F., Machado, A. J., & Soares, J. (2002). Correlation models of diffuse solar-radiation applied to the city of Sa˜o Paulo, Brazil. *Applied Energy*, 59-73.

Orgill, J. F., & Hollands, K. G. (1977). Correlation Equation For Hourly Diffuse Radiation On A Horizontal Surface. *Solar Energy*, 357-359.

Raichijk, C., Fasulo, A., & Gallegos, H. G. (2009). Estudio De Validación De Las Correlaciones Para La Fracción Difusa De La Irradiación Solar En San Luis. *Avances en Energías Renovables y Medio Ambiente*, 11.17-11.24.

Reindl, D. T., Beckman, W. A., & Duffle, J. A. (1990). Diffuse Fraction Correlations. *Solar Energy*, 1-7.

Rivington, M., Bellocchi, G., Matthews, K. B., & Buchan, K. (2005). Evaluation of three model estimations of solar radiation at 24 UK stations. *Agricultural and Forest Meteorology*, 228–243.

Sen, Z. (2008). *Solar Energy Fundamentals and Modeling Techniques: Atmosphere, Environment, Climate Change.* Springer-Verlag London Limited.

Singh, J., Bhattacharya, B. l., Kumar, M., & Mallick, K. (2013). Modelling monthly diffuse solar radiation fraction and its validity over the Indian sub-tropics. *Climatology*, 77-86.

Soteris, K. (2009). *Solar energy engineering : processes and systems.* Burlington: Elsevier Inc.

Souza, A. P., & Escobedo, J. F. (2013). Estimates of Hourly Diffuse Radiation on Tilted Surfaces in Southeast of Brazil. *Renewable Energy Research*.

Talebizadeh, P., Mehrabian, M., & Abdolzadeh, M. (2011). Prediction of the optimum slope and surface azimuth angles using the Genetic Algorithm. *Energy and Buildings*, 2998-3005.

Team, E. W. (2005, October 1). *Education and Outreach : Teacher Lesson Plans*. Retrieved October 15, 2014, from Earth System Research Laboratory: Global Monitoring Division: http://www.esrl.noaa.gov/gmd/outreach/lesson_plans/

The Sun as a Source of energy: Part 1: Solar Astronomy. (n.d.). Retrieved October 10, 2014, from ITACA: http://www.itacanet.org/the-sun-as-a-source-of-energy/part-1-solar-astronomy/

Viorel, B. (2008). *Modeling Solar Radiation at the Earth's Surface Recent Advances.* Berlin Heidelberg: Springer.

Web materials shown in class. (n.d.). Retrieved October 20, 2014, from Earth System science Center: http://www.essc.psu.edu/~dbabb/Chapter_2/sun-earth-radiation.jpg

Wong, L., & Chow, W. (2001). Solar radiation model. *Applied Energy*, 191–224.

Appendix A Monthly averaged hourly global horizontal insolation

Monthly averaged hourly Global horizontal insolation $\bar{I}$												
	January	February	March	April	May	June	July	August	September	October	November	December
Hour	MJ/m^2	MJ/m^2	MJ/m^2	MJ/m^2	MJ/m^2	MJ/m^2	MJ/m^2	MJ/m^2	MJ/m^2	MJ/m^2	MJ/m^2	MJ/m^2
5-6	0.00	0.00	0.00	0.00	0.00	0.00	0.00	0.00	0.00	0.00	0.00	0.00
6-7	0.07	0.05	0.10	0.22	0.26	0.21	0.19	0.18	0.20	0.22	0.20	0.10
7-8	0.63	0.50	0.77	1.00	0.94	0.81	0.89	0.80	0.97	0.96	0.77	0.58
8-9	1.43	1.27	1.62	1.80	1.66	1.49	1.67	1.59	1.76	1.72	1.49	1.26
9-10	2.18	1.91	2.37	2.32	2.36	2.12	2.26	2.21	2.40	2.19	1.98	1.85
10-11	2.79	2.58	2.83	2.67	2.84	2.55	2.85	2.60	2.86	2.57	2.34	2.18
11-12	3.20	2.93	2.80	2.70	3.14	2.71	3.11	2.86	3.11	2.77	2.29	2.32
12-13	2.97	2.94	3.18	2.76	3.17	2.58	2.96	2.98	3.06	2.90	2.20	2.32
13-14	2.83	2.75	3.08	2.58	2.87	2.46	2.78	2.71	2.79	2.57	2.19	2.17
14-15	2.14	2.25	2.73	2.12	2.50	2.14	2.43	2.29	2.26	2.17	1.57	1.69
15-16	1.66	1.64	1.85	1.35	1.75	1.55	1.75	1.70	1.59	1.32	1.01	1.17
16-17	0.90	0.91	1.03	0.55	0.97	0.91	0.99	1.01	0.81	0.58	0.39	0.55
17-18	0.21	0.27	0.31	0.14	0.29	0.31	0.33	0.33	0.19	0.10	0.05	0.10
18-19	0.00	0.00	0.01	0.00	0.00	0.01	0.01	0.01	0.00	0.00	0.00	0.00
Total	21.02	19.99	22.69	20.21	22.75	19.83	22.22	21.26	22.01	20.09	16.48	16.30

Appendix B Monthly averaged hourly beam horizontal insolation

Monthly averaged hourly beam horizontal insolation $\bar{I}_b$												
	January	February	March	April	May	June	July	August	September	October	November	December
Hour	MJ/m^2	MJ/m^2	MJ/m^2	MJ/m^2	MJ/m^2	MJ/m^2	MJ/m^2	MJ/m^2	MJ/m^2	MJ/m^2	MJ/m^2	MJ/m^2
5-6	0.00	0.00	0.00	0.00	0.00	0.00	0.00	0.00	0.00	0.00	0.00	0.00
6-7	0.02	0.01	0.01	0.05	0.08	0.03	0.04	0.04	0.04	0.06	0.05	0.02
7-8	0.35	0.19	0.39	0.47	0.45	0.27	0.40	0.35	0.51	0.57	0.33	0.23
8-9	0.93	0.67	1.04	0.96	0.94	0.59	0.92	0.82	1.04	1.04	0.75	0.65
9-10	1.49	1.07	1.54	1.21	1.43	0.96	1.33	1.16	1.43	1.27	1.00	1.05
10-11	2.01	1.44	1.86	1.33	1.78	1.19	1.77	1.34	1.68	1.51	1.21	1.16
11-12	2.38	1.65	1.68	1.26	1.99	1.27	2.05	1.52	1.83	1.61	1.07	1.14
12-13	2.03	1.57	1.92	1.37	2.02	1.20	1.85	1.64	1.81	1.78	0.97	1.12
13-14	1.92	1.45	1.94	1.40	1.78	1.07	1.73	1.50	1.65	1.56	0.99	1.03
14-15	1.30	1.13	1.79	1.16	1.51	0.94	1.54	1.26	1.27	1.26	0.66	0.73
15-16	0.96	0.74	1.17	0.63	0.99	0.58	1.05	0.94	0.83	0.69	0.38	0.47
16-17	0.43	0.34	0.57	0.16	0.45	0.29	0.52	0.49	0.35	0.26	0.08	0.16
17-18	0.05	0.06	0.10	0.02	0.09	0.06	0.11	0.12	0.05	0.03	0.00	0.02
18-19	0.00	0.00	0.00	0.00	0.00	0.00	0.00	0.00	0.00	0.00	0.00	0.00
Total	13.87	10.32	14.01	10.03	13.52	8.44	13.32	11.18	12.48	11.62	7.47	7.79

Appendix C Monthly averaged hourly diffuse horizontal insolation

Monthly averaged hourly diffuse horizontal insolation $\bar{I}_{dt}$												
	January	February	March	April	May	June	July	August	September	October	November	December
Hour	MJ/m^2	MJ/m^2	MJ/m^2	MJ/m^2	MJ/m^2	MJ/m^2	MJ/m^2	MJ/m^2	MJ/m^2	MJ/m^2	MJ/m^2	MJ/m^2
5-6	0.00	0.00	0.00	0.00	0.00	0.00	0.00	0.00	0.00	0.00	0.00	0.00
6-7	0.05	0.04	0.09	0.17	0.19	0.18	0.15	0.13	0.16	0.15	0.15	0.07
7-8	0.29	0.31	0.38	0.53	0.50	0.54	0.49	0.45	0.46	0.39	0.44	0.35
8-9	0.50	0.59	0.58	0.84	0.72	0.90	0.75	0.76	0.72	0.69	0.75	0.61
9-10	0.70	0.84	0.83	1.11	0.93	1.16	0.92	1.05	0.97	0.92	0.98	0.80
10-11	0.78	1.14	0.97	1.34	1.05	1.36	1.08	1.26	1.18	1.07	1.13	1.02
11-12	0.83	1.28	1.12	1.44	1.15	1.44	1.06	1.33	1.28	1.16	1.23	1.18
12-13	0.94	1.37	1.26	1.39	1.14	1.38	1.11	1.34	1.25	1.12	1.23	1.20
13-14	0.91	1.30	1.15	1.19	1.08	1.39	1.05	1.21	1.14	1.01	1.21	1.14
14-15	0.84	1.12	0.93	0.96	0.98	1.20	0.89	1.03	0.99	0.91	0.92	0.97
15-16	0.69	0.90	0.68	0.72	0.75	0.96	0.70	0.76	0.76	0.63	0.64	0.70
16-17	0.47	0.57	0.46	0.38	0.51	0.62	0.47	0.52	0.47	0.33	0.31	0.39
17-18	0.16	0.21	0.22	0.12	0.21	0.25	0.22	0.22	0.15	0.07	0.04	0.08
18-19	0.00	0.00	0.01	0.00	0.00	0.01	0.01	0.01	0.00	0.00	0.00	0.00
Total	7.15	9.67	8.68	10.18	9.23	11.40	8.90	10.08	9.53	8.46	9.02	8.51

Appendix D Monthly averaged hourly global tilted (β = 7°) insolation

Monthly averaged hourly Global tilted insolation $\bar{I}_{t(\beta=7°)}$												
	January	February	March	April	May	June	July	August	September	October	November	December
Hour	MJ/m^2	MJ/m^2	MJ/m^2	MJ/m^2	MJ/m^2	MJ/m^2	MJ/m^2	MJ/m^2	MJ/m^2	MJ/m^2	MJ/m^2	MJ/m^2
5-6	0.00	0.00	0.00	0.00	0.00	0.00	0.00	0.00	0.00	0.00	0.00	0.00
6-7	0.10	0.06	0.11	0.23	0.26	0.21	0.19	0.18	0.22	0.27	0.24	0.12
7-8	0.83	0.59	0.87	1.04	0.93	0.78	0.85	0.83	1.06	1.11	0.91	0.71
8-9	1.63	1.37	1.69	1.79	1.55	1.41	1.57	1.55	1.76	1.79	1.62	1.41
9-10	2.29	1.95	2.33	2.21	2.12	1.94	2.06	2.07	2.29	2.17	2.04	1.94
10-11	2.81	2.55	2.70	2.49	2.54	2.31	2.55	2.40	2.68	2.50	2.35	2.22
11-12	3.12	2.83	2.62	2.51	2.82	2.45	2.75	2.61	2.89	2.65	2.29	2.34
12-13	2.84	2.80	2.94	2.55	2.84	2.34	2.64	2.71	2.83	2.78	2.21	2.33
13-14	2.77	2.64	2.89	2.42	2.60	2.26	2.51	2.49	2.63	2.52	2.23	2.22
14-15	2.19	2.21	2.65	2.04	2.31	2.00	2.23	2.15	2.20	2.20	1.67	1.79
15-16	1.83	1.70	1.89	1.35	1.67	1.48	1.66	1.66	1.62	1.41	1.13	1.31
16-17	1.10	1.02	1.13	0.57	0.94	0.88	0.96	1.03	0.88	0.68	0.45	0.66
17-18	0.28	0.32	0.36	0.16	0.29	0.30	0.32	0.33	0.22	0.12	0.06	0.14
18-19	0.00	0.00	0.01	0.00	0.00	0.01	0.02	0.01	0.00	0.00	0.00	0.00
Total	21.78	20.05	22.19	19.37	20.88	18.38	20.32	20.02	21.28	20.19	17.21	17.18

Appendix E Monthly averaged hourly beam tilted (β = 7°) insolation

Monthly averaged hourly beam tilted insolation $\bar{I}_{bt\,(\beta = 7°)}$												
	January	February	March	April	May	June	July	August	September	October	November	December
Hour	MJ/m^2	MJ/m^2	MJ/m^2	MJ/m^2	MJ/m^2	MJ/m^2	MJ/m^2	MJ/m^2	MJ/m^2	MJ/m^2	MJ/m^2	MJ/m^2
5-6	0.00	0.00	0.00	0.00	0.00	0.00	0.00	0.00	0.00	0.00	0.00	0.00
6-7	0.04	0.01	0.02	0.05	0.06	0.02	0.02	0.03	0.03	0.07	0.06	0.04
7-8	0.41	0.21	0.40	0.45	0.41	0.23	0.35	0.33	0.51	0.60	0.37	0.27
8-9	1.02	0.72	1.05	0.94	0.89	0.54	0.85	0.79	1.04	1.08	0.80	0.71
9-10	1.59	1.12	1.56	1.19	1.37	0.90	1.26	1.13	1.44	1.30	1.06	1.13
10-11	2.13	1.49	1.88	1.31	1.72	1.13	1.70	1.30	1.68	1.55	1.27	1.24
11-12	2.51	1.71	1.70	1.24	1.92	1.21	1.97	1.49	1.84	1.65	1.12	1.21
12-13	2.15	1.63	1.94	1.35	1.95	1.15	1.78	1.60	1.82	1.82	1.01	1.19
13-14	2.04	1.51	1.95	1.38	1.72	1.02	1.66	1.46	1.66	1.61	1.04	1.10
14-15	1.39	1.18	1.81	1.14	1.45	0.88	1.47	1.22	1.27	1.30	0.70	0.78
15-16	1.04	0.78	1.18	0.61	0.94	0.54	0.98	0.91	0.83	0.71	0.41	0.52
16-17	0.48	0.37	0.58	0.15	0.41	0.26	0.47	0.46	0.35	0.27	0.09	0.19
17-18	0.07	0.07	0.10	0.02	0.07	0.04	0.09	0.10	0.04	0.03	0.01	0.03
18-19	0.00	0.00	0.00	0.00	0.00	0.00	0.00	0.00	0.00	0.00	0.00	0.00
Total	14.87	10.79	14.17	9.82	12.90	7.93	12.62	10.80	12.51	12.00	7.95	8.40

Appendix F Monthly averaged hourly diffuse tilted (β = 7°) insolation

Monthly averaged hourly diffuse tilted insolation $\bar{I}_{dt\,(\beta = 7°)}$												
	January	February	March	April	May	June	July	August	September	October	November	December
Hour	MJ/m^2	MJ/m^2	MJ/m^2	MJ/m^2	MJ/m^2	MJ/m^2	MJ/m^2	MJ/m^2	MJ/m^2	MJ/m^2	MJ/m^2	MJ/m^2
5---6	0.00	0.00	0.00	0.00	0.00	0.00	0.00	0.00	0.00	0.00	0.00	0.00
6-7	0.06	0.05	0.10	0.19	0.20	0.19	0.17	0.15	0.18	0.19	0.09	0.18
7-8	0.43	0.39	0.47	0.59	0.52	0.55	0.50	0.50	0.55	0.51	0.44	0.54
8-9	0.61	0.68	0.63	0.86	0.67	0.86	0.72	0.76	0.72	0.71	0.70	0.81
9-10	0.69	0.86	0.77	1.02	0.75	1.04	0.79	0.95	0.85	0.86	0.81	0.98
10-11	0.67	1.09	0.82	1.19	0.82	1.18	0.85	1.10	1.00	0.95	0.99	1.08
11-12	0.60	1.16	0.92	1.27	0.90	1.24	0.78	1.12	1.05	1.00	1.13	1.17
12-13	0.70	1.21	1.00	1.20	0.89	1.19	0.86	1.11	1.02	0.95	1.13	1.19
13-14	0.73	1.17	0.94	1.04	0.89	1.24	0.85	1.03	0.97	0.91	1.11	1.19
14-15	0.80	1.07	0.83	0.89	0.86	1.12	0.76	0.93	0.93	0.90	1.00	0.97
15-16	0.78	0.95	0.71	0.74	0.73	0.94	0.68	0.76	0.79	0.70	0.79	0.72
16-17	0.62	0.68	0.55	0.42	0.53	0.62	0.49	0.57	0.53	0.41	0.47	0.36
17-18	0.22	0.26	0.26	0.14	0.22	0.26	0.23	0.23	0.18	0.09	0.11	0.06
18-19	0.00	0.00	0.01	0.00	0.00	0.01	0.02	0.01	0.00	0.00	0.00	0.00
Total	6.91	9.58	8.01	9.55	7.97	10.44	7.70	9.21	8.76	8.19	8.77	9.25

Appendix G Monthly averaged hourly beam normal insolation

Monthly averaged hourly beam normal insolation $\bar{I}_{bn}$												
	January	February	March	April	May	June	July	August	September	October	November	December
Hour	MJ/m^2	MJ/m^2	MJ/m^2	MJ/m^2	MJ/m^2	MJ/m^2	MJ/m^2	MJ/m^2	MJ/m^2	MJ/m^2	MJ/m^2	MJ/m^2
5---6	0.00	0.00	0.00	0.00	0.00	0.00	0.00	0.00	0.00	0.00	0.00	0.00
6-7	0.33	0.11	0.15	0.44	0.51	0.20	0.33	0.36	0.26	0.43	0.26	0.38
7-8	1.32	0.71	1.24	1.28	1.16	0.73	1.14	0.98	1.32	1.45	0.78	0.93
8-9	1.95	1.36	1.89	1.63	1.56	1.01	1.62	1.42	1.71	1.70	1.27	1.33
9-10	2.25	1.55	2.07	1.55	1.84	1.27	1.78	1.51	1.81	1.62	1.55	1.37
10-11	2.53	1.73	2.10	1.46	1.98	1.36	2.02	1.48	1.83	1.67	1.45	1.43
11-12	2.73	1.80	1.74	1.28	2.06	1.34	2.16	1.56	1.86	1.67	1.32	1.19
12-13	2.29	1.67	1.95	1.38	2.09	1.26	1.92	1.66	1.84	1.87	1.30	1.08
13-14	2.29	1.62	2.07	1.50	1.96	1.20	1.90	1.60	1.80	1.79	1.28	1.21
14-15	1.78	1.43	2.19	1.44	1.92	1.19	1.92	1.55	1.61	1.71	1.06	0.96
15-16	1.69	1.18	1.80	0.99	1.61	0.94	1.63	1.46	1.38	1.25	0.91	0.74
16-17	1.17	0.81	1.31	0.40	1.12	0.69	1.19	1.13	0.92	0.78	0.52	0.28
17-18	0.37	0.32	0.52	0.15	0.52	0.31	0.55	0.60	0.34	0.27	0.17	0.05
18-19	0.00	0.00	0.01	0.00	0.00	0.02	0.07	0.01	0.00	0.00	0.00	0.00
Total	20.70	14.29	19.03	13.48	18.34	11.53	18.22	15.32	16.67	16.20	11.87	10.94

Appendix H Monthly averaged daily global insolation

Surface Angle β	Monthly averaged daily global insolation $\bar{I}_t$												
	January	February	March	April	May	June	July	August	September	October	November	December	Annual
°	MJ/m^2	MJ/m^2	MJ/m^2	MJ/m^2	MJ/m^2	MJ/m^2	MJ/m^2	MJ/m^2	MJ/m^2	MJ/m^2	MJ/m^2	MJ/m^2	MJ/m^2
-45	9.92	12.31	16.86	18.08	23.07	20.38	23.13	20.01	17.46	12.99	9.35	8.36	16.02
-44	10.21	12.55	17.10	18.23	23.20	20.48	23.25	20.16	17.67	13.23	9.56	8.58	16.21
-43	10.51	12.80	17.34	18.38	23.32	20.57	23.36	20.30	17.87	13.45	9.76	8.79	16.39
-42	10.81	13.04	17.57	18.52	23.44	20.66	23.46	20.43	18.07	13.68	9.96	9.00	16.58
-41	11.10	13.27	17.79	18.66	23.55	20.74	23.56	20.56	18.27	13.90	10.16	9.21	16.75
-40	11.40	13.51	18.02	18.79	23.66	20.82	23.65	20.69	18.46	14.13	10.37	9.42	16.93
-39	11.70	13.74	18.23	18.93	23.76	20.90	23.74	20.81	18.65	14.34	10.57	9.63	17.10
-38	11.99	13.97	18.45	19.05	23.85	20.97	23.82	20.92	18.83	14.56	10.77	9.83	17.27
-37	12.28	14.20	18.66	19.17	23.94	21.03	23.89	21.03	19.01	14.77	10.96	10.04	17.44
-36	12.57	14.42	18.86	19.29	24.02	21.09	23.96	21.13	19.18	14.97	11.16	10.24	17.60
-35	12.86	14.64	19.06	19.40	24.09	21.15	24.02	21.23	19.35	15.18	11.36	10.45	17.75
-34	13.15	14.86	19.25	19.51	24.16	21.20	24.07	21.32	19.51	15.38	11.55	10.66	17.91
-33	13.43	15.08	19.44	19.61	24.22	21.24	24.12	21.41	19.67	15.58	11.74	10.87	18.06
-32	13.72	15.29	19.63	19.71	24.28	21.28	24.16	21.50	19.83	15.77	11.93	11.07	18.20
-31	14.01	15.50	19.81	19.80	24.33	21.31	24.20	21.57	19.98	15.96	12.12	11.28	18.34
-30	14.30	15.70	19.98	19.89	24.37	21.34	24.23	21.64	20.12	16.15	12.30	11.48	18.48
-29	14.58	15.91	20.15	19.97	24.41	21.37	24.25	21.71	20.26	16.33	12.48	11.68	18.61
-28	14.86	16.10	20.32	20.05	24.44	21.38	24.27	21.77	20.40	16.51	12.66	11.88	18.74
-27	15.13	16.30	20.48	20.12	24.46	21.40	24.28	21.83	20.53	16.69	12.84	12.08	18.86
-26	15.40	16.49	20.63	20.19	24.48	21.41	24.29	21.88	20.65	16.86	13.01	12.27	18.98
-25	15.67	16.68	20.78	20.26	24.49	21.41	24.28	21.92	20.77	17.02	13.18	12.47	19.10
-24	15.93	16.86	20.92	20.32	24.50	21.41	24.28	21.96	20.88	17.19	13.35	12.65	19.21

Monthly averaged daily global insolation $\bar{I}_t$ continued													
Surface Angle β	Monthly averaged daily global insolation $\bar{I}_t$												
	January	February	March	April	May	June	July	August	September	October	November	December	Annual
°	MJ/m^2	MJ/m^2	MJ/m^2	MJ/m^2	MJ/m^2	MJ/m^2	MJ/m^2	MJ/m^2	MJ/m^2	MJ/m^2	MJ/m^2	MJ/m^2	MJ/m^2
-23	16.19	17.04	21.06	20.37	24.50	21.40	24.26	22.00	20.99	17.35	13.52	12.84	19.31
-22	16.45	17.22	21.19	20.42	24.49	21.39	24.24	22.03	21.10	17.50	13.68	13.02	19.41
-21	16.70	17.39	21.32	20.46	24.48	21.37	24.21	22.05	21.20	17.65	13.84	13.20	19.51
-20	16.95	17.56	21.44	20.50	24.46	21.35	24.18	22.07	21.29	17.80	14.00	13.38	19.60
-19	17.19	17.72	21.56	20.53	24.43	21.32	24.14	22.08	21.38	17.94	14.15	13.55	19.68
-18	17.43	17.88	21.67	20.56	24.40	21.29	24.09	22.08	21.46	18.08	14.30	13.73	19.76
-17	17.67	18.04	21.78	20.59	24.36	21.25	24.04	22.08	21.54	18.21	14.45	13.89	19.84
-16	17.90	18.19	21.88	20.60	24.31	21.21	23.98	22.08	21.61	18.34	14.60	14.06	19.91
-15	18.13	18.33	21.97	20.62	24.26	21.16	23.92	22.07	21.67	18.46	14.74	14.22	19.98
-14	18.36	18.48	22.06	20.63	24.20	21.10	23.85	22.05	21.74	18.58	14.88	14.38	20.04
-13	18.58	18.61	22.14	20.63	24.14	21.05	23.77	22.03	21.79	18.70	15.02	14.54	20.10
-12	18.79	18.75	22.22	20.63	24.07	20.98	23.69	22.01	21.84	18.81	15.15	14.70	20.15
-11	19.00	18.88	22.29	20.62	23.99	20.91	23.60	21.97	21.88	18.92	15.28	14.85	20.20
-10	19.21	19.00	22.35	20.61	23.91	20.84	23.50	21.94	21.92	19.02	15.41	15.00	20.24
-9	19.42	19.12	22.41	20.59	23.82	20.76	23.40	21.89	21.96	19.11	15.54	15.15	20.28
-8	19.61	19.24	22.47	20.57	23.73	20.68	23.30	21.84	21.98	19.20	15.66	15.29	20.31
-7	19.81	19.35	22.52	20.54	23.63	20.59	23.18	21.79	22.01	19.29	15.77	15.43	20.34
-6	20.00	19.45	22.56	20.51	23.52	20.50	23.06	21.73	22.02	19.37	15.89	15.56	20.36
-5	20.18	19.56	22.59	20.47	23.40	20.40	22.94	21.67	22.04	19.45	15.99	15.70	20.38
-4	20.36	19.65	22.62	20.43	23.29	20.29	22.81	21.59	22.04	19.52	16.10	15.83	20.39
-3	20.53	19.74	22.65	20.38	23.16	20.19	22.67	21.52	22.04	19.59	16.20	15.95	20.40
-2	20.70	19.83	22.67	20.33	23.03	20.07	22.53	21.44	22.04	19.65	16.30	16.07	20.40
-1	20.86	19.91	22.68	20.27	22.89	19.96	22.38	21.35	22.02	19.71	16.39	16.19	20.40

Monthly averaged daily global insolation $\bar{I}_t$ continued													
Surface Angle β	Monthly averaged daily global insolation $\bar{I}_t$												
	January	February	March	April	May	June	July	August	September	October	November	December	Annual
°	MJ/m^2	MJ/m^2	MJ/m^2	MJ/m^2	MJ/m^2	MJ/m^2	MJ/m^2	MJ/m^2	MJ/m^2	MJ/m^2	MJ/m^2	MJ/m^2	MJ/m^2
0	21.02	19.99	22.69	20.21	22.75	19.83	22.22	21.26	22.01	19.76	16.48	16.30	20.39
1	21.17	20.06	22.69	20.14	22.60	19.71	22.06	21.16	21.99	19.81	16.57	16.41	20.37
2	21.32	20.13	22.68	20.07	22.45	19.58	21.90	21.06	21.96	19.85	16.65	16.52	20.36
3	21.46	20.19	22.67	19.99	22.29	19.44	21.73	20.95	21.93	19.89	16.73	16.62	20.33
4	21.59	20.25	22.65	19.91	22.12	19.30	21.55	20.84	21.89	19.92	16.81	16.72	20.30
5	21.72	20.30	22.63	19.82	21.95	19.15	21.37	20.72	21.84	19.95	16.88	16.81	20.27
6	21.84	20.35	22.60	19.73	21.77	19.00	21.18	20.60	21.79	19.97	16.94	16.90	20.23
7	21.96	20.39	22.57	19.64	21.59	18.85	20.99	20.47	21.74	19.99	17.01	16.99	20.19
8	22.07	20.43	22.53	19.53	21.40	18.69	20.79	20.34	21.68	20.00	17.07	17.07	20.14
9	22.18	20.46	22.48	19.43	21.21	18.53	20.59	20.20	21.61	20.01	17.12	17.15	20.09
10	22.28	20.49	22.43	19.32	21.01	18.36	20.38	20.06	21.54	20.01	17.17	17.22	20.03
11	22.38	20.51	22.37	19.20	20.81	18.19	20.16	19.91	21.46	20.01	17.22	17.29	19.97
12	22.47	20.53	22.31	19.08	20.60	18.02	19.95	19.76	21.38	20.00	17.26	17.36	19.90
13	22.55	20.54	22.24	18.96	20.38	17.84	19.72	19.60	21.29	19.99	17.30	17.42	19.82
14	22.63	20.55	22.16	18.83	20.16	17.65	19.49	19.44	21.20	19.97	17.34	17.48	19.75
15	22.70	20.55	22.08	18.69	19.94	17.47	19.26	19.27	21.10	19.95	17.37	17.53	19.66
16	22.76	20.55	21.99	18.56	19.71	17.27	19.02	19.10	21.00	19.92	17.39	17.58	19.58
17	22.82	20.54	21.90	18.41	19.47	17.08	18.78	18.92	20.89	19.89	17.41	17.62	19.48
18	22.88	20.53	21.80	18.27	19.23	16.88	18.53	18.74	20.77	19.85	17.43	17.66	19.39
19	22.92	20.51	21.70	18.11	18.99	16.68	18.28	18.56	20.66	19.81	17.45	17.70	19.28
20	22.96	20.49	21.59	17.96	18.74	16.47	18.03	18.37	20.53	19.76	17.46	17.73	19.18
21	23.00	20.46	21.47	17.80	18.49	16.26	17.77	18.17	20.40	19.71	17.46	17.76	19.07
22	23.03	20.43	21.35	17.63	18.23	16.05	17.51	17.97	20.27	19.65	17.46	17.78	18.95

Monthly averaged daily global insolation $\bar{I}_t$ continued													
Surface Angle β	Monthly averaged daily global insolation $\bar{I}_t$												
	January	February	March	April	May	June	July	August	September	October	November	December	Annual
°	MJ/m^2	MJ/m^2	MJ/m^2	MJ/m^2	MJ/m^2	MJ/m^2	MJ/m^2	MJ/m^2	MJ/m^2	MJ/m^2	MJ/m^2	MJ/m^2	MJ/m^2
23	23.05	20.39	21.23	17.47	17.97	15.84	17.24	17.83	20.13	19.59	17.46	17.80	18.83
24	23.07	20.35	21.10	17.29	17.70	15.62	16.97	17.56	19.98	19.52	17.45	17.82	18.70
25	23.08	20.30	20.96	17.12	17.43	15.40	16.70	17.35	19.83	19.45	17.44	17.83	18.57
26	23.09	20.25	20.82	16.94	17.16	15.17	16.42	17.14	19.68	19.37	17.43	17.83	18.44
27	23.08	20.19	20.67	16.75	16.88	14.95	16.14	16.92	19.52	19.29	17.41	17.83	18.30
28	23.08	20.12	20.52	16.56	16.60	14.72	15.85	16.70	19.36	19.20	17.39	17.83	18.16
29	23.06	20.06	20.36	16.37	16.32	14.49	15.56	16.47	19.19	19.11	17.36	17.83	18.01
30	23.05	19.98	20.20	16.17	16.04	14.25	15.27	16.24	19.01	19.01	17.33	17.81	17.86
31	23.02	19.91	20.03	15.97	15.75	14.01	14.98	16.01	18.84	18.91	17.29	17.80	17.71
32	22.99	19.82	19.85	15.77	15.46	13.77	14.68	15.77	18.65	18.80	17.25	17.78	17.55
33	22.95	19.74	19.67	15.57	15.17	13.53	14.38	15.53	18.47	18.69	17.21	17.76	17.39
34	22.91	19.64	19.49	15.36	14.87	13.29	14.07	15.29	18.28	18.58	17.16	17.73	17.22
35	22.86	19.55	19.30	15.14	14.57	13.04	13.77	15.04	18.08	18.46	17.11	17.69	17.05
36	22.80	19.45	19.11	14.93	14.27	12.79	13.46	14.79	17.88	18.33	17.05	17.66	16.87
37	22.74	19.34	18.91	14.71	13.96	12.53	13.15	14.54	17.67	18.21	16.99	17.62	16.69
38	22.67	19.23	18.71	14.49	13.65	12.28	12.83	14.28	17.47	18.07	16.93	17.57	16.51
39	22.60	19.11	18.50	14.26	13.34	12.02	12.52	14.02	17.25	17.93	16.86	17.52	16.32
40	22.52	18.99	18.29	14.03	13.02	11.76	12.20	13.76	17.04	17.79	16.79	17.47	16.13
41	22.44	18.87	18.07	13.80	12.70	11.50	11.87	13.50	16.81	17.65	16.71	17.41	15.94
42	22.35	18.74	17.85	13.57	12.38	11.23	11.55	13.23	16.59	17.49	16.63	17.35	15.74
43	22.25	18.60	17.62	13.33	12.06	10.97	11.22	12.96	16.36	17.34	16.55	17.28	15.54
44	22.15	18.46	17.39	13.09	11.73	10.70	10.89	12.69	16.13	17.18	16.46	17.21	15.33
45	22.04	18.32	17.16	12.85	11.40	10.43	10.56	12.42	15.89	17.02	16.37	17.14	15.12

Appendix I Monthly averaged daily beam insolation

Surface Angle β	Monthly averaged daily beam insolation $\bar{I}_{bt}$												
	January	February	March	April	May	June	July	August	September	October	November	December	Annual
°	MJ/m^2	MJ/m^2	MJ/m^2	MJ/m^2	MJ/m^2	MJ/m^2	MJ/m^2	MJ/m^2	MJ/m^2	MJ/m^2	MJ/m^2	MJ/m^2	MJ/m^2
-45	3.74	4.20	8.38	7.86	12.60	8.54	12.94	9.59	8.13	5.49	2.24	1.81	7.15
-44	3.99	4.38	8.58	7.97	12.71	8.59	13.04	9.70	8.29	5.67	2.37	1.96	7.30
-43	4.25	4.56	8.77	8.07	12.82	8.65	13.14	9.80	8.46	5.85	2.51	2.11	7.44
-42	4.51	4.73	8.96	8.18	12.92	8.70	13.23	9.90	8.62	6.03	2.65	2.26	7.58
-41	4.77	4.91	9.15	8.28	13.02	8.75	13.32	10.00	8.77	6.21	2.79	2.40	7.72
-40	5.02	5.08	9.34	8.38	13.12	8.80	13.41	10.09	8.93	6.39	2.92	2.55	7.86
-39	5.28	5.25	9.53	8.47	13.21	8.84	13.49	10.19	9.08	6.57	3.06	2.70	8.00
-38	5.54	5.42	9.71	8.57	13.30	8.89	13.56	10.27	9.23	6.74	3.20	2.84	8.13
-37	5.80	5.59	9.89	8.66	13.39	8.92	13.64	10.36	9.38	6.91	3.34	2.99	8.26
-36	6.05	5.76	10.06	8.75	13.47	8.96	13.71	10.44	9.52	7.08	3.47	3.13	8.39
-35	6.30	5.92	10.24	8.84	13.54	9.00	13.77	10.52	9.66	7.25	3.61	3.28	8.52
-34	6.56	6.09	10.40	8.92	13.61	9.03	13.83	10.60	9.80	7.41	3.74	3.43	8.64
-33	6.81	6.25	10.57	9.00	13.68	9.05	13.89	10.67	9.93	7.58	3.88	3.58	8.77
-32	7.07	6.41	10.73	9.08	13.74	9.08	13.94	10.74	10.06	7.74	4.01	3.74	8.89
-31	7.32	6.57	10.89	9.15	13.80	9.10	13.98	10.81	10.19	7.90	4.14	3.89	9.01
-30	7.58	6.73	11.05	9.23	13.86	9.12	14.03	10.87	10.32	8.05	4.27	4.04	9.12
-29	7.83	6.88	11.20	9.30	13.91	9.14	14.07	10.93	10.44	8.21	4.40	4.18	9.23
-28	8.08	7.04	11.35	9.36	13.96	9.15	14.10	10.99	10.56	8.36	4.53	4.33	9.34
-27	8.32	7.19	11.50	9.43	14.00	9.17	14.13	11.04	10.67	8.51	4.65	4.47	9.45
-26	8.57	7.34	11.64	9.49	14.04	9.18	14.16	11.09	10.79	8.65	4.78	4.62	9.55
-25	8.81	7.49	11.78	9.55	14.07	9.18	14.18	11.14	10.89	8.80	4.90	4.76	9.65
-24	9.05	7.63	11.92	9.60	14.10	9.18	14.20	11.18	11.00	8.94	5.02	4.90	9.75

Monthly averaged daily beam insolation $\bar{I}_{bt}$ continued													
Surface Angle β	Monthly averaged daily beam insolation $\bar{I}_{bt}$												
	January	February	March	April	May	June	July	August	September	October	November	December	Annual
°	MJ/m^2	MJ/m^2	MJ/m^2	MJ/m^2	MJ/m^2	MJ/m^2	MJ/m^2	MJ/m^2	MJ/m^2	MJ/m^2	MJ/m^2	MJ/m^2	MJ/m^2
-23	9.28	7.77	12.05	9.65	14.13	9.19	14.21	11.22	11.10	9.08	5.15	5.04	9.85
-22	9.52	7.91	12.18	9.70	14.15	9.18	14.22	11.25	11.20	9.21	5.27	5.18	9.94
-21	9.75	8.05	12.30	9.75	14.16	9.18	14.22	11.29	11.30	9.35	5.38	5.32	10.03
-20	9.98	8.19	12.42	9.79	14.18	9.17	14.22	11.32	11.39	9.48	5.50	5.45	10.12
-19	10.20	8.32	12.54	9.83	14.19	9.16	14.22	11.34	11.48	9.61	5.61	5.58	10.20
-18	10.42	8.45	12.66	9.87	14.19	9.15	14.21	11.37	11.57	9.73	5.73	5.72	10.28
-17	10.64	8.58	12.77	9.91	14.19	9.13	14.20	11.38	11.65	9.85	5.84	5.84	10.36
-16	10.86	8.70	12.87	9.94	14.18	9.11	14.18	11.40	11.73	9.97	5.95	5.97	10.43
-15	11.07	8.82	12.97	9.97	14.17	9.09	14.16	11.41	11.80	10.09	6.06	6.10	10.50
-14	11.29	8.94	13.07	9.99	14.16	9.06	14.13	11.42	11.87	10.20	6.17	6.22	10.57
-13	11.49	9.06	13.16	10.01	14.14	9.04	14.10	11.43	11.94	10.31	6.27	6.35	10.63
-12	11.70	9.18	13.25	10.03	14.12	9.01	14.07	11.43	12.00	10.42	6.38	6.47	10.70
-11	11.90	9.29	13.34	10.05	14.09	8.97	14.03	11.43	12.06	10.52	6.48	6.59	10.75
-10	12.10	9.40	13.42	10.06	14.06	8.94	13.99	11.42	12.12	10.62	6.58	6.71	10.81
-9	12.29	9.50	13.50	10.07	14.03	8.90	13.94	11.41	12.17	10.71	6.68	6.83	10.86
-8	12.48	9.61	13.57	10.08	13.99	8.86	13.89	11.40	12.22	10.81	6.77	6.95	10.91
-7	12.67	9.71	13.64	10.08	13.95	8.82	13.83	11.38	12.27	10.90	6.87	7.06	10.95
-6	12.85	9.80	13.71	10.09	13.90	8.77	13.77	11.36	12.31	10.99	6.96	7.17	11.00
-5	13.03	9.90	13.77	10.08	13.85	8.72	13.71	11.34	12.35	11.07	7.05	7.28	11.04
-4	13.21	9.99	13.83	10.08	13.79	8.67	13.64	11.31	12.38	11.15	7.14	7.39	11.07
-3	13.38	10.08	13.88	10.07	13.73	8.61	13.57	11.28	12.41	11.23	7.22	7.49	11.10
-2	13.55	10.16	13.93	10.06	13.66	8.56	13.49	11.25	12.44	11.30	7.31	7.59	11.13
-1	13.71	10.24	13.97	10.04	13.60	8.50	13.41	11.22	12.46	11.37	7.39	7.69	11.16

Monthly averaged daily beam insolation $\bar{I}_{bt}$ continued													
Surface Angle β	Monthly averaged daily beam insolation $\bar{I}_{bt}$												
	January	February	March	April	May	June	July	August	September	October	November	December	Annual
°	MJ/m^2	MJ/m^2	MJ/m^2	MJ/m^2	MJ/m^2	MJ/m^2	MJ/m^2	MJ/m^2	MJ/m^2	MJ/m^2	MJ/m^2	MJ/m^2	MJ/m^2
0	13.87	10.32	14.01	10.03	13.52	8.44	13.32	11.18	12.48	11.44	7.47	7.79	11.18
1	14.03	10.40	14.05	10.01	13.45	8.37	13.23	11.13	12.50	11.50	7.54	7.89	11.20
2	14.18	10.47	14.08	9.98	13.37	8.30	13.14	11.09	12.51	11.56	7.62	7.98	11.21
3	14.32	10.54	14.10	9.96	13.28	8.23	13.04	11.04	12.51	11.61	7.69	8.07	11.22
4	14.47	10.61	14.13	9.93	13.19	8.16	12.94	10.98	12.52	11.67	7.76	8.16	11.23
5	14.60	10.67	14.15	9.89	13.10	8.09	12.84	10.93	12.52	11.71	7.82	8.24	11.23
6	14.74	10.73	14.16	9.86	13.00	8.01	12.73	10.87	12.51	11.76	7.89	8.32	11.24
7	14.87	10.79	14.17	9.82	12.90	7.93	12.62	10.80	12.51	11.80	7.95	8.40	11.23
8	14.99	10.84	14.18	9.78	12.79	7.85	12.50	10.73	12.50	11.84	8.01	8.48	11.23
9	15.11	10.89	14.18	9.73	12.68	7.76	12.38	10.66	12.48	11.87	8.07	8.56	11.22
10	15.23	10.94	14.17	9.69	12.57	7.68	12.26	10.59	12.46	11.90	8.12	8.63	11.21
11	15.34	10.98	14.17	9.64	12.46	7.59	12.13	10.52	12.44	11.93	8.18	8.70	11.19
12	15.44	11.02	14.15	9.58	12.33	7.50	12.00	10.44	12.41	11.96	8.23	8.77	11.17
13	15.54	11.06	14.14	9.53	12.21	7.40	11.86	10.35	12.38	11.98	8.27	8.83	11.15
14	15.64	11.09	14.12	9.47	12.08	7.31	11.73	10.27	12.35	11.99	8.32	8.89	11.12
15	15.73	11.12	14.09	9.40	11.95	7.21	11.58	10.18	12.31	12.00	8.36	8.95	11.09
16	15.82	11.15	14.06	9.34	11.82	7.11	11.44	10.09	12.27	12.01	8.40	9.01	11.06
17	15.90	11.17	14.03	9.27	11.68	7.01	11.29	9.99	12.22	12.02	8.44	9.06	11.02
18	15.98	11.19	13.99	9.20	11.53	6.90	11.14	9.89	12.17	12.02	8.47	9.12	10.99
19	16.05	11.21	13.95	9.13	11.39	6.79	10.98	9.79	12.12	12.02	8.51	9.16	10.94
20	16.12	11.22	13.91	9.05	11.24	6.69	10.82	9.69	12.06	12.01	8.54	9.21	10.90
21	16.18	11.23	13.86	8.97	11.09	6.58	10.66	9.58	12.00	12.00	8.56	9.25	10.85
22	16.24	11.23	13.80	8.89	10.93	6.47	10.50	9.47	11.94	11.99	8.59	9.29	10.79

Monthly averaged daily beam insolation $\bar{I}_{bt}$ continued													
Surface Angle β	Monthly averaged daily beam insolation $\bar{I}_{bt}$												
	January	February	March	April	May	June	July	August	September	October	November	December	Annual
°	MJ/m^2	MJ/m^2	MJ/m^2	MJ/m^2	MJ/m^2	MJ/m^2	MJ/m^2	MJ/m^2	MJ/m^2	MJ/m^2	MJ/m^2	MJ/m^2	MJ/m^2
23	16.29	11.24	13.74	8.81	10.77	6.35	10.33	9.39	11.87	11.97	8.61	9.33	10.74
24	16.34	11.24	13.68	8.72	10.61	6.24	10.16	9.24	11.80	11.95	8.63	9.36	10.68
25	16.38	11.23	13.61	8.63	10.44	6.12	9.99	9.12	11.73	11.93	8.64	9.39	10.62
26	16.42	11.22	13.54	8.54	10.27	6.00	9.81	9.00	11.65	11.90	8.66	9.42	10.55
27	16.45	11.21	13.47	8.44	10.10	5.88	9.63	8.88	11.57	11.87	8.67	9.45	10.48
28	16.48	11.20	13.39	8.34	9.93	5.76	9.45	8.75	11.48	11.84	8.68	9.47	10.41
29	16.50	11.18	13.30	8.24	9.75	5.64	9.27	8.62	11.39	11.80	8.68	9.49	10.34
30	16.52	11.16	13.22	8.14	9.58	5.51	9.08	8.49	11.30	11.76	8.69	9.51	10.26
31	16.53	11.13	13.12	8.04	9.40	5.39	8.89	8.36	11.20	11.71	8.69	9.52	10.18
32	16.54	11.11	13.03	7.93	9.21	5.26	8.70	8.22	11.10	11.66	8.69	9.53	10.10
33	16.54	11.08	12.93	7.82	9.03	5.13	8.51	8.08	11.00	11.61	8.68	9.54	10.01
34	16.54	11.04	12.83	7.71	8.84	5.00	8.31	7.94	10.90	11.55	8.67	9.55	9.92
35	16.53	11.00	12.72	7.59	8.65	4.87	8.11	7.80	10.79	11.49	8.66	9.55	9.83
36	16.52	10.96	12.61	7.48	8.46	4.74	7.91	7.65	10.67	11.43	8.65	9.55	9.73
37	16.50	10.92	12.49	7.36	8.27	4.60	7.71	7.50	10.56	11.36	8.64	9.55	9.63
38	16.48	10.87	12.37	7.24	8.07	4.46	7.51	7.35	10.44	11.29	8.62	9.54	9.53
39	16.45	10.82	12.25	7.12	7.87	4.33	7.30	7.20	10.32	11.22	8.60	9.53	9.43
40	16.42	10.76	12.12	6.99	7.67	4.19	7.09	7.05	10.19	11.14	8.58	9.52	9.32
41	16.38	10.70	11.99	6.86	7.46	4.05	6.88	6.90	10.06	11.06	8.55	9.50	9.21
42	16.34	10.64	11.86	6.74	7.26	3.91	6.67	6.74	9.93	10.98	8.52	9.49	9.10
43	16.29	10.58	11.72	6.61	7.05	3.76	6.45	6.58	9.80	10.89	8.49	9.46	8.98
44	16.24	10.51	11.58	6.47	6.84	3.62	6.23	6.42	9.66	10.80	8.46	9.44	8.86
45	16.18	10.44	11.44	6.34	6.62	3.47	6.01	6.26	9.52	10.71	8.42	9.41	8.74

Appendix J Monthly averaged daily diffuse insolation

Surface Angle β	Monthly averaged daily diffuse insolation $\bar{I}_{dt}$												
	January	February	March	April	May	June	July	August	September	October	November	December	Annual
°	MJ/m^2	MJ/m^2	MJ/m^2	MJ/m^2	MJ/m^2	MJ/m^2	MJ/m^2	MJ/m^2	MJ/m^2	MJ/m^2	MJ/m^2	MJ/m^2	MJ/m^2
-45	5.84	7.79	8.12	9.89	10.10	11.52	9.83	10.08	8.97	7.19	6.85	6.29	8.54
-44	5.90	7.87	8.17	9.95	10.14	11.58	9.86	10.13	9.03	7.25	6.93	6.37	8.59
-43	5.95	7.94	8.23	10.01	10.17	11.63	9.89	10.18	9.09	7.31	7.00	6.44	8.65
-42	6.00	8.02	8.28	10.06	10.20	11.68	9.92	10.23	9.14	7.37	7.08	6.52	8.70
-41	6.06	8.10	8.33	10.11	10.22	11.73	9.94	10.28	9.20	7.42	7.16	6.59	8.76
-40	6.11	8.17	8.38	10.16	10.24	11.77	9.96	10.32	9.25	7.48	7.23	6.66	8.81
-39	6.16	8.25	8.43	10.20	10.27	11.81	9.98	10.36	9.30	7.53	7.30	6.73	8.86
-38	6.21	8.32	8.47	10.25	10.28	11.85	9.99	10.40	9.34	7.59	7.38	6.80	8.90
-37	6.26	8.39	8.52	10.29	10.30	11.89	10.01	10.43	9.39	7.64	7.45	6.87	8.95
-36	6.30	8.45	8.56	10.33	10.31	11.92	10.02	10.47	9.43	7.69	7.52	6.94	8.99
-35	6.35	8.52	8.60	10.36	10.32	11.95	10.03	10.50	9.47	7.73	7.59	7.00	9.03
-34	6.39	8.59	8.64	10.40	10.33	11.98	10.03	10.53	9.51	7.78	7.65	7.07	9.07
-33	6.44	8.65	8.67	10.43	10.34	12.01	10.04	10.55	9.55	7.83	7.72	7.14	9.11
-32	6.48	8.71	8.70	10.46	10.34	12.03	10.04	10.58	9.58	7.87	7.78	7.20	9.14
-31	6.52	8.77	8.74	10.49	10.35	12.05	10.04	10.60	9.61	7.91	7.85	7.27	9.18
-30	6.57	8.83	8.76	10.51	10.34	12.07	10.04	10.62	9.64	7.95	7.91	7.33	9.21
-29	6.61	8.88	8.79	10.54	10.34	12.09	10.03	10.63	9.67	7.99	7.97	7.39	9.24
-28	6.64	8.94	8.82	10.56	10.34	12.10	10.03	10.65	9.70	8.02	8.03	7.45	9.27
-27	6.68	8.99	8.84	10.58	10.33	12.11	10.02	10.66	9.72	8.06	8.09	7.51	9.29
-26	6.72	9.04	8.86	10.59	10.32	12.12	10.00	10.67	9.74	8.09	8.14	7.56	9.32
-25	6.75	9.09	8.88	10.61	10.30	12.13	9.99	10.68	9.76	8.12	8.20	7.62	9.34
-24	6.78	9.14	8.90	10.62	10.29	12.13	9.97	10.68	9.78	8.15	8.25	7.67	9.36

Monthly averaged daily diffuse insolation $\bar{I}_{dt}$ continued													
Surface Angle β	Monthly averaged daily diffuse insolation $\bar{I}_{dt}$												
	January	February	March	April	May	June	July	August	September	October	November	December	Annual
°	MJ/m^2	MJ/m^2	MJ/m^2	MJ/m^2	MJ/m^2	MJ/m^2	MJ/m^2	MJ/m^2	MJ/m^2	MJ/m^2	MJ/m^2	MJ/m^2	MJ/m^2
-23	6.82	9.18	8.91	10.63	10.27	12.13	9.95	10.69	9.79	8.18	8.30	7.73	9.37
-22	6.85	9.23	8.92	10.63	10.25	12.12	9.93	10.69	9.81	8.21	8.35	7.78	9.39
-21	6.88	9.27	8.94	10.64	10.23	12.12	9.91	10.68	9.82	8.23	8.40	7.83	9.40
-20	6.90	9.31	8.94	10.64	10.20	12.11	9.88	10.68	9.82	8.25	8.44	7.88	9.41
-19	6.93	9.34	8.95	10.64	10.18	12.10	9.86	10.67	9.83	8.28	8.49	7.92	9.42
-18	6.95	9.38	8.95	10.64	10.15	12.09	9.82	10.66	9.83	8.29	8.53	7.97	9.43
-17	6.98	9.41	8.96	10.63	10.12	12.07	9.79	10.65	9.84	8.31	8.57	8.01	9.44
-16	7.00	9.44	8.96	10.62	10.08	12.05	9.76	10.64	9.84	8.33	8.61	8.05	9.44
-15	7.02	9.47	8.96	10.61	10.04	12.03	9.72	10.62	9.83	8.34	8.65	8.09	9.44
-14	7.04	9.50	8.95	10.60	10.01	12.01	9.68	10.60	9.83	8.35	8.69	8.13	9.44
-13	7.06	9.52	8.94	10.59	9.96	11.98	9.64	10.58	9.82	8.36	8.72	8.17	9.44
-12	7.07	9.55	8.94	10.57	9.92	11.95	9.59	10.55	9.81	8.37	8.76	8.20	9.43
-11	7.09	9.57	8.93	10.55	9.88	11.92	9.55	10.53	9.80	8.38	8.79	8.24	9.42
-10	7.10	9.59	8.91	10.53	9.83	11.88	9.50	10.50	9.79	8.38	8.82	8.27	9.41
-9	7.11	9.61	8.90	10.50	9.78	11.85	9.45	10.47	9.77	8.38	8.85	8.30	9.40
-8	7.12	9.62	8.88	10.48	9.72	11.81	9.40	10.43	9.75	8.38	8.87	8.33	9.39
-7	7.13	9.63	8.86	10.45	9.67	11.77	9.34	10.40	9.73	8.38	8.90	8.36	9.37
-6	7.14	9.64	8.84	10.42	9.61	11.72	9.29	10.36	9.71	8.38	8.92	8.39	9.36
-5	7.14	9.65	8.82	10.38	9.55	11.67	9.23	10.32	9.68	8.38	8.94	8.41	9.34
-4	7.15	9.66	8.80	10.35	9.49	11.62	9.17	10.28	9.66	8.37	8.96	8.44	9.32
-3	7.15	9.66	8.77	10.31	9.43	11.57	9.10	10.23	9.63	8.36	8.98	8.46	9.29
-2	7.15	9.67	8.74	10.27	9.36	11.52	9.04	10.19	9.60	8.35	8.99	8.48	9.27
-1	7.15	9.67	8.71	10.23	9.30	11.46	8.97	10.14	9.56	8.34	9.01	8.50	9.24

Monthly averaged daily diffuse insolation $\bar{I}_{dt}$ continued													
Surface Angle β	Monthly averaged daily diffuse insolation $\bar{I}_{dt}$												
	January	February	March	April	May	June	July	August	September	October	November	December	Annual
°	MJ/m^2	MJ/m^2	MJ/m^2	MJ/m^2	MJ/m^2	MJ/m^2	MJ/m^2	MJ/m^2	MJ/m^2	MJ/m^2	MJ/m^2	MJ/m^2	MJ/m^2
0	7.15	9.67	8.68	10.18	9.23	11.40	8.90	10.08	9.53	8.33	9.02	8.51	9.21
1	7.14	9.66	8.64	10.14	9.15	11.34	8.83	10.03	9.49	8.31	9.03	8.53	9.18
2	7.14	9.66	8.60	10.09	9.08	11.27	8.76	9.97	9.45	8.29	9.04	8.54	9.15
3	7.13	9.65	8.56	10.03	9.00	11.20	8.68	9.92	9.41	8.27	9.04	8.55	9.11
4	7.12	9.64	8.52	9.98	8.93	11.14	8.60	9.86	9.37	8.25	9.05	8.56	9.07
5	7.11	9.63	8.48	9.93	8.85	11.06	8.52	9.79	9.32	8.23	9.05	8.57	9.03
6	7.10	9.61	8.44	9.87	8.76	10.99	8.44	9.73	9.27	8.21	9.05	8.57	8.99
7	7.09	9.60	8.39	9.81	8.68	10.91	8.36	9.66	9.22	8.18	9.05	8.58	8.95
8	7.07	9.58	8.34	9.74	8.60	10.83	8.28	9.59	9.17	8.15	9.05	8.58	8.90
9	7.06	9.56	8.29	9.68	8.51	10.75	8.19	9.52	9.12	8.12	9.04	8.58	8.85
10	7.04	9.54	8.24	9.61	8.42	10.67	8.10	9.45	9.06	8.09	9.04	8.58	8.81
11	7.02	9.51	8.18	9.55	8.33	10.58	8.01	9.37	9.00	8.06	9.03	8.58	8.75
12	7.00	9.49	8.12	9.48	8.23	10.50	7.92	9.30	8.94	8.02	9.02	8.57	8.70
13	6.98	9.46	8.07	9.40	8.14	10.41	7.83	9.22	8.88	7.98	9.00	8.56	8.65
14	6.95	9.43	8.01	9.33	8.04	10.31	7.73	9.13	8.82	7.95	8.99	8.56	8.59
15	6.93	9.40	7.94	9.25	7.94	10.22	7.64	9.05	8.75	7.91	8.97	8.55	8.53
16	6.90	9.36	7.88	9.17	7.84	10.12	7.54	8.97	8.68	7.86	8.96	8.53	8.47
17	6.87	9.32	7.82	9.09	7.74	10.03	7.44	8.88	8.61	7.82	8.94	8.52	8.41
18	6.84	9.29	7.75	9.01	7.64	9.93	7.34	8.79	8.54	7.78	8.92	8.50	8.35
19	6.81	9.25	7.68	8.93	7.54	9.82	7.23	8.70	8.47	7.73	8.89	8.49	8.28
20	6.78	9.20	7.61	8.84	7.43	9.72	7.13	8.61	8.39	7.68	8.87	8.47	8.21
21	6.74	9.16	7.54	8.75	7.32	9.61	7.03	8.51	8.32	7.63	8.84	8.45	8.14
22	6.71	9.11	7.46	8.66	7.21	9.51	6.92	8.42	8.24	7.58	8.81	8.43	8.07

Monthly averaged daily diffuse insolation $\bar{I}_{dt}$ continued													
Surface Angle β	Monthly averaged daily diffuse insolation $\bar{I}_{dt}$												
	January	February	March	April	May	June	July	August	September	October	November	December	Annual
°	MJ/m^2	MJ/m^2	MJ/m^2	MJ/m^2	MJ/m^2	MJ/m^2	MJ/m^2	MJ/m^2	MJ/m^2	MJ/m^2	MJ/m^2	MJ/m^2	MJ/m^2
23	6.67	9.07	7.39	8.57	7.10	9.40	6.81	8.35	8.16	7.53	8.78	8.40	8.00
24	6.63	9.02	7.31	8.48	6.99	9.29	6.70	8.22	8.08	7.47	8.75	8.38	7.93
25	6.59	8.96	7.23	8.38	6.88	9.18	6.59	8.12	7.99	7.41	8.71	8.35	7.85
26	6.55	8.91	7.15	8.29	6.76	9.06	6.48	8.02	7.91	7.36	8.68	8.32	7.78
27	6.51	8.85	7.07	8.19	6.65	8.95	6.37	7.91	7.82	7.30	8.64	8.29	7.70
28	6.46	8.80	6.98	8.09	6.53	8.83	6.26	7.81	7.73	7.24	8.60	8.26	7.62
29	6.42	8.74	6.90	7.99	6.41	8.71	6.14	7.70	7.64	7.17	8.56	8.22	7.54
30	6.37	8.68	6.81	7.88	6.29	8.59	6.03	7.59	7.55	7.11	8.52	8.19	7.45
31	6.32	8.61	6.72	7.78	6.18	8.47	5.91	7.48	7.46	7.05	8.47	8.15	7.37
32	6.27	8.55	6.63	7.67	6.06	8.35	5.79	7.37	7.37	6.98	8.43	8.11	7.28
33	6.22	8.48	6.54	7.57	5.93	8.23	5.67	7.26	7.27	6.91	8.38	8.07	7.20
34	6.17	8.42	6.45	7.46	5.81	8.10	5.55	7.15	7.17	6.84	8.33	8.03	7.11
35	6.12	8.35	6.36	7.35	5.69	7.97	5.43	7.03	7.07	6.77	8.28	7.98	7.02
36	6.06	8.27	6.26	7.24	5.57	7.84	5.31	6.92	6.97	6.70	8.23	7.94	6.93
37	6.01	8.20	6.17	7.12	5.44	7.71	5.19	6.80	6.87	6.62	8.17	7.89	6.83
38	5.95	8.13	6.07	7.01	5.32	7.58	5.07	6.68	6.77	6.55	8.12	7.84	6.74
39	5.89	8.05	5.97	6.90	5.19	7.45	4.95	6.56	6.67	6.47	8.06	7.79	6.65
40	5.83	7.97	5.87	6.78	5.06	7.32	4.82	6.44	6.56	6.40	8.00	7.74	6.55
41	5.77	7.89	5.77	6.66	4.93	7.18	4.70	6.32	6.45	6.32	7.94	7.69	6.45
42	5.71	7.81	5.67	6.55	4.80	7.05	4.57	6.19	6.35	6.24	7.88	7.63	6.35
43	5.65	7.73	5.57	6.43	4.67	6.91	4.44	6.07	6.24	6.16	7.82	7.58	6.25
44	5.58	7.65	5.46	6.31	4.54	6.77	4.32	5.95	6.13	6.08	7.75	7.52	6.15
45	5.52	7.56	5.36	6.18	4.41	6.63	4.19	5.82	6.02	5.99	7.68	7.46	6.05